NASA/TM–20220013820
NESC-TI-21-01657

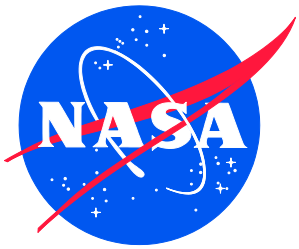

A Survey of NASA Standard Nondestructive Evaluation (NDE)

Peter A. Parker
Langley Research Center, Hampton, Virginia

Ajay Koshti
Johnson Space Center, Houston, Texas

David S. Forsyth
NDTAnalysis, St John, U.S. Virgin Islands

Michael W. Suits, James L. Walker
Marshall Space Flight Center, Huntsville, Alabama

William H. Prosser/NESC
Langley Research Center, Hampton, Virginia

September 2022

NASA STI Program . . . in Profile

Since its founding, NASA has been dedicated to the advancement of aeronautics and space science. The NASA scientific and technical information (STI) program plays a key part in helping NASA maintain this important role.

The NASA STI program operates under the auspices of the Agency Chief Information Officer. It collects, organizes, provides for archiving, and disseminates NASA's STI. The NASA STI program provides access to the NTRS Registered and its public interface, the NASA Technical Reports Server, thus providing one of the largest collections of aeronautical and space science STI in the world. Results are published in both non-NASA channels and by NASA in the NASA STI Report Series, which includes the following report types:

- TECHNICAL PUBLICATION. Reports of completed research or a major significant phase of research that present the results of NASA Programs and include extensive data or theoretical analysis. Includes compilations of significant scientific and technical data and information deemed to be of continuing reference value. NASA counter-part of peer-reviewed formal professional papers but has less stringent limitations on manuscript length and extent of graphic presentations.

- TECHNICAL MEMORANDUM. Scientific and technical findings that are preliminary or of specialized interest, e.g., quick release reports, working papers, and bibliographies that contain minimal annotation. Does not contain extensive analysis.

- CONTRACTOR REPORT. Scientific and technical findings by NASA-sponsored contractors and grantees.

- CONFERENCE PUBLICATION. Collected papers from scientific and technical conferences, symposia, seminars, or other meetings sponsored or co-sponsored by NASA.

- SPECIAL PUBLICATION. Scientific, technical, or historical information from NASA programs, projects, and missions, often concerned with subjects having substantial public interest.

- TECHNICAL TRANSLATION. English-language translations of foreign scientific and technical material pertinent to NASA's mission.

Specialized services also include organizing and publishing research results, distributing specialized research announcements and feeds, providing information desk and personal search support, and enabling data exchange services.

For more information about the NASA STI program, see the following:

- Access the NASA STI program home page at *http://www.sti.nasa.gov*

- E-mail your question to help@sti.nasa.gov

- Phone the NASA STI Information Desk at 757-864-9658

- Write to:

NASA STI Information Desk
Mail Stop 148
NASA Langley Research Center
Hampton, VA 23681-2199

NASA/TM–20220013820
NESC-TI-21-01657

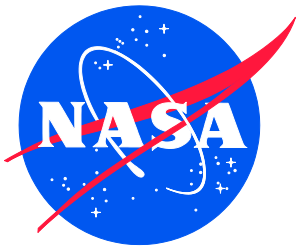

A Survey of NASA Standard Nondestructive Evaluation (NDE)

Peter A. Parker
Langley Research Center, Hampton, Virginia

Ajay Koshti
Johnson Space Center, Houston, Texas

David S. Forsyth
NDTAnalysis, St John, U.S. Virgin Islands

Michael W. Suits, James L. Walker
Marshall Space Flight Center, Huntsville, Alabama

William H. Prosser/NESC
Langley Research Center, Hampton, Virginia

National Aeronautics and
Space Administration

Langley Research Center
Hampton, Virginia 23681-2199

September 2022

Available from:

NASA STI Program / Mail Stop 148
NASA Langley Research Center
Hampton, VA 23681-2199
Fax: 757-864-6500

Preface

Purpose – This document provides a comprehensive review to trace the evolution of NASA's Standard nondestructive evaluation (NDE) flaw sizes provided in NASA-STD-5009B for fracture-critical metallic spaceflight hardware. A NASA Standard NDE flaw size is considered to be conservative such that most inspectors, trained and certified in the specific method, are expected to provide the required 90/95 probability of detection (POD) for that flaw size. As such, individual certified inspectors are not required to perform POD demonstration testing to be allowed to inspect fracture-critical hardware for that specific method.

Table of Contents

List of Figures

List of Tables

Nomenclature

2c	Flaw Length, designating total length of an open surface flaw
2c/a	Flaw Aspect Ratio
a	Flaw Depth
a/t	Flaw Depth-to-Thickness
CIFS	Critical Initial Flaw Size
EDM	Electrical Discharge Machining
MIL-HDBK	Military Handbook
MSFC	Marshall space Flight Center
NDE	Nondestructive Evaluation
NDI	Nondestructive Inspection
NDT	Nondestructive Testing
NIST	National Institute of Standards and Technology
NSTS	National Space Transportation System
NTIAC	Nondestructive Testing Information Analysis Center
OFCP	Orbiter Fracture Control Plan
PEM	Point Estimate Method
PFIB	Plasma Focused Ion Beam
POD	Probability of Detection
PTC	Partly Through Crack
RMS	Root Mean Squared
SGAM	Sorted Group Ascent Method
SI	International System of Units
STD	Standard
t	Specimen Thickness
TC	Through Crack
USAF	United States Air Force

Definitions (adapted from NASA Standard (STD) 5009B (2019))

Capability Demonstration Specimens: A set of specimens made from material similar to the material of the hardware to be inspected with known flaws used to estimate the capability of indication detection (i.e., Probability of Detection (POD) or other methods of capability assessment) of a nondestructive evaluation (NDE) method.

Cracks or Crack-Like Flaws: A discontinuity assumed to behave like a crack for assessment of material or structural integrity. Referred to as induced flaws, whether naturally occurring or laboratory simulated.

Critical Initial Flaw Size (CIFS): The naturally occurring flaw size that is assumed to exist in the part for damage tolerance analysis that is required to be detectable with 90/95 POD.

Defect: One or more flaws whose aggregate size, shape, orientation, location, or properties do not meet specified acceptance criteria and are rejectable.

Flaw: An imperfection or discontinuity that may be detectable by nondestructive testing and is not necessarily rejectable. Examples of flaws in metallic articles include cracks, deep scratches and sharp notches that behave like cracks, material inclusions, forging laps, welding incomplete fusion, penetration, and slag or porosity with a crack-like tail. For additive manufactured metallics, skipped layers, thermal or stress induced cracks, or inclusions are examples.

Hit-Miss NDE Data: Data resulting from an NDE inspection where only the determination of whether an indication is present or not is recorded. Thus, the data at each measurement point corresponds to either a yes or no, or is sometimes represented numerically as a 1 (i.e., indication present) or 0 (no indication). No signal measurements from any NDE sensor output are recorded.

Initial Crack (Flaw) Size: The crack size that is assumed to exist in the part for damage tolerance analysis.

Naturally Occurring Flaw: A flaw that is present in a component as a result of the normally occurring manufacturing processes or usage of the component.

Nondestructive Evaluation (NDE), Nondestructive Inspection (NDI), Nondestructive Testing (NDT): The development and application of technical methods to examine materials or components in ways that do not impair future usefulness and serviceability in order to detect, locate, measure, and evaluate flaws; to assess integrity, properties, and composition; and to measure geometrical characteristics.

NDE Procedure: A written plan providing detailed information on ‘how-to’ perform a hardware-specific inspection.

NDE Simulated Fabricated Flaw**:** A flaw that is intentionally placed in a component for the purpose of generating an NDE signal response. These can be produced by a variety of material removal processes (e.g., cutting, drilling, electrical discharge machining (EDM), laser notching, plasma focused ion beam (PFIB) notching, etc.) or additive material forming processes.

NDE Simulated Induced Flaw**:** A flaw that is intentionally placed in a component for the purpose of generating an NDE signal response. Induced flaws are produced by intentional

loading (thermal, mechanical, etc.) to induce damage (e.g., cracks, delaminations, disbonds, etc.).

NDE Transfer Function: A function that describes the relationship between signal responses for an NDE method as a function of flaw size for different types of flaws (e.g., naturally occurring flaws, load induced or material removal NDE simulated flaws) or for flaws in different types of components (e.g., simple geometries such as cylinders or flat plates or structural component of interest with complex geometry).

Signal Response NDE Data: Data from an inspection where the NDE sensor produces a signal output (e.g., voltage, current, etc.) that is measured and proportional to flaw size. The determination for whether an indication is present is typically made based on a threshold value of the signal response NDE data.

Special NDE: Nondestructive inspections of fracture-critical hardware that are capable of detecting cracks or crack-like flaws smaller than those assumed detectable by Standard NDE or do not conform to the requirements for Standard NDE as set forth in NASA Standard 5009B. Special NDE methods are not limited to fluorescent penetrant, radiography, ultrasonic, eddy current, and magnetic particle.

Standard NDE: NDE methods of metallic materials for which a statistically based flaw detection capability has been established. Standard NDE methods addressed by NASA Standard 5009B are limited to the fluorescent penetrant, radiographic, ultrasonic, eddy current, and magnetic particle methods employing techniques with established capabilities.

Similarity: The outcome of an assessment that the same POD is expected in different NDE inspection situations that might include variations in NDE method/procedure, components being inspected, and/or inspection conditions.

1.0 Introduction

The concept of NASA Standard nondestructive evaluation (NDE) flaw sizes was introduced in the Space Shuttle Program (SSP) Orbiter Fracture Control Plan (OFCP), see King and Johnson (1974). It was carried forth in following documents including the Fracture Control Requirements for Payloads Using the National Space Transportation System (NSTS) NHB 8071.1 (1988), Marshall Space Flight Center (MSFC)-STD-1249 Standard NDE Guidelines and Requirement for Fracture Control Programs (1985), and eventually into NASA-STD-5009B Nondestructive Evaluation Requirements for Fracture-Critical Metallic Components (2019). Anecdotal history suggests the flaw sizes were linked to a series of probability of detection (POD) test programs performed by SSP prime contractors, which were combined and jointly analyzed by Bishop (1973). This review showed that the history was considerably more complicated. First, none of the referenced standards provided details, specifics, or references to the data sources that resulted in the original NASA Standard NDE flaw sizes, or changes that have evolved in later NASA requirements documents. Second, conversations with personnel involved in the development of these original documents and the text contained therein, have revealed that while some of the values are based on the quantitative analysis performed by Bishop, others are based on more undocumented engineering judgement, while others are based on additional unnamed data sources. Lastly, more recent analysis of the historical data in the Bishop report using POD analysis methods described in MIL-HDBK-1823A Nondestructive Evaluation System Reliability Assessment (2009) show that the rudimentary methods used by Bishop were non-conservative in estimating POD parameters and additionally other mathematical errors were made.

The definition of Standard NDE from NASA-STD-5009B, and repeated in this document, is "NDE methods of metallic materials for which a statistically based flaw detection capability has been established. Standard NDE methods addressed by NASA Standard 5009B are limited to the fluorescent penetrant, radiographic, ultrasonic, eddy current, and magnetic particle methods employing techniques with established capabilities." This definition is woefully lacking in terms of how it is described within the NASA NDE and Fracture Control Communities and what it is intended to represent. What Bishop attempted to analyze from the POD studies was what was termed a90/95/95 (i.e., the flaw size for the given method for which 95-percent of inspectors would be able to provide $\geq$ 90/95 POD). Thus, it was intended to be a conservative flaw size used in structural analysis representing the reliably detectable NDE limit such that trained and certified inspectors are assumed to provide the required 90/95 POD. As such, in practice per NASA-STD-5009, properly trained and certified inspectors are not required to perform individual 90/95 POD demonstration testing as is required for NASA Special NDE.

While these Standard NDE flaw sizes have been successfully applied to many NASA programs and projects since the SSP, as noted and described in the following, in most cases they do not represent a90/95/95 values for the original SSP POD demonstration test data. Further, the methodology for performing and analyzing data from a Standard NDE POD study was not codified in any of the NASA requirements documents. Thus, at present, there is no established methodology to develop Standard NDE flaw sizes for new NDE methods, nor to reassess the Standard NDE flaw size for an existing Standard NDE method considering advances in NDE tools, processes, and equipment since the 1970s. This document provides a retrospective survey to trace the evolution of the Standard NDE flaw sizes contained in NASA-STD-5009B. The lessons learned throughout this review were used to develop a methodology for designing, performing, analyzing,

and documenting a NASA Standard NDE POD study, described in Guidebook for Planning and Analyzing NASA Standard Nondestructive Evaluation (NDE) Probability of Detection (POD) Studies, NASA/TM–20220013822 (2022).

2.0 Literature Review of NASA's Standard NDE Flaw Sizes

This literature review traces the evolution of NASA's Standard NDE flaw sizes provided in NASA-STD-5009B (2019) that originated during the SSP in the early 1970s. NASA's Standard NDE flaw sizes are used in the majority of fracture analyses of human spaceflight components, and this motivates the need for a traceable lineage of their derivation. Retrospectively following their evolution spanning 50 years was challenging. This detailed review is based on all known resources, including interviews with key personnel involved in the 1970s. This review follows a chronological order of the primary references, starting with the earliest POD study and progressing to NASA-STD-5009B, as shown below.

- Bishop (1973), Rummel et al. (1974), Anderson et al. (1973)
- Orbiter Fracture Control Plan, King and Johnson (1974)
- MSFC-STD-1249 (1985)
- NASA-STD-5009 (2008) and NASA-STD-5009B (2019)

This review serves as the first cohesive documentation to support NASA-STD-5009B Standard NDE flaw sizes, and is intended to provide a historical benchmark for evaluating consistency with the new NASA Standard NDE methodology proposed in NASA/TM–20220013822 (2022).

Salkowski (1995) provides a high-level overview of the fracture control motivation for assessing NDE detection reliably, and identifies the foundational POD studies used in the SSP development in early 1970s. Salkowski explains that the reusable orbiter design drove NDE to detect smaller flaws than could be found in proof test, which was the first approach used in 1966 for Apollo-era pressure vessels. The SSP OFCP required the definition of reliably detectable flaw sizes for common NDE methods that are assumed to exist by fracture analysts for the purpose of crack growth analysis. These requirements drove significant advancements in POD study design and analysis. Salkowski does not provide sufficient detail to quantitatively trace the NASA-STD-5009B's Standard NDE flaw sizes.

There are other surveys in the literature that provide a historical perspective of the development of POD methodology. For example, Rummel (2010) provides a helpful overview of the history of nondestructive inspection reliability and highlights the initiatives by NASA and the United States Air Force (USAF) to develop NDE methods and reliability assessments in the 1970s. The SSP's introduction of the linear elastic fracture mechanics is cited as motivating the first POD data analysis procedures, which became the ubiquitous metric of NDE reliability. Forsyth (2018) provides an excellent overview of the practice of assessing NDE performance and provides early references to the first discussions of nondestructive testing reliability dating to 1965 involving the Atomic Energy Commission and motivating subsequent advancement with application to the nuclear power industry. Forsyth also cites the concurrent 1970s initiatives of NASA and the USAF motivated by damage-tolerance philosophies in design and maintenance, where it is assumed that parts contain undetected flaws in their as-manufactured condition that could propagate under operational service conditions. Rummel (2010) and Forsyth (2018) provide the historical context

of NDE reliability assessment state-of-practice when NASA's Standard NDE flaw sizes were developed.

2.1 Review of POD Study Design and Analysis of Bishop (1973), "Nondestructive Evaluation of Fatigue Cracks"

Bishop (1973) was a pioneering POD study that included multiple inspectors from three facilities with the objective of assessing estimate inspector-to-inspector variability in the a90/95 flaw sizes for common NDE methods that included radiographic, ultrasonic, eddy current, and penetrant. This study is the first known reference to propose an approach to estimate the flaw size that a large proportion of inspectors would reliably detect, which would become the Standard NDE flaw size. As will be shown, the first definition of Standard NDE flaw sizes in the SSP OFCP were based on the results of this study, and ultimately, NASA-STD-5009B's flaw size for penetrant and radiography can be directly traced to Bishop (1973).

Rummel et al. (1974) and Anderson et al. (1973) are complementary reports to Bishop (1973) that provide more information on the NDE methods and specimen fabrication. They also contain portions of Bishop's inspection results, some alternative analyses, and inspection data from flaws in different conditions (i.e., as-machined, after-etch, and post-proof loading). In this review, these complementary reports are utilized to provide clarification of Bishop (1973), rather than an in-depth review of all data contained in them.

2.1.1 Bishop Flaw Design, Specimen Preparation, and Execution Protocol

The Bishop POD study featured 420 fatigue cracks in 2219-T87 aluminum alloy specimens presented to 5 to 7 inspectors for each NDE method. The 420 flaws were induced in 164 specimens fabricated by two contractors, summarized in Table 2.1-1, with nominal dimensions of 4 inches wide and 16 inches long in thicknesses (t) of 0.060 inch and 0.210 inch, which are labeled as Thin and Thick. Each specimen contained multiple fatigue cracks, with some specimens having fatigue cracks on both sides, summarized in Table 2.1-2. All of the flaws in this study were open surface, partly through cracks (PTCs). Bishop reports that "The location and occurrence of the flaws were carefully selected to eliminate any pattern effect which may have been detected by the inspectors." Details on the specimen fabrication are provided in Rummel et al. (1974) and Anderson et al. (1973). Contrary to current NDE best practices, there were no blank (unflawed) specimens included in this POD study, and therefore the probability of a false call could not be estimated.

The study included flaws of varying aspect ratios, and the practice of inducing the specified crack sizes from starter notches in the specimens was reported to require significant development effort. Bending and tension-tension loading were utilized, and in some cases sequential combinations of bending and tension-tension were employed to induce fatigue cracks in the specimens. From an interview with Ward Rummel, a lead engineer in this study, it was reported that the bending mode was employed to grow longer cracks, while tension-tension was used to grow deeper cracks. Bending cracks tended to produce more open cracks and were sometimes finished by tension-tension loading to close the cracks more tightly. Conversely, cracks grown in tension-tension may be tightly closed, and some may have been finished using a bending mode to open the cracks. The specific loads and cycles to produce the specimens were not documented. The challenges in producing consistent crack specimens is relevant to the interpretation of the POD results in that some cracks may have been more detectable based on the manner in which they were induced. For

example, more open cracks are likely more detectable by methods (e.g., penetrant and radiography).

Table 2.1-1. Total Number of Specimens and Induced Flaws from Bishop (1973) Table 1.

	Size	Number of Specimens	Number of Flaws	Specimen Numbers
Convair	Thin Thick	24 24 48	57 59 116	A001 through A024 B001 through B024
Martin Marietta	Thin Thick	55 61 116	141 163 304	C001 through C055 C056 through C060, C062 through C089, C091 through C118*
Total	Thin Thick	79 85 164	198 222 420	*Specimen numbers C061 and C090 were not received from Martin Marietta

Table 2.1-2. Incidence of Flaws from Bishop (1973) Table 2.

Number of Flaws	Martin Marietta		Convair (flawed one side only)
	Side A	Side B	
0	22	73	8
1	22	25	10
2	34	14	6
3	23	1	8
4	8	1	10
5	1	0	6
6	6	2	0

After the cracks were grown and the specimens were machined to final size, they were chemically etched at two levels of material removal by the two fabricators. Rummel et al. (1974) reports that about 75% of Bishop's specimens were chemically milled to remove 0.002 inch of material thickness, while Anderson et al. (1973) reports an etching rate and time of exposure that suggest a material removal of about 0.0008 inch thickness for the other 25% of the cracks. Rummel reports with respect to the 0.002-inch etched specimens that "Many of the cracks were visible on close visual inspection after chemical milling." It was a significant finding of this review that all of the inspection data published in Bishop's POD study were conducted on etched cracks, and therefore the estimated detectable flaw sizes for some methods may not be representative of inspections on as-machined (un-etched) condition. While the requirement for etching was known for penetrant, Rummel et al. (1974) indicates that etching improved the performance of other methods (e.g., eddy current). Of particular interest, the performance of radiographic inspections were greatly enhanced by etching.

The flaw length (2c) and depth (a) were measured by specimen destructive analysis after the inspections were completed. From the measured flaw length and depth, the projected elliptical face area of the flaw (i.e., a thumbnail crack shape) and the flaw depth to specimen thickness ratio were computed. The detectable flaw size for radiography was reported as the ratio of flaw depth-to-thickness (a/t) of specimen, and the detectable flaw size for eddy current was reported as a function of flaw depth. For penetrant and ultrasonic, the detectable flaw sizes were reported as a function

of crack face area. It is noted that flaw length is now the most common parameter typically for penetrant POD analysis. Bishop's rationale for using face area was:

> "For penetrant inspection, flaw detection is dependent on the visibility of the fluorescence against the test specimen background. The brightness of the indication is the controlling factor and is proportional to the amount of fluorescent material absorbed by the developer. Although the proper flaw parameter for penetrant would appear to be crack volume, crack area was used in this study because the actual crack width information was not available. Since the crack volume equals the crack area times a factor (crack opening), crack area best approximates crack volume for this study."

It is important to note that the inability to measure crack opening width drove Bishop's choice of flaw parameterization in the analysis, and there was not an explicit assumption that detection capability depends on the flaw area. In subsequent usage of Bishop's results, there was an extrapolation that cracks of equivalent area are equally detectable. However, that was not the original motivation. Furthermore, no POD study has been discovered that supports this general assumption of detectability based on equivalent area.

While varying crack aspect ratios were included in Bishop's dataset, the reported detectable flaw sizes were not reported as a function of aspect ratio. Furthermore, it will be shown that the distribution of flaw sizes does not support modelling the detectable flaw size as a function of aspect ratio. Figure 2.1-1 shows the flaw length versus depth, and Figure 2.1-2 shows the flaw depth-to-thickness ratio versus specimen thickness.

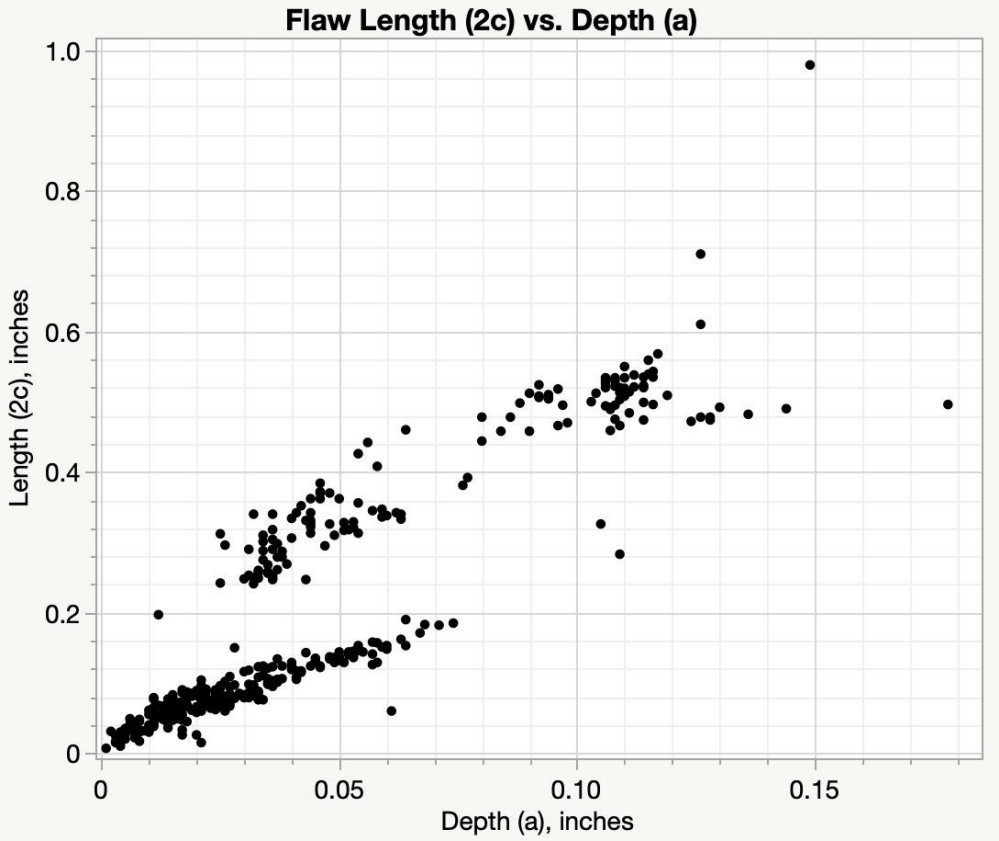

Figure 2.1-1. Flaw length versus depth in Bishop (1973) study.

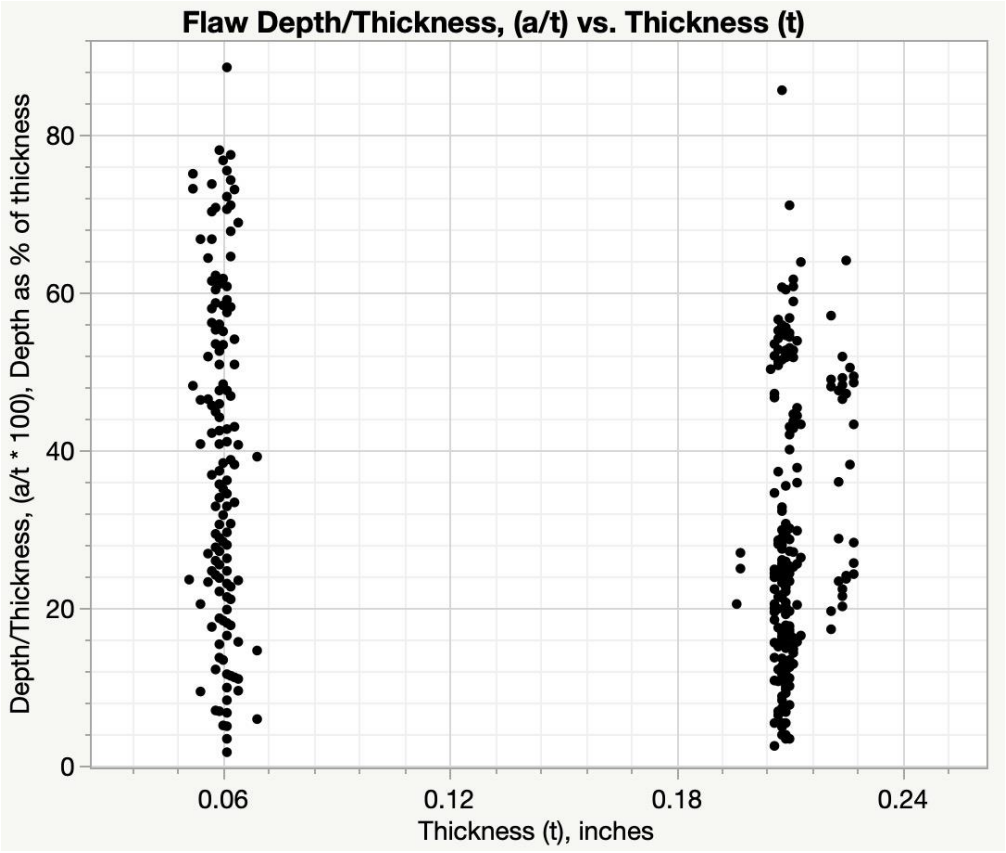

Figure 2.1-2. Flaw a/t ratio versus specimen thickness in Bishop (1973) study.

In Bishop's study, the inspectors for a given NDE method were presented with all of the flaws. Each inspector reported a flaw was present (i.e., a hit), or that a flaw was not present (i.e., a miss). Recall, there were no blank (unflawed) specimens included, and therefore if an inspector does not detect the flaw, it is a miss rather than a true negative of no flaw being present. The inspectors were alphabetically labeled in the reported data, and they were not associated with their respective facility. There were 5 inspectors for ultrasonic and eddy current methods, and 7 inspectors for radiographic and penetrant. The complete dataset was transcribed from Bishop's report, and it is contained in Appendix A.

Spencer (2020) inferred the inspector-to-facility affiliation for the eddy current inspections and was able to describe differences in the eddy current inspection methods at the three facilities. Two facilities employed an automated scanning and recording of the eddy current signal, which was compared to a threshold value to call a hit or miss, and the third was manually scanned and the inspector's hit or miss call was recorded. In Section 1.3 (Spencer (2020)), potential anomalies in the dataset due to manual recording are discussed. Based on this finding, Spencer suggests that it may be more appropriate to refer to facility-to-facility variability, which could include variability associated with different equipment and inspection procedures, rather than inspector-to-inspector variability, which tends to attribute the source of variability to human factors only. In the analysis and conclusions section, Bishop recognizes the significant variability among inspectors, who were referred to as "operators":

> "A great amount of operator dependence is indicated in the results by large value of estimated deviations (*among individual inspector detection capability*). The large deviations take into account the fact that many variables exist."
>
> "Operator variability appears to be one of the most significant factors in establishing flaw sensitivity limits."

However, there was not an acknowledgement that differences in facilities involving different implementations of the same method may be significant. There are important implications for the design of Standard NDE POD studies, specifically whether it is appropriate to stipulate the details of a method's implementation, or whether to allow each facility to utilize their own process. Furthermore, the influence of different implementations may violate the assumptions that all inspectors are drawn from a single population. In the remainder of this review, inspector-to-inspector variability will be used since it is more common terminology. However, it is acknowledged that it may encompass more sources of variability in addition to human variability. The affiliation of inspectors to facilities for the other NDE methods in Bishop's study has not been documented in the literature.

Inspection data for all methods were recorded as hit/miss, even though some methods produced signal responses (e.g., eddy current and ultrasonic). Additionally, for signal-based methods, the determination of the threshold signal level to indicate a hit appeared rudimentary compared to current methods that are typically based on the probability of false calls, which are methods not in broad usage at the time of Bishop's study.

2.1.2 Summary of Bishop Flaw Design, Specimen Preparation, and Execution Protocol

The following is a summary of key findings relevant to the lineage of NASA's Standard NDE flaw sizes.

- Involved open surface, PTCs
- A range of flaw aspect ratios were included
- All fatigue cracks were etched before inspection for all methods
- No blank (i.e., unflawed) specimens were included to estimate the false call rate
- NDE method implementation varied from facility-to-facility for some methods
- Hit/miss responses were recorded and analyzed for all methods, even if signal-based
- Magnetic particle was not included in this study, due to aluminum specimens

2.1.3 Review of Bishop POD Analysis Methodology

Bishop's approach to estimating the expected detection capability for a large proportion of inspectors involved two stages, where the first is to estimate each individual inspector's 90/95 detection capability (i.e., a90/95 flaw size). This individual POD analysis approach was based on a binomial distribution that assumes the probability of detecting a flaw increases with flaw size (i.e., larger flaws are more probable to detect than smaller ones). Conceptually, Bishop's approach is similar to the point estimate method (PEM) referenced in NASA-STD-5009B and commonly used in NASA Special NDE demonstration. NASA's implementation of PEM was derived from Rummel (1982). In a typical PEM approach, 29 flaws of the same nominal size are presented to an inspector, with a number of blank (unflawed) specimens, and the inspector must find all 29 flaws to demonstrate they possess at least 90% POD of that flaw size with 95% statistical

confidence. If the inspector misses a flaw, the demonstration can be expanded to consider 45 detections from 46 flaw inspections, where 45/46 detections demonstrate at least 90% POD with 95% confidence. PEM is conceptually the same method as devised by Bishop. However, a range of flaw sizes were included in the study, rather than a single nominal flaw size in a PEM demonstration. Bishop called the analysis approach the "sorted group ascent method" (SGAM), which is described as:

> "The sorted group ascent method was devised in order to determine a subset of flaws, characterized by a flaw size, which met set values of test confidence and probability of detection. Starting at the bottom of a sorted list, the largest consecutive subset is determined which meets the … size requirement for the number of misses encountered. The smallest value of the sorted flaw size completely contained with this subset characterizes the subset and can be reasonably called the flaw sensitivity limit."

Similar to the PEM, the number of misses from the number of inspections had to meet a specified threshold to demonstrate at least 90% POD with 95% confidence. However, the flaw sizes within the Bishop group of inspections were widely variable. For example, in the analysis of one eddy current inspector, the flaw depth with the subset ranged from 0.017 inch to 0.178 inch in depth. By including a range of flaw sizes, it violates the assumption that the detectability of all flaws within a subset have the same POD. Furthermore, Spencer (2020), in regard to the eddy current example, states that "This technique *(SGAM)* is not conservative and ignores the detection rates immediately surrounding the minimum flaw size in the group, which is said to be the 90/95 flaw size."

Salkowski (1995) discusses the motivation for employing the SGAM and its technical faults, as:

> "As was typical for the time, Rockwell based its statistical analysis on the binomial distribution. The binomial approach assumes that the POD for all cracks of a given size is constant. In order to obtain a reasonable confidence bound on the POD it is necessary to have a large sample of equal size cracks. Since the test panels contained only a few cracks at any given size, Rockwell was forced to increase the effective sample size by grouping together cracks of different sizes. Since different cracks cannot logically have the same POD, grouping violates the necessary assumption that the POD is constant. While the lower confidence bound derived from grouped cracks is technically not valid, it was the only method available at the time."

While this criticism of the analysis was published in 1995, there were no revised analyses of Bishop's dataset discovered during this NESC literature review.

The SGAM analysis was reproduced as a part of this NESC review to evaluate its performance and additional technical issues with the methodology were discovered regarding non-unique flaw size solutions that satisfied the algorithm, and there was no explanation of how those cases were resolved in Bishop's data analysis section. Of more concern, Bishop reported that extrapolation was required to report the detectable flaw size when the specified number of hits out of a number of trials to provide 90/95 detection capability were not achieved. However, the details of how that extrapolation was conducted were not documented and could not be fully reproduced. It is notable that extrapolation was required for 9 of 24 individual inspector analyses, and for the Radiographic method, extrapolation was required for 6 of 7 inspectors. In the independent reproduction of SGAM for radiographic inspectors, three of the inspector's a90/95 flaw sizes represented 90% POD with 50% confidence or less, and two inspectors were below 20% confidence. The need to

extrapolate reflects on a weakness of the SGAM approach, and the sufficiency of the flaw size distribution to define the transition from an inspector's probability of non-detection-to-detection as a function of flaw sizes (i.e., POD curve transition region).

While SGAM appears crude compared to analysis approaches in MIL-HBDK-1823A (2009), Bishop's analysis represented significant advancement compared to the state-of-the-practice in 1973 based on a cursory review of uncited NDE literature. SGAM was subsequently refined by others, including Rummel et al. (1974) to create smaller subgroups of flaws with less variable flaw sizes (i.e., the "moving average approach") that better conforms to the constant flaw size assumption of the PEM method. In less than 10 years after Bishop's report, these binomial point estimate methods began to be replaced by the generalized linear model regression approaches, where the most common is logistic regression, originally proposed by Berens and Hovey (1981).

As a note, Bishop reported flaw sizes for 95% POD and 90% POD, both with 95% statistical confidence. At the time of Bishop's report, 90% POD with 95% confidence had not been agreed upon as the standard for reporting detection capability. Bishop offers the following discussion regarding a95/95 and a90/95. However, there is not a definitive recommendation as to which detection limit should be used in practice.

> "An evaluation of the 0.90/95% and 0.95/95% limits for the data of this study are shown… It is logical to think in terms of 95% test confidence and 95% operator confidence because these figures represent the two-sigma limit, a commonly used value for process control and other quality control statistics. The probability-of-detection value should be selected near the bend in the top part of the S-curve. The larger the value at which the fraction can be chosen, the more reliable the inspection process will be and the more confidence the inspection will generate."

For the remainder of this report, only a90/95 is discussed, since it is the requirement in NASA-STD-5019A Fracture Control Requirements, and it is the intended basis of NASA-STD-5009B Standard NDE flaw sizes.

The second step in estimating the flaw size that a large proportion of inspectors are expected to detect involves computing the average and standard deviation across the individual inspector a90/95 flaw sizes. Using these statistical quantities, a Student's t-distribution was employed to estimate a 95% coverage over the group of inspectors. The objective of this calculation was to estimate a flaw size that a large portion of all qualified and certified inspectors performing field inspections would reliably find, inferred from the small sample of inspectors contained in this particular POD study. Bishop makes the following claim regarding the representativeness of the individual inspector capabilities.

> "Because the operators, techniques, or grouping is randomly selected, homogeneous, and representative of the larger population, this flaw sensitivity limit becomes a measure of flaw sensitivity for the larger population."

As discussed, differences among implementation practices at different facilities using different equipment (e.g., for manual and automatic eddy current inspection techniques) seems to not support this strong statistical assumption of a homogenous sample. If the implementation of specific NDE methods is a significant contributor to the variability, then it could violate this assumption of a representative, random sample. This non-homogeneity could lead to increased variability attributed to inspectors, resulting in an overly conservative estimate of the detectable

flaw size by a large proportion of inspectors. The definition of the representative population is an important and consequential choice in the design of a Standard POD study, as discussed in NASA/TM–20220013822(2022).

Bishop's summary of reported flaw sizes are provided in Figure 2.1-3. The reported area of 0.0096 in^2 for penetrant is a result of the miscalculation of the square root of 152.3E-08 on page 40 of Bishop's report. It appears that the square root of 152.3E-07 was mistakenly taken. Using Bishop's algorithm with the corrected square root results in a penetrant area of 0.0040 in^2 as the 0.90/95%/95% flaw size. This miscalculation ultimately becomes inadvertently favorable based on the NESC's independent analysis of Bishop's data, as will be discussed in Section 2.1.5.

VI. CONCLUSIONS

Within the limitations of this study, crack detection sensitivities have been derived for the four nondestructive testing techniques. Fatigue cracks greater in size than the detection levels shown below can be maintained at the appropriate probability of detection (or greater) with 95-percent confidence.

All Operators (95% Confidence)

	0.90	0.95
X-radiography (crack-depth-to-material-thickness ratio)	70%	77%
Fluorescent penetrant (crack area)	0.0096 $in.^2$	0.012 $in.^2$
Ultrasonics (crack area)	0.0071 $in.^2$	0.018 $in.^2$
Eddy current (crack depth)	0.038 in.	0.046 in.

The fact that X-radiography was by far the least sensitive of the techniques examined came as no surprise, since radiography alone is not generally used for detection of fatigue cracks.

Operator variability appears to be one of the most significant factors in establishing flaw sensitivity limits. It can be shown that under certain conditions (best operator), the flaw sensitivity limits are much smaller than those which generally occur (all operators).

Best Operator

	0.90	0.95
X-radiography (crack-depth-to-material-thickness ratio)	53%	61%
Fluorescent penetrant (crack area)	0.0002 $in.^2$	0.0002 $in.^2$
Ultrasonics (crack area)	0.0002 $in.^2$	0.0002 $in.^2$
Eddy current (crack depth)	0.010 in.	0.019 in.

The 0.0002-square-inch area limit is the lower limit of the available data in this study. A larger population of smaller crack sizes than were available would be necessary to reflect a detection-level change between the 0.90 and 0.95 probability of detection.

Figure 2.1-3. Bishop (1973) reported 90/95 flaw sizes for radiographic, penetrant, ultrasonic, and Eddy current for all operators and best operator.

Regardless of the various weaknesses that have been cited throughout this review of Bishop's analysis, this study is commended for its pioneering contribution of proposing an approach to quantitatively estimate a flaw size that would be detectable by a large proportion of inspectors based on a representative sample of inspectors. Bishop's original explanation of how this quantity is to be interpreted is shown in Figure 2.1-4. The reported 0.90/95%/95% is the basis of what ultimately became referred to as the Standard NDE flaw size in NASA-STD-5009B.

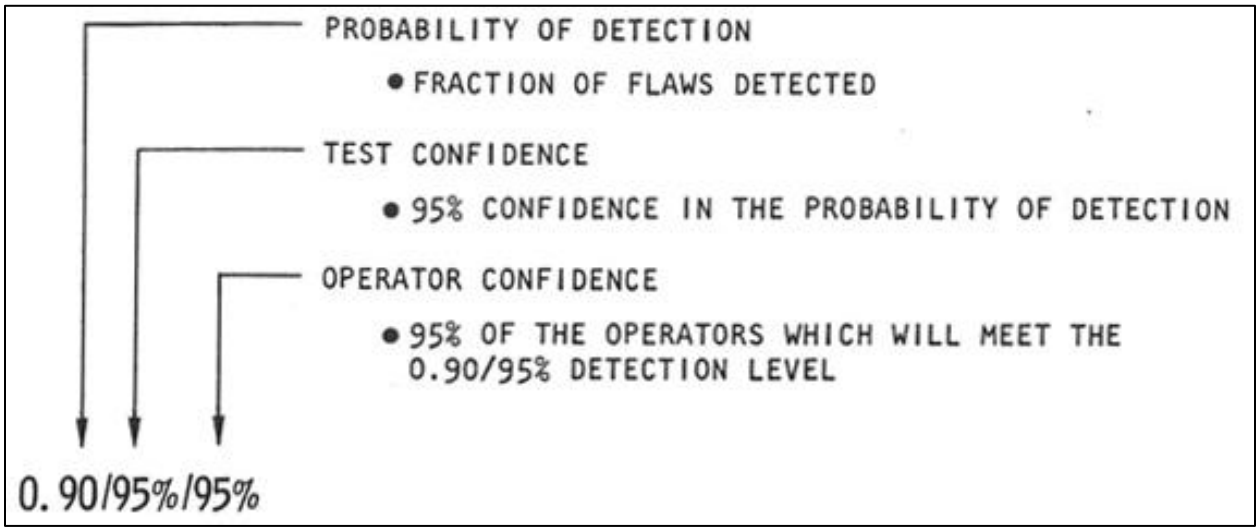

Figure 2.1-4. Interpretation of the 0.90/95%/95% flaw size from Bishop (1973) Figure 20.

2.1.4 Summary of Bishop Analysis Methodology

The following is a summary of key findings relevant to the lineage of NASA Standard NDE flaw sizes and suggested lessons learned for future Standard NDE POD studies.

- SGAM used in Bishop (1973) is conceptually similar to the binomial PEM. However, grouping of flaws with vastly ranging sizes violates the assumption of constant POD within a subgroup of flaws that are the same nominal size.
- A miscalculated square root was discovered in the estimate of a90/95/95 for penetrant that results in a larger detectable area than would have been reported using Bishop analysis methodology.
- Claims of a representative sample of inspectors could be challenged, and they have important implications in the estimated Standard NDE flaw size and future Standard NDE study designs.

2.1.5 NESC Independent Analyses of Bishop's dataset

In this section, independent analyses of Bishop's dataset using current POD analysis methods contained in MIL-HDBK-1823A are presented. As a preamble to this analysis, it is acknowledged that the relevance of the Bishop dataset has been criticized based on advancements in NDE methods over the past 50 years, and whether they represent current detection capability. While some methods (e.g., eddy current and ultrasonic) have experienced technological advancements, others (e.g., penetrant) may not have substantially progressed, and therefore the dataset remains relevant. It is even more difficult to speculate on whether inspector-to-inspector variability has been reduced based on additional training and qualification requirements enacted since 1973.

However, there are few comparable datasets that comprehensively study variation in multiple inspectors at multiple facilities, with the exception of Lewis et al. (1978) that conducted a broad study of inspector capability for the USAF "Have Cracks, Will Travel" database. Considering these caveats, the primary purpose of these independent analyses is to trace the lineage of NASA-STD-5009B Standard NDE flaw sizes and their statistically defensible basis.

Spencer (2020) provides an independent analysis of eddy current method, which discovered the non-conservative nature of Bishop's SGAM. Furthermore, Spencer found indications of misses for reasons independent of flaw size, and speculated "There is a good chance that a step in the inspection procedure (including the recording and control of inspection forms) led to either a "non-inspection" or a non-reporting of the inspection." To address this scenario of hits or misses independent of flaw size, Spencer explored more complex statistical models that included upper and lower asymptotes in the POD curve. As exemplified by this detailed investigation of the eddy current data, other undocumented anomalies may exist in the dataset, which have not been investigated, nor could be sufficiently since the study was conducted 50 years ago.

Spencer (2020) presented a technique to estimate the Standard NDE flaw sizes that involves the estimation of the a90 flaw size from each inspector, considering the coverage probability with a specified confidence interval. Spencer argues that this is a more statistically rigorous approach in considering that the a90 value represents an individual inspector's capability, not a a90/95. While this discussion of theoretical concepts can appear confusing, even to a statistician, there are important implications in the practical implementation of this approach since it was found to be overly conservative for a small number of inspectors (i.e., 5) included for eddy current in Bishop's study. More discussion on analysis approaches to infer the flaw size detectable from a large proportion of the population of inspectors is contained in NASA/TM–20220013822 (2022).

In 2022, the NESC conducted independent analyses of the data for all four NDE methods adopting Bishop's flaw parameterizations of a/t for radiography, flaw face area for penetrant and ultrasonic, and flaw depth for eddy current. The POD modeling relied on generalized linear model regression, as per MIL-HDBK-1823A, and consistently used a probit link function. In the modeling, there was no transformation applied to the radiographic flaw size (a/t), a natural logarithm transformation of the flaw area was applied for penetrant and ultrasonic, and a natural logarithm of flaw depth was utilized for eddy current. As a note, this common practice of applying a log transformation of flaw size would have had no effect on the SGAM used by Bishop since that method does employ the flaw size directly. Following the same two-step process of Bishop, individual inspector average and standard deviation of a90/95 flaw sizes were computed. A statistical tolerance interval for 95% coverage with 50% confidence was used to estimate the a90/95/95 flaw size, which differs from the Student's t-distribution used by Bishop. Use of this distribution generally produces a more conservative estimate of a90/95/95, especially for a small number of inspectors.

There were no individual inspector responses or flaws removed from Bishop's dataset in this analysis, regardless of whether they appeared anomalous. It was decided that without first-hand knowledge of the study a consistent rationale could not be developed to exclude individual inspections or specimens. However, an engineering judgement was made to remove two individual inspectors when estimating the a90/95/95 flaw size, since they produced considerably larger detectable flaw sizes relative to the group of inspectors. Inspectors L for penetrant and V for eddy current were found to have an unacceptably strong influence on the estimated a90/95/95 flaw size and were removed. It is interesting to note that both of these inspectors required extrapolation in Bishop's SGAM. Tables 2.1-3 through 2.1-6 provide the results of individual inspector capabilities

published by Bishop and independently modeled by the NESC. Inspectors L and V are shown grayed out to indicate that they were not used in the estimation of a90/95/95 flaw size.

Table 2.1-3. Radiography Detectable Flaw Sizes

Radiography		**Individual-Inspector a90/95**		
Depth/Thickness, a/t	**Inspector**	**Bishop (1973)**	**NESC (2022)**	
	A	53	59	%
	B	64	66	%
	C	66	67	%
	D	59	70	%
	E	65	79	%
	F	60	77	%
	G	58	74	%
Inspector Average a90/95		61	70	%
Standard NDE a90/95/95		**70**	**83**	%

Table 2.1-4. Penetrant Detectable Flaw Sizes

Penetrant		**Individual-Inspector a90/95**		
Projected Area	**Inspector**	**Bishop (1973)**	**NESC (2022)**	
	H	0.0002	0.0024	in^2
	I	0.0013	0.0035	in^2
	J	0.0015	0.0070	in^2
	K	0.0002	0.0019	in^2
	L	0.0030	0.0717	in^2
	M	0.0003	0.0027	in^2
	N	0.0034	0.0078	in^2
Inspector Average a90/95		0.0014	0.0042	in^2
Reported Standard NDE a90/95/95		0.0096	**0.0087**	in^2
Corrected Standard NDE a90/95/95		**0.0040**		in^2

Table 2.1-5. Ultrasonic Detectable Flaw Sizes

Ultrasonic		**Individual-Inspector a90/95**		
Projected Area	**Inspector**	**Bishop (1973)**	**NESC (2022)**	
	O	0.0030	0.0156	in^2
	P	0.0002	0.0009	in^2
	Q	0.0057	0.0111	in^2
	R	0.0020	0.0088	in^2
	S	0.0003	0.0029	in^2
Inspector Average a90/95		0.0022	0.0079	in^2
Standard NDE a90/95/95		**0.0071**	**0.0185**	in^2

Table 2.1-6. Eddy Current Detectable Flaw Sizes

Eddy Current		**Individual-Inspector a90/95**		
Depth, a	**Inspector**	**Bishop (1973)**	**NESC (2022)**	
	T	0.017	0.032	in
	U	0.010	0.019	in
	V	0.032	0.070	in
	W	0.023	0.049	in
	X	0.021	0.037	in
Inspector Average a90/95		0.021	0.034	in
Standard NDE a90/95/95		**0.038**	**0.057**	in

By inspection of Tables 2.1-3 through 2.1-6, Bishop's individual inspector a90/95 estimates are generally non-conservative compared to applying a MIL-HDBK-1823A approach. This result is not surprising based on the earlier discussion of Bishop's SGAM, and it is influenced by the distribution of flaw sizes relative to each method in the study. It follows that Bishop's a90/95/95s are generally non-conservative, with the exception of penetrant based on a flaw surface area miscalculation. The fortuitous nature of this miscalculated square root for penetrant resulted in a 0.0096 in^2 flaw area that is in agreement with this independent analysis result of 0.0087 in^2 where using Bishop's approach with a corrected calculation results in a smaller detectable area of 0.0040 in^2.

A review of the flaw size design (i.e., distribution of flaw) was conducted to evaluate its quality for estimating the individual inspector a90/95 flaw size for each method. Conceptually, it is desired to have some flaws that are consistently missed below the a90/95 flaw size and flaws that are consistently found (i.e., hit) above the a90 flaw size. The region of overlap between almost always misses and almost always hits is important in the POD modeling using generalized linear model regression, which is referred to as the transition region. However, an excessive number of misses indicates that there are too many small flaws included in the study that are not informative, and an excessive number of hits above the a90 flaw sizes indicates that there are too many large flaws. Beyond the practical implications of an excessive number of either too small or too large flaws,

there are diminishing benefits for the statistical model estimation. Unnecessary flaw production cost and diminishing statistical benefits can be thought of as a measure of inefficiency of the flaw design in estimating a90/95 flaw size, as discussed in the NASA/TM–20220013822 (2022). Figures 2.1-5 through 2.1-8 illustrate the calls made by every inspector plotted versus their respective flaw parameter, where individual inspectors are not distinguished in these plots. Vertical reference lines for the average inspector performance are shown using Bishop's SGAM, and the NESC's MIL-HDBK-1823A method. All plots illustrate the uniformly non-conservative results of Bishop's a90/95/95 flaw sizes.

For radiography, there appears to be an excessive number of small flaws and a deficiency of larger flaws approaching a through crack (TC) (i.e., 100% penetration) to support a better estimate of the a90/95 flaw size. For penetrant, ultrasonic, and eddy current there appears to be adequate overlap of misses and hits in the transition region. However, there appears to be too many large flaws that provide little statistical benefit to the a90/95 estimate. It is assumed that Bishop's flaw size design was chosen to cover all four methods and the flaws were inspected for every method to simplify the study logistics. This action simplified the flaw production of a single set of flaws, inspection protocols that did not require a subset of flaws to be inspected by a specific method, and the consistent analyses across methods. Furthermore, there may not have been reliable estimates of the a90 flaw size for each method prior to this study that would have informed a more strategic flaw size specification.

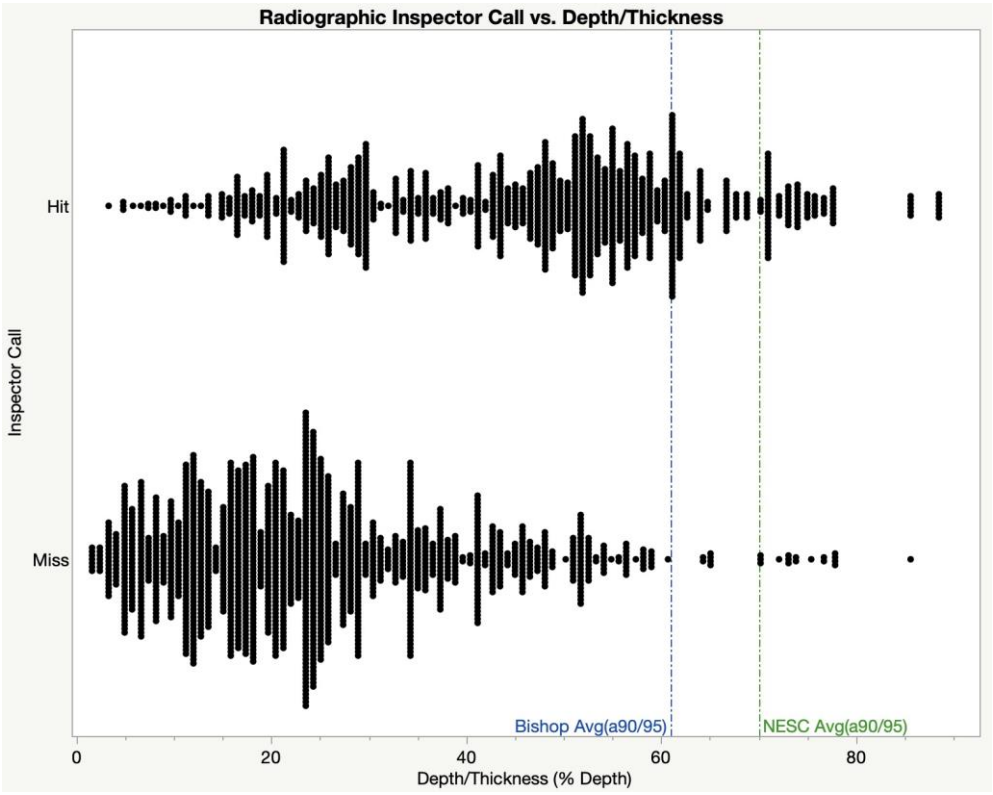

Figure 2.1-5. Radiography inspector calls versus depth/thickness (% depth) with estimated a90/95 by Bishop and the NESC.

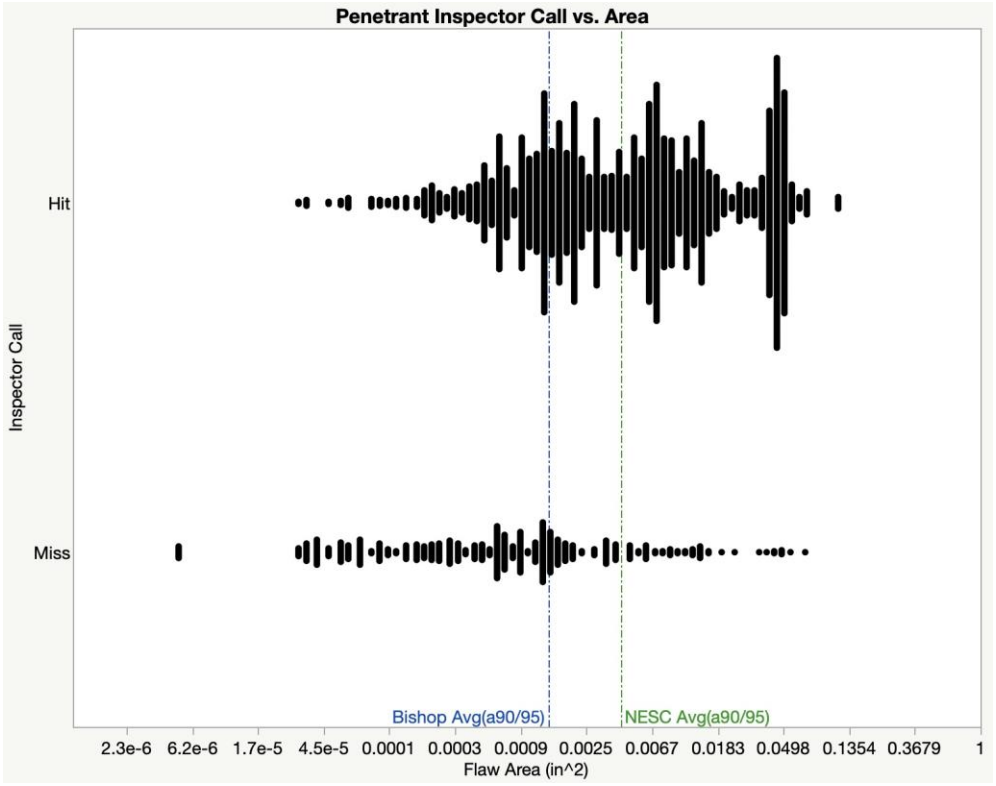

Figure 2.1-6. Penetrant inspector calls versus flaw area with estimated a90/95 by Bishop and the NESC.

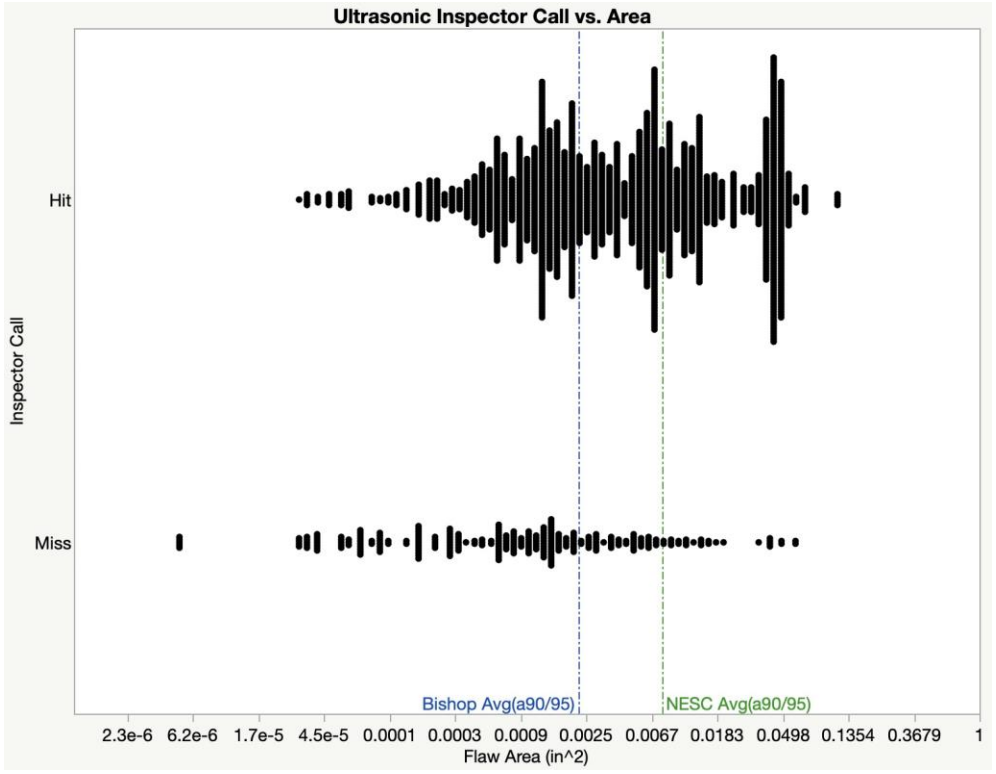

Figure 2.1-7. Ultrasonic inspector calls versus flaw area with estimated a90/95 by Bishop and the

NESC.

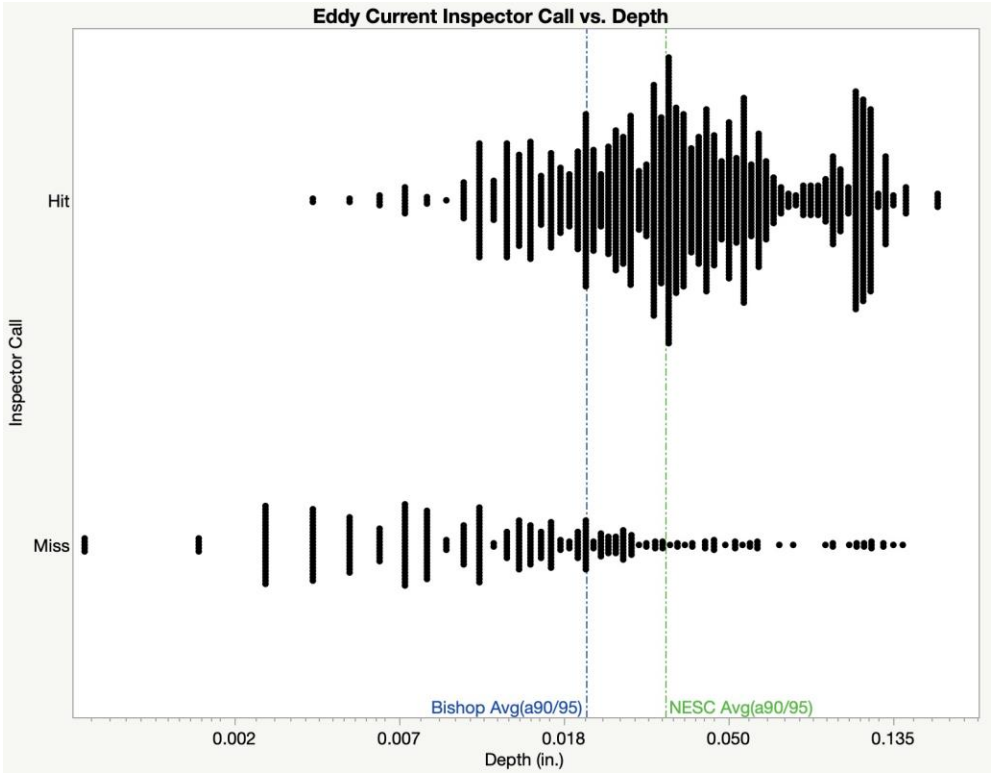

Figure 2.1-8. Eddy current inspector calls versus flaw depth with estimated a90/95 by Bishop and the NESC.

Bishop combines all of the cracks with different aspect ratios to estimate each inspector's a90/95 flaw size, while the Standard NDE flaw sizes in NASA-STD-5009B are provided at different aspect ratios. In Bishop's approach, the a90/95 flaw sizes are independent of aspect ratio, and the analysis essentially produces an average a90/95 over different aspect ratios. Therefore, an exploration of Bishop's dataset was conducted to determine if an aspect ratio effect could be found. Stated as a question for penetrant, "Does an inspector's a90/95 flaw area depend on aspect ratio?" For penetrant in NASA-STD-5009B, the elliptical flaw area for a 0.075-inch-deep by 0.150-inch-long flaw (i.e., aspect ratio of 2) is 0.0088 in^2, while the flaw area for a 0.025-inch-deep by 0.250-inch-long flaw (i.e., aspect ratio of 10) is 0.0049 in^2. This implies that there is better detection capability of longer, shallower flaws compared to shorter, deeper flaws. The following analysis of Bishop's dataset seeks to determine if it supports this assertion.

The most straightforward analytical approach to explore the influence of aspect ratio is to augment the POD model with an additional flaw characteristic. Therefore, additive and two-factor interaction terms of aspect ratio were included in the model. The natural log of area was used, consistent with the NESC modeling, and aspect ratio was explored as untransformed and log transformed. The modeling results, not presented, show that neither the additive nor two-factor interaction terms involving aspect ratio were statistically significant. This analysis shows that the Bishop dataset does not support the different flaw area at an aspect ratio of 10 in NASA-STD-5009B. A further exploration of the flaw size distribution in the study to support this model was performed since a number of flaws ranging in area at different aspect ratios would need to be present to support the modeling, regardless of inspector responses.

To further investigate the potential effect of aspect ratio, the distribution of flaw area was partitioned into two groups that are above and below an aspect ratio of 5. There are 272 flaws with an aspect ratio of less than 5 and 148 flaws with an aspect ratio ≥ 5. Figure 2.1-9 shows a histogram of flaw area within each aspect ratio group, and it includes a vertical reference line for the estimated inspector average a90/95 from the NESC analysis. The y-axis denotes the number of flaws in each of the histogram bins of the 420 total flaws in the study. The histogram shows that at a lower aspect ratio (i.e., < 5) there are many smaller flaws below the average a90/95, but there is a gap of flaws sizes in the neighborhood of the a90/95 flaw size. At this lower aspect ratio, there are fewer larger flaws. Conversely, for the higher aspect ratio (i.e., > 5) there are many flaws in the vicinity of the average a90/95 flaw size and larger, but there are fewer smaller flaws. Figure 2.1-9 reveals the limitations of the flaw size design in this study for evaluating the influence of aspect ratio on penetrant or ultrasonic detection capability, since they were both modeled as a function or area.

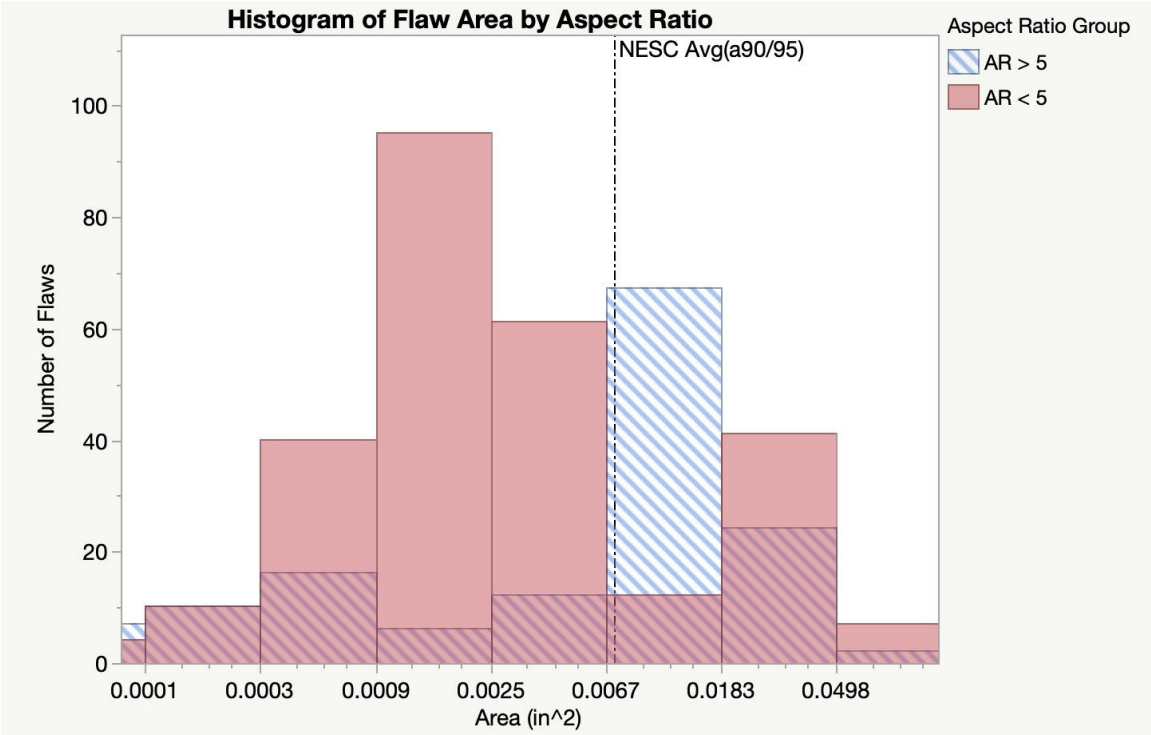

Figure 2.1-9. Histogram of flaw area for aspect ratio above and below 5.

Bishop's analysis of eddy current as a function of depth was also published as being independent of aspect ratio. However, in NASA-STD-5009B, the Standard NDE flaw depth is presented as 0.050 inch at an aspect ratio of 2, and 0.020 inch at an aspect ratio of 10. This implies that shallower-depth flaws are more detectable at a higher aspect ratio compared to low aspect ratio flaws. To investigate whether this assertion is supported in Bishop's dataset, aspect ratio terms were added to the primary flaw parameter of depth in eddy current POD models. For eddy current, there are indications that flaw depth detection capability has some dependence on aspect ratio based on the modeling approach chosen for specific inspectors. The details and results of this modeling were deemed beyond the scope of this review. However, using a logistic model, with a log transform of depth, no transformation of aspect ratio, and focusing on inspectors T and U as being qualitatively representative of the best detection capability, shows significant aspect ratio effects. Table 2.1-7 summarizes estimated a90/95 values from the NESC analysis as a function of

depth as presented in Table 2.1-6, with the estimated a90/95 flaw sizes for an aspect ratio of 2 and 10 predicted by a POD model that includes aspect ratio terms.

Table 2.1-7. Eddy Current Detectable Depth as a Function of Aspect Ratio

		Individual-Inspector a90/95		
Eddy Current		*Depth Only*	*Depth and Aspect Ratio*	
Depth, a	**Inspector**	**NESC (2022)**	**2c/a = 2**	**2c/a = 10**
	T	0.032	0.069	0.014
	U	0.019	0.037	0.011

Table 2.1-7 tends to support the assertion that shallower depths are detectable for higher aspect ratio flaws compared to low aspect ratio flaws for eddy current. However, what appears to be an aspect ratio effect may indicate that the method is more sensitive to crack length. For inspector T, the crack length (2c) would be essentially equal for the two different aspect ratios, while it is ~30% longer for the shallower crack for inspector U. This analysis illustrates that modeling POD as a function of depth, as suggested by Bishop, results in an average a90/95 depth over the aspect ratios contained in this study, since it falls between the depths at the two aspect ratios. The results of this cursory analysis may warrant further investigation into the effects of aspect ratio effect on detectability.

2.1.6 Summary of NESC Independent Analyses of Bishop's dataset

The following is a summary of key findings from independent analyses of Bishop's dataset:

- Bishop's SGAM produced uniformly non-conservative individual inspector a90/95 flaw sizes compared to MIL-HDBK-1823A methods.
- The individual inspector estimate non-conservatism directly translates to non-conservative 0.90/95%/95% (i.e., Standard NDE) flaw sizes for radiographic, ultrasonic, and eddy current.
- For penetrant, the miscalculated square root inadvertently resulted in an estimate of a90/95/95 flaw area that correlates with the NESC independent analysis. Using the corrected square root for penetrant supports that Bishop's 0.90/95%/95% flaw sizes are uniformly non-conservative for all methods.
- Flaw size distribution was assumed to be chosen to cover the NDE methods. However, it was not tailored for estimating a90/95 for individual methods.
- Bishop's flaw size distribution does not support estimation of detection capability as a function of flaw aspect ratio for penetrant and ultrasonic. This finding does not support the smaller detectable area at an aspect ratio of 10 published as the Standard NDE flaw sizes in NASA-STD-5009B.
- For eddy current, there is cursory evidence of an aspect ratio effect on the detectable depth, with shallower depths being more detectable at higher aspect ratios. This trend is consistent with the Standard NDE flaw depths published in NASA-STD-5009B.

2.2 Review of Orbiter Fracture Control Plan (OFCP) (1974)

The SSP OFCP, King and Johnson (1974), documents the engineering design and quality assurance plan "to design components that provide structural integrity in the presence of

undetected flaws," and that "assurance shall be maintained with minimum impact to weight and cost." The objective was "to establish those criteria, procedures, and controls necessary to prevent orbiter structural failures due to the presence of defects and flaws, assumed to be present in all fabricated metal products." The four main elements of the plan were engineering structural design, engineering structural analysis, engineering materials and process, and quality assurance. The primary objective of the quality assurance element was "to institute procedures required to ascertain maintenance of material properties and to provide non-destructive evaluation techniques adequate to detect flaws of the size identified in the predictive analysis."

This report is primarily addressed to the engineering fracture analysis community to provide initial flaw sizes that "shall be used in analysis and shall be representative of NDE capabilities." This intended audience is evidenced by the lack of NDE method details and POD analysis discussion. An important finding is that there are no POD studies explicitly referenced in the SSP OFCP Revision A. However, Bishop references the original version of the OFCP, not found in this review. It appears that Bishop's POD study and the OFCP were developed concurrently by Rockwell International Space Division, and their linkage may have been commonly known at the time and explicitly cross-referencing could have been overlooked. Throughout the NESC review, it became increasingly apparent that Bishop's POD study was the primary, if not the sole, source for the OFCP.

The SSP OFCP is the first reference to introduce and define the terminology of "Standard Flaws", which is the heritage of the Standard NDE in NASA-STD-5009, as quoted in the following excerpt:

> "The analyst shall assume for the purpose of crack growth analysis using standard NDE (as cited in Figure 1), that standard NDE will detect surface flaws having lengths in excess of 0.150 inch and depths in excess of 0.075 inch except that the curve for standard NDE in Figure 2 shall be utilized for other length and depth combinations."

The SSP OFCP's Figure 1 refers to a flow chart that begins with the completion of the part normal static and fatigue analysis, and if the part's structural failure is deemed to cause loss of vehicle, then the part life is computed using the flaw size limits of Standard NDE. If that life analysis shows in excess of 4 lifetimes, then the Standard NDE flaw size limits are considered sufficient. If less than 4 lifetimes are predicted or if it is a pressure vessel, then Special NDE flaw limits are used in the fracture analysis. For Special NDE, inspector demonstration statistical analysis to support 90/95 detection capability was required in the OFCP.

The 0.150-inch-long by 0.075-inch-deep flaw reported as the Standard NDE flaw size has a projected elliptical area of 0.0088 in^2, which is comparable to the reported a90/95/95 flaw area of 0.0096 in^2 for penetrant reported in Bishop (1973), that includes a miscalculation. Note that penetrant is not explicitly associated with this standard flaw size in the OFCP definition, but additional references and analyses discussed later support that it was based on penetrant. The supposed rounding-down of Bishop's reported flaw area is conjectured to report nominal dimensions for flaw length and depth. The flaw area is nearly equal to the NESC independently estimated a90/95/95 flaw area of 0.0087 in^2 for penetrant based on Bishop's dataset, and therefore, this flaw area represents a statistically based estimate of the a90/95/95 detection capability of penetrant and is published in NASA-STD-5009B.

The SSP OFCP's Figure 2 referenced in the definition of Standard NDE is reproduced in Figure 2.2-1. It defines an upper bounded region of flaw sizes for Standard NDE, and a lower bounded region for Special NDE. There are lines from the origin denoting constant flaw aspect ratio. When

the OFCP was written, aspect ratio was defined as crack depth over length (a/2c); however, the modern convention is crack length over depth (2c/a). In the subsequent sections, the modern convention of 2c/a is used consistently in the discussion and parenthetical clarifications are added when referring to a historical figure or table that uses a/2c. Unless specifically noted, aspect ratio indicates 2c/a.

The depth and length limits are noted for Standard and Special NDE boundaries. As expected, the standard flaw size of 0.150 inch long by 0.075 inch deep occurs at the intersection of the aspect ratio of 2 line (a/2c = 0.5) and the Standard NDE boundary drawn on the figure. This penetrant detectable area from Bishop anchors the Standard NDE boundary. Salkowski (1995) confirms this finding by stating that "The standard curve was based on the 90/95 flaw sensitivity limit for penetrant and on a review of the inspection data for low aspect ratio cracks." For clarification, Salkowski's terminology of "90/95 flaw sensitivity limit" is understood to refer to the a90/95/95 flaw area reported by Bishop. The reference to low aspect ratio refers to the historical a/2c = 0.1, which is a high aspect ratio of 2c/a = 10, the "review" mentioned by Salkowski is discussed in a subsequent paragraph.

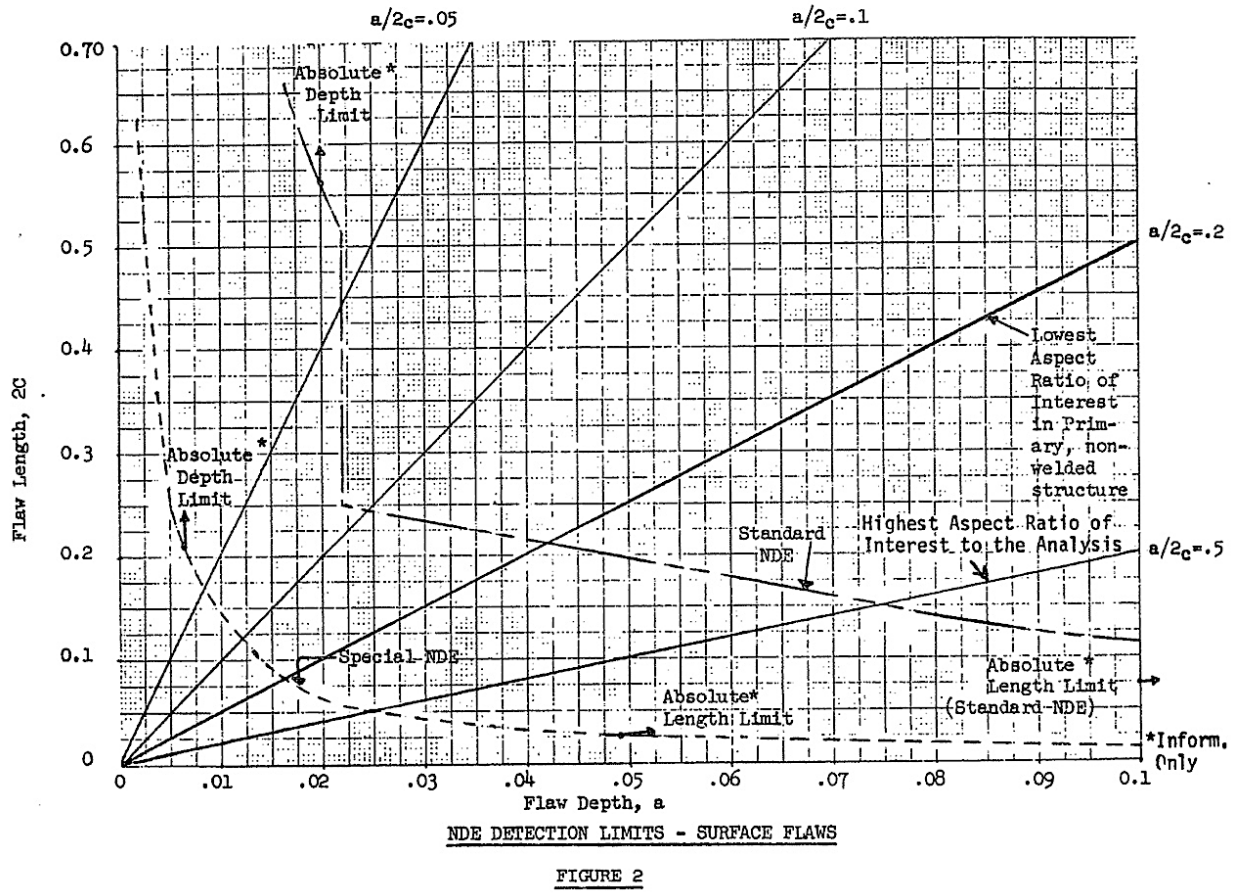

Figure 2.2-1. NDE detection limits of surface flaws from the OFCP[1]

For flaw depths exceeding 0.075 inch deep (i.e., to the right of the anchoring point at a/2c = 0.5), the boundary is defined by curve of constant area, and a slight curvature in the boundary line can

[1] Aspect ratio in OFCP was defined as depth/length, a/2c

be seen from careful inspection. For flaw depths shallower than 0.075 inch deep (i.e., to the left of the anchor point) there is a straight-line boundary through a point that intersects the aspect ratio of 10 line (a/2c = 0.1) near the coordinate of a flaw size of 0.250 inch long by 0.025 inch deep. Note this is the Standard NDE flaw size published in NASA-STD-5009B for penetrant at an aspect ratio of 10. This flaw size deviates from Bishop's reported a90/95/95 detectable area with a smaller area of 0.0049 in^2, and was shown to be unsupported by Bishop's original analysis or the NESC independent analysis. The SSP OFCP provides no rationale for the selection of this flaw size that establishes the straight-line boundary of Standard NDE. However, Salkowski (1995) refers to "…a review of the inspection data for low aspect ratio cracks" in the vicinity of an aspect ratio of 10 and provides the following additional clarification.

> "An angular bulge was included in the standard curve to take advantage of the high percentage of low[2] aspect ratio cracks that were detected."

The description of how this point was chosen was independently confirmed by interviews with the personnel involved when the SSP OFCP was created. Salkowski offers an augmented version of the OFCP's "Figure 2" with markers that indicate the flaw sizes from Bishop's study, which is reproduced in Figure 2.2-2.

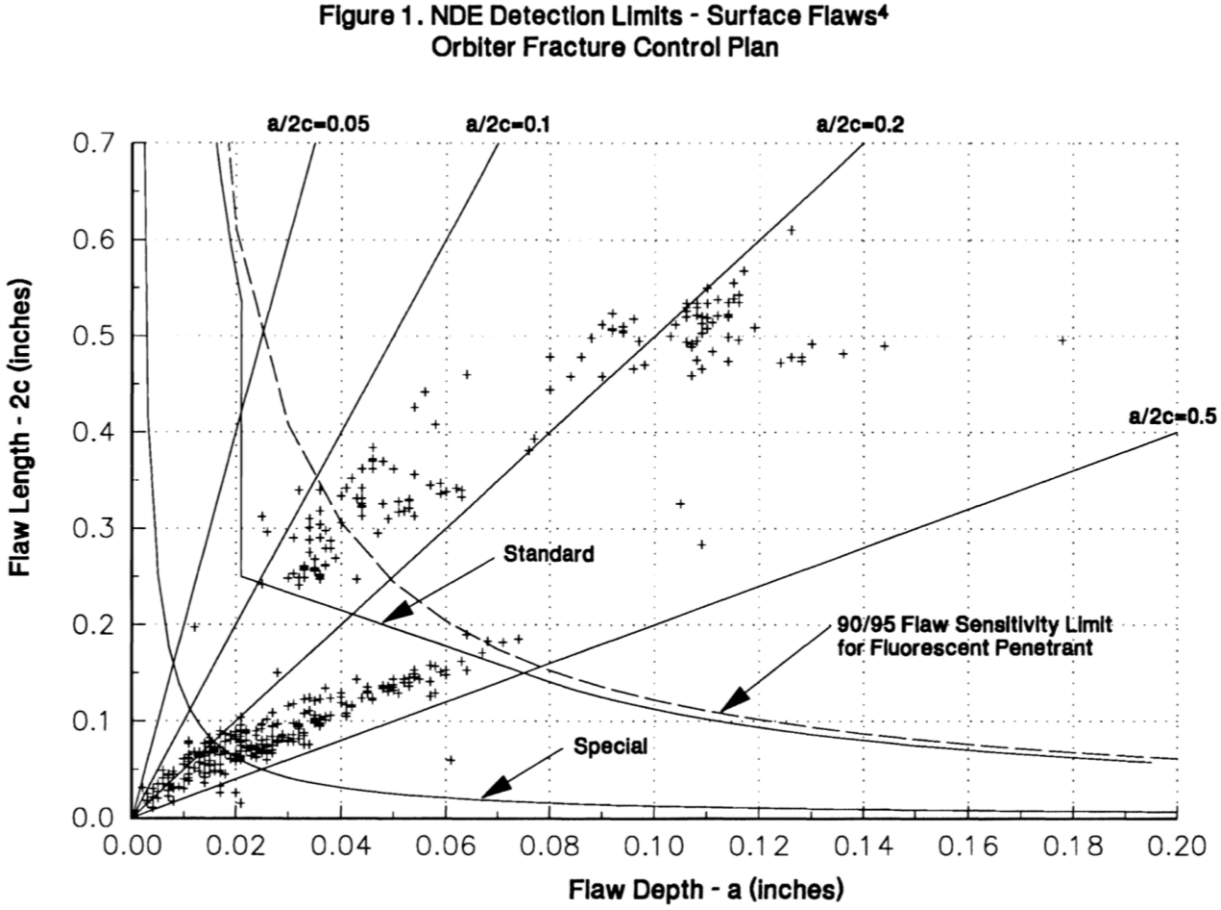

Figure 2.2-2. Reproduction of OFCP with markers representing the flaws in Bishop (1973).

[2] Historical reference to low aspect ratio is a/2c.

Further augmenting Salkowski's figure, Figure 2.2-3 includes more informative markers that indicate penetrant inspector hits and misses. Recall that each flaw is inspected once by each of the 7 penetrant inspectors. A dot marker with no surrounding square indicates that all 7 inspectors detected the flaw (i.e., all hit responses), a square without an inscribed dot indicates that none of the 7 inspectors detected the flaw, and a dot with a square indicates that there was a mixture of hits and misses among the inspectors for that flaw. A "pocket" of hits can be observed below the equivalent area curve, to the right of aspect ratio of 10 line, and above the Standard NDE boundary. In this "pocket" there were 33 unique flaws that resulted in 230 hits and 1 miss across the 7 penetrant inspector responses. This extremely high percentage of detections motivated the "angular bulge" that deviates from the equivalent area curve defined by Bishop's reported a90/95/95 flaw area, which is shown with a curved dotted line. While the rationale of considering this concentration of hits is intuitive, it tends to ignore the presence of misses for larger area flaws where square markers are present. This qualitatively chosen flaw size of 0.250 inch long by 0.025 inch deep was used to anchor the left side of the straight-line portion of the Standard NDE boundary, and is the penetrant flaw size published in NASA-STD-5009B for penetrant at an aspect ratio of 10.

It is acknowledged that this "pocket" of concentrated hits is intriguing, and it is conjectured that these 33 flaws may have had characteristics that made them more detectable with penetrant inspections. For example, if these flaws had exhibited a wider crack opening due to the manner in which there were induced, then the crack volume would be increased and the width of the penetrant indication would be more prevalent, both of which would increase their detection probability. Based on the discussion in Section 2.1.1, this is plausible since some flaws were induced by bending that tended to produce longer more open flaws at shallower depths. Regrettably, a more thorough investigation of this specific group of flaws was not possible for this review since they were destructively analyzed.

To left of the 0.250 inch long by 0.025 inch deep an absolute depth limit is depicted with a vertical line at about 0.022 inch deep, which is a value approximately read from the original plot in the OFCP. The report provides no discussion of the absolute depth limits shown in Figure 2.2-1, and no reference was found to support these absolute depth limits. At the location where the vertical line depth limit intersects the equivalent area curve, the Standard NDE boundary is completed for shallower flaws with a curve of constant flaw area.

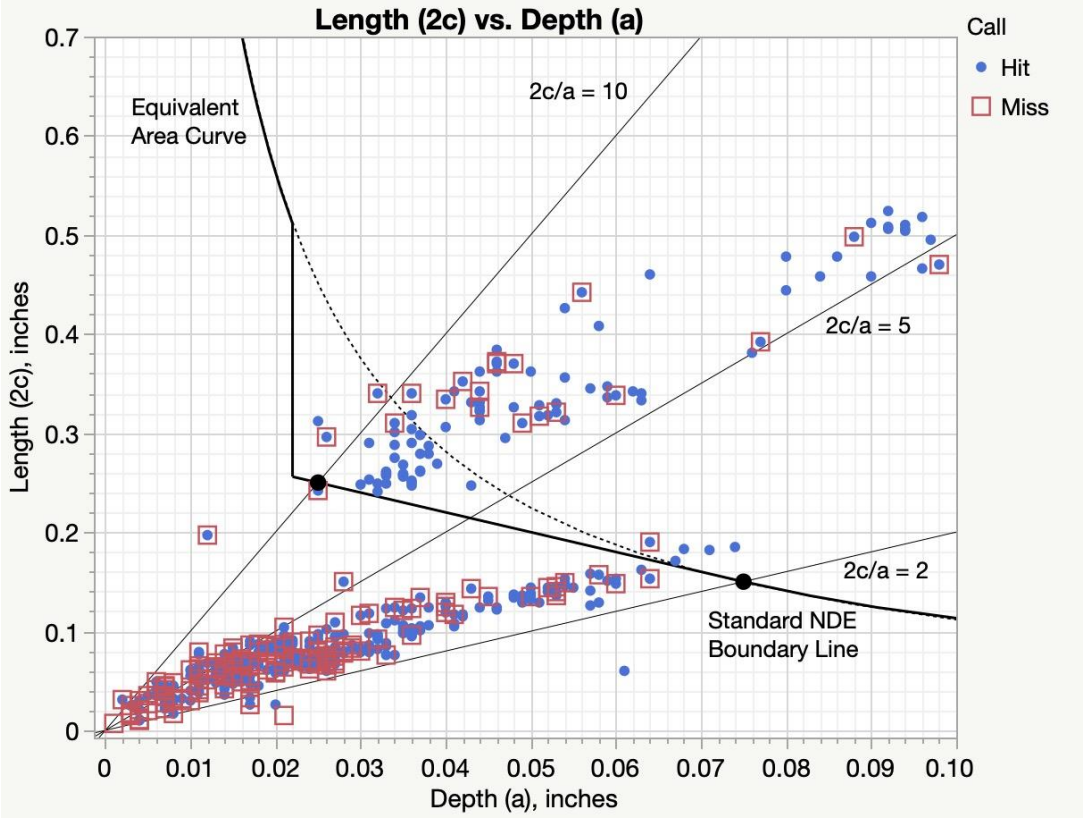

Figure 2.2-3. OFCP diagram with penetrant flaw sizes and detections from Bishop (1973) overlaid.

It is noteworthy that the OFCP's constructed Standard NDE boundary is not claimed to be statistically based nor is it asserted to have a probabilistic interpretation for inspector detection capability or coverage probability of certified inspectors. There is no mention of 0.90/95% detection capability or 95% inspector coverage in the OFCP's discussion of Standard NDE.

Combining information from the multiple sources cited, it appears certain that the Standard NDE boundary in the OFCP's "Figure 2" was based on Bishop's analysis results and qualitative observations of Bishop's dataset to choose the flaw size at an aspect ratio of 10. It is important to note that Bishop's a90/95/95 flaw area for penetrant, derived over a range of flaw aspect ratios, was notionally extended to claim that it represented the detectable flaw size at an aspect ratio of 2. For this to be demonstrated and statistically based, a POD study exclusively containing nominal aspect ratio of 2 flaws is required. Recall, Bishop's a90/95/95 flaw area represents an average over a wide range of aspect ratio flaws, and Bishop's flaw size distribution is limited in evaluating the influence of aspect ratio independently from flaw area. The SSP OFCP interpretation and extension of Bishop's reported flaw area is most likely the heritage of the "equivalent area" assumption, which claims that detection capability is based on flaw area. No other references that substantiate the rationale for the assumption of equivalent area were found. Recall that Bishop used flaw area as a surrogate parameter for crack volume since crack opening width was not measured. However, this did not appear to be intended as directly supporting an equivalent area assumption. Bishop's results are best interpreted as the average detectable flaw size area over a range of aspect ratios.

Standard flaws are discussed for ultrasonic and radiographic methods. For ultrasonic, the OFCP states "Also, the analyst shall assume that standard ultrasonic will reveal hidden flaws in excess of 0.100 inch in diameter (or equivalent)." This specification of this flaw size for ultrasonic detection capability implies that a POD study with embedded flaws was conducted. However, there is no POD study cited nor a reference found during this review to support this flaw size. Recall, Bishop's study consisted of open surface, PTCs, and no embedded flaws were included.

For radiographic inspections, the OFCP states

> "The standard capability for radiography shall be the detection of a crack which has a depth in excess of 70 percent of the material thickness. However, the crack length on the surface of the part shall be assumed to be 0.150 inches or longer in the analysis and the Quality Assurance Function shall require that a surface flaw detection method is utilized in addition to the radiographic technique employed."

Bishop's a90/95/95 flaw size for radiography was 70% (i.e., 0.7t), and while not cited explicitly, it is believed to be the source. The reference or rationale for the minimum flaw length is unknown.

Standard flaw sizes for eddy current and magnetic particle methods are not provided in the SSP OFCP. However, eddy current is discussed subsequently in regard to Special NDE.

The OFCP introduces and distinguishes "Flaws by Special NDE" as:

> "Satisfactory accomplishment of a flaw detection demonstration by the Quality Assurance function of each Orbiter system/subsystem will permit the following flaw sizes to be assumed in the analysis. A 0.90 probability of detection at a 95 percent confidence level statistical base is required in the demonstration. Also, a specific inspection procedure document shall be prepared for each fracture critical component to assure this statistical base."

In contrast to Standard NDE, OFCP's definition of Special NDE is based on demonstration of 0.90/95% detection capability. However, the OFCP does not specifically require inspector demonstration, even though that may be implied and is required in NASA-STD-5009B's implementation of Special NDE. While Special NDE does not suggest a coverage probability over the population of inspectors, it could be inferred that it is referring to individual inspectors. However, the concept of inspector coverage probability is not included in Standard NDE either. The nuances of the OFCP's distinction between Standard NDE as a starting point for engineering fracture analysis, not asserted to be statistical based or requiring demonstration, and Special NDE requiring statistical basis with 0.90/95% demonstration evolved into NASA-STD-5009B's distinction between Standard and Special NDE. In NASA-STD-5009B there is no requirement for inspector demonstration of Standard NDE flaw sizes (i.e., only inspector certification). However, every inspector must demonstrate the 90/95 detection capability for Special NDE.

The SSP OFCP defines the Special NDE flaw size boundary as:

> "When the use of special NDE is required to achieve increased component life (per Figure 1), the analyst may assume that surface flaws will be detected if the surface length is 0.050 inch or greater and the depth into the surface (as applicable) is 0.025 inch or greater. The dimensions are for an aspect ratio of 0.5 (2c/a = 2). The crack front area relationships depicted in Figure 2 shall prevail for other aspect ratios of interest in the analysis, e.g., shallower cracks must be longer on the surface. Dye penetrant methods will be the

predominant method used for surface flaw detection; however, eddy current and ultrasonic techniques can be applied in the detection of surface flaws."

Similar to the SSP OFCP's Standard NDE, the defined Special NDE boundary appears to be based on penetrant since it was the most common method. Special NDE is defined as an increased inspection capability beyond Standard NDE, and the term Special and Standard seem to refer to the process or level of inspection and/or the qualification of the inspector. This differs from the implementation of Special NDE in NASA-STD-5009B, that does not specify a flaw size. Instead, NASA-STD-500B refers to Special NDE more generically as it applies to flaw sizes smaller than Standard NDE or specific component geometry or inspection access conditions. Any influence of the material, component geometry, or inspection access restrictions on detection capability are not mentioned in the OFCP, even though Bishop's study was based on flat aluminum panels. As a final note, while eddy current is mentioned in the OFCP's Special NDE discussion, the OFCP does not provide flaw sizes for eddy current detection capability.

The source for the 0.050-inch-long by 0.025-inch-deep flaw with an elliptical area of 0.00098 in^2 Special NDE flaw size is not cited. Salkowski (1995) provides the following explanation.

"The special curve was based on a review of the inspection data for the best penetrant inspectors. The area of a 0.050- x 0.025-inch semi-circular crack was reportedly chosen because it marked the transition between those cracks which were generally missed and those which were generally detected."

It appears that the best individual reported a90/95 flaw area anchored an equivalent area curve to form the boundary of Special NDE. A qualitative ranking with an analysis of regions in the length by depth diagram of inspector hits and misses was performed. Furthermore, Salkowski reports that flaw area to anchor the Special NDE curve was based on the "best" penetrant inspectors. From Bishop's reported individual inspector capability shown in Table 2.1-4, if the individual inspector a90/95 flaw areas are averaged, excluding inspectors L and N since they have larger detectable areas, it produces a flaw area of 0.00070 in^2. This flaw area is close to the 0.00098 in^2 for the OFCP Special NDE flaw size. Therefore, 0.00070 in^2 could be interpreted at the 0.90/95%/50% of the best inspectors, since it represents the 0.90/95% detection capability expected to be exceeded by 50% of the best inspectors.

The OFCP Special NDE flaw size of 0.050-inch-long by 0.025-inch-deep continues to be used for fracture analysis of pressure vessels, including composite overwrap and metallic pressure vessels. While technical issues in Bishop's analysis and the OFCP's qualitative selection of this flaw size have been cited, it has been routinely used in Special NDE by a specialized group of pressure vessel inspectors to successfully demonstrate 0.90/95% detection capability.

The Special NDE flaws for ultrasonic are discussed as:

"Embedded (sub-surface) flaws may be assumed to be detected by ultrasonic if the area of the crack is equivalent to the area of a 3/64 inch diameter flat surface or larger. The ultrasonic testing proficiency required by Quality Assurance shall be a 2/64 inch diameter flat bottom hole in the materials of concern."

Similar to Standard NDE, the ultrasonic flaw type is embedded, and it appears that the detectable flaw area for open surface PTCs from Bishop's study may have been the basis for extrapolating to an embedded flaw. However, the description is insufficient to make this link without significant speculation.

The Special NDE flaws for radiographic inspections are discussed as:

> "Radiographic inspection is a technique routinely applied to the detection of voids and inclusions. The method has limited applicability in the detection of cracks; however, the analyst may assume that radiographic inspection will detect a material separation (crack) which has penetrated more than 60 percent through the thickness of the material. However, the crack length on the surface of the part shall be assumed to be 0.050 inches or longer in the analysis and the Quality Assurance function shall require that surface flaw detection method is utilized in addition to the radiographic techniques employed."

The 60% through thickness penetration is about equal to Bishop's inspector average a90/95 flaw size in Table 2.1-3, and represents the 0.90/95% for 50% of the inspectors. The source for the minimum length of 0.050 inch is not cited. In a similar manner as ultrasonic, the radiographic "void and inclusions" is extrapolated from Bishop's POD study of open surface, partly through, fatigue cracks not embedded flaws. Moreover, the SSP OFCP states that radiographic should not be relied upon for surface flaw detection, which was the sole flaw type in Bishop's POD study.

In addition to Standard and Special NDE, the OFCP discusses "Flaws Screened by Proof Testing" as a viable method for select metallic alloys in primary structure and pressure vessels. It further discusses NDE inspections performed on pressure vessel interiors following proof testing and states the usage of the Special NDE flaw sizes as:

> "It is recognized that accessibility problems can prohibit reasonable determination of the flaws of the size listed under the special NDE section. However, when demonstrated by fracture mechanics methods that flaws at the detection limit of special NDE methods will not enlarge during the proof test, those flaws, when screened by inspection of components prior to assembly (i.e., hemispheres, cylinder sections, etc.) will be acceptable as initial flaw sizes for safe crack growth fracture mechanics analysis of those portions of the structure."

The discussion largely resembles current design and inspection practice of composite overwrap pressure vessels and metallic tanks. The section discusses applications of post-proof inspections for other structural components that includes NDE inspection methods.

Moving from inspection methods and focusing on NDE fracture analysis assumptions, the SSP OFCP offers a section entitled "Flaws Out of Holes" that includes other flaw geometries including in the vicinity of holes and corners as:

> "The analyst shall assume that drilled holes have a 0.100 inch long through cracks (where $t \leq 0.100$) or 0.100 inch corner cracks ($t > 0.100$) emanating from one side of the hole. Establishment of a requirement to ream holes will permit the assumption of the initial flaws no greater than 0.050 inch through cracks ($t \leq 0.050$ inch) or 0.050 inch corner cracks ($t >$ 0.050 inch). The respective flaw sizes for very thick material when the flaw is assumed to be on the surface of the hole shall be 0.100 inch for drilled holes and 0.050 inch for reamed holes, respectively. The installation of driven rivets in standard structure will permit an assumption of an 0.005 inch corner crack out of the rivet holes."

The OFCP "Figures A3 and A4" are shown in Figures 2.2-4 and 2.2-5. These figures and the flaw sizes discussed form the heritage of NASA-STD-5009B Standard NDE flaw sizes for other crack geometries. Conspicuously missing from this discussion is reference to experimental POD demonstrations that involve these other crack geometries to support these flaw sizes, nor is there

a mention of specific NDE methods considered. It appears that these flaw sizes are being reported primarily for engineering analysis and are not representative of detection capability or statistically based.

Figure A3

Initial Crack Geometries –
Parts Without Holes

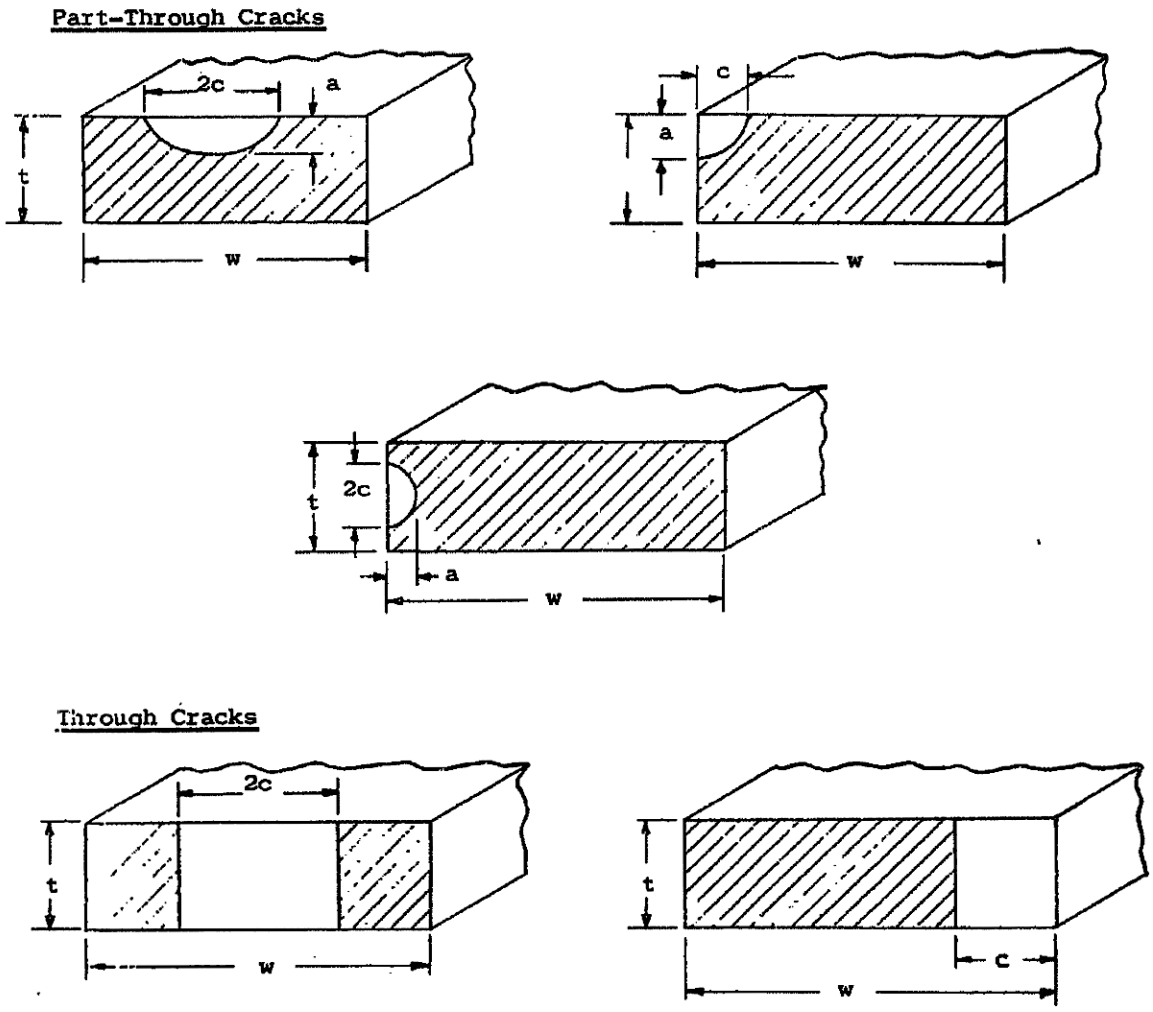

Figure 2.2-4. Initial crack geometries – parts without holes.

Figure A4

Initial Crack Geometries

Parts with Holes

Part-through Cracks

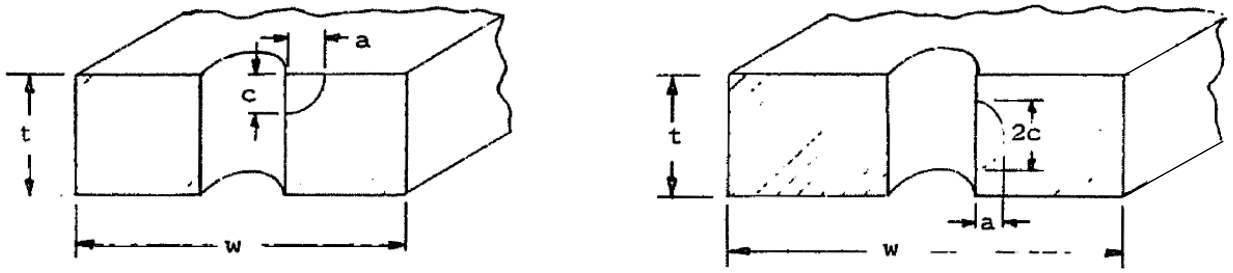

Drilled: $t \geq .10$ in.
$a = c = .10$ in.

Reamed: $t \geq .05$ in.
$a = c = .05$ in.

Through Crack

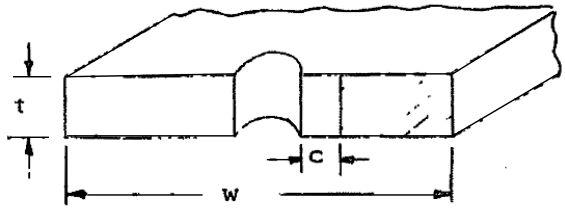

Drilled: $t \geq .10$ in.
$c = .10$ in.

Reamed: $t \geq .05$ in.
$c = .05$ in.

Figure 2.2-5. Initial crack geometries – parts with holes.

As a suitable conclusion to the SSP OFCP review, the final section related to NDE is entitled "Precautions on Assumed Flaw Sizes" that states the guidance:

> "When the analyst assumes a flaw not to exceed the size dictated by the capabilities of a given NDE method, it is the responsibility of the board/team to assure that the method is employed to inspect the part. As an example, weld inspection would require that radiographic and/or ultrasonic methods be used for hidden flaws, since penetrant methods would not detect such flaws. Therefore, a weld analyzed assuming X-ray [radiographic] or ultrasonic method detection limits must be 100 percent radiographically inspected and/or ultrasonic inspected."

This concluding section emphasizes the necessary reliance of coordinated efforts between fracture analysts and NDE engineers, who possess the knowledge of the inspection method and its detection capabilities, to help ensure the predicted performance of fracture critical components.

2.2.1 Summary of the SSP Orbiter Fracture Control Plan (OFCP) (1974)

The SSP OFCP was a seminal document in translating NDE detection capability from Bishop (1973) for use in fracture analysis, and the OFCP guidance remains as the foundation practice 50 years later. The OFCP serves as the twin foundational document, with Bishop (1973), that evolved into NASA-STD-5009B. Furthermore, Salkowski (1995) states that the fracture analysis computer program (i.e., FLAGRO) released in 1986 by NASA "included a set of initial flaw size assumptions derived mainly from the OFCP." In addition, Salkowski reports that "The orbiter payload and space station fracture control documents, released in 1988 and 1991, respectively contain tables of initial flaw size assumptions that are essentially the same as those embedded in FLAGRO." Significant findings from this NESC review are:

- The OFCP introduced and defined Standard and Special NDE concepts and set their flaw size limits.
- Flaw size limits were primarily based on Bishop's inspection dataset and analysis results for penetrant since it was the most common method in practice.
- Standard NDE limits were constructed from an interpretation of Bishop's a90/95/95 flaw size area for penetrant at an aspect ratio of 2, a qualitative adjustment at an aspect ratio of 10 based on an observed concentration of detected flaws, a minimum depth limit, and an equivalent area assumption for smaller and larger flaws that exceed those aspect ratios.
- The constructed Standard NDE boundary is not claimed to be statistically based nor is it asserted to have a probabilistic interpretation for inspector detection capability or coverage over the population of inspectors. However, it is anchored by Bishop's reported a90/95/95 flaw size for penetrant.
- Standard NDE does not consistently apply an equivalent area assumption, which claims that detection capability is based on flaw area only.
- Absolute detection limits are defined without a reference to their source.
- Special NDE limits were constructed from the best inspector a90/95 detectable area at an aspect ratio of 2 and perpetuated the equivalent area assumption.
- Special NDE flaw size of 0.050-inch-long by 0.025-inch-deep remains in common usage for pressure vessel fracture analysis, and it is routinely used in Special NDE demonstrations to have a90/95 capability by pressure vessel inspectors.
- Other crack geometries were introduced and include parts with holes, TCs in an open surface and on an edge, and cracks on corners and edges, all of which are flaws other than open surface PTCs included in Bishop's POD study.
- Guidance for flaw sizes in the vicinity of holes and corners for use in fracture analysis is provided. However, this guidance does not appear to be established on statistically-based demonstration of NDE detection capability of these flaw geometries.
- Flaw size limits for ultrasonic and radiography are discussed for embedded, hidden flaws, which appear to be extrapolations of Bishop's flaw area results from surface cracks.
- Radiographic Standard NDE flaw sizes appear to originate from Bishop's reported a90/95/95 flaw size of 70% (i.e., 0.7t), and radiographic Special NDE came from Bishop's average inspector a90/95 flaw size of 60% (0.6t).
- No Standard or Special NDE flaw sizes for magnetic particle or eddy current are provided in the OFCP.

2.3 Review of MSFC-STD-1249 (1985)

In 1985, MSFC published MSFC-STD-1249 "Standard NDE Guidelines and Requirements for Fracture Control Programs" with the scope of:

> "The standard provides guidelines for selection and prescription of NDE (Nondestructive Evaluation) techniques required to fulfill the demands of a Fracture Control Program. Also provided are the minimum crack-like flaw sizes deemed reliably (90% probability, 95% confidence) detectable via the traditional NDE techniques, Penetrant, Eddy Current, Magnetic Particle, Ultrasonic, and (manual) Radiography, when implemented as prescribed herein."

This document appears to be written by and for NDE engineers based on the details included on specific NDE methods that would not be particularly useful for fracture analysts. In the introduction, MSFC-STD-1249 states the responsibility of NDE in providing reliable estimates of Critical Initial Flaw Size (CIFS) that would not grow to catastrophic-failure size within the number of cyclic exposures dictated for mission assurance. The NDE objective is stated as:

> "NDE then is obligated to assure that the CIFS does not exist in the newly fabricated hardware. The CIFS may prove to be smaller than is reliably detectable by standard "normally," economically practiced NDE; causing special efforts in the form of special attention by the NDE operator/inspector, refinements in inspection material and equipment selection, and refinements in inspection technique/procedure. Occasionally, the CIFS still may be beyond the reliable detectability of implementable NDE, necessitating other considerations such as redesign or periodic reinspection for larger flaws."

Notice that terminology usage of "standard" and "special" refer to inspection practices, rather than flaw sizes or proportions of certified inspectors that would be expected to demonstrate 90/95 detection capability. This terminology is further reinforced in the appendix of MSFC-STD-1249 as "STD – Standard practices" and "SPCL – Special Practices." This is consistent with the OFCP's definition of standard and special, and it is relevant distinction since the term evolved to Standard NDE flaw sizes and Special NDE POD demonstration in NASA-STD-5009B.

The sections of MSFC-STD-1249 provide guidance on the selection of methods for various applications and constraints, at various times during the fabrication and testing of components. As an overarching requirement, it references MIL-STD-410 "Nondestructive Testing Personnel Qualification and Certification", the predecessor of NAS-410 cited in NASA-STD-5009. In addition, it enumerates high-level inspection conditions for each NDE method, which it refers to as "basic assumptions" of effecting factors to formulate levels of detectability. For example, under penetrant, it lists the following:

1. "Unrestricted accessible surface without sharp-root recesses.
2. Roll-formed surface, or machined surface, which was effectively etched to remove smeared masking material.
3. Surface not contaminated with paints, coatings, oils, etc., which would prevent surface wetting or restrict penetrant flow into cracks.
4. Surface finish of 125 root mean squared (RMS) or better quality (roughness, pattern), typical of aerospace hardware.
5. Penetrant family employed certified as meeting the Group VI level of sensitivity."

A similar number of basic assumptions are provided for each method. It is assumed that these are considered best-practice assumptions, but not necessarily derived by experimental POD demonstrations that evaluate these factors. As a specific example, from the discussion in Section 2.1.1 it is accepted that etching influences POD detectability. However, the level of etching for penetrant is not specified in MSFC-STD-1249. Furthermore, there is no mention of etching for radiography, which was performed on the cracks used to evaluate radiographic POD in Bishop's study.

MSFC-STD-1249 is the first reference to tabulate flaw sizes for Standard and Special NDE. Figure 2.3-1 reproduces the tables provided in MSFC-STD-1249 for the included inspection methods. Under "NDE Detectability Assumptions", MSFC-STD-1249 states:

> "Based on NDE technique implementation criteria set forth in Section 3.2, and fundamental assumptions set forth in Section 3.1.2, minimum size crack-like flaws deemed reliably (90% probability / 95% confidence) detectable by NDE techniques have been identified. The compilation presented in Appendix B draws upon various studies and summations previously derived by industry and Government agencies, including guideline documents derived by other NASA Centers."

While "…draws upon various studies and summations previously derived by industry and Government agencies, including guideline documents derived by other NASA Centers" are mentioned, there are no specific references provided in MSFC-STD-1249 to support the flaw sizes contained in these tables. Therefore, the NESC attempted to trace the possible sources of values presented in the tables. As an example, for penetrant, the top region of the table in Figure 2.3-1a provides Standard flaw sizes for open surface TC and PTC for a part thickness of less than and greater than or equal to 0.075 inch at three aspect ratios[3] of 10, 5, 2. For $t \geq 0.075$ inch, PTC, at aspect ratios of 10 and 2, the Standard flaw sizes are reported as 0.250 inch long by 0.025 inch deep, and 0.150 inch long by 0.075 inch deep, respectively. These are the flaw sizes reported in NASA-STD-5009B, and appear to be those that anchor the Standard NDE boundary specified by the SSP OFCP, derived from the POD study in Bishop (1973), even though neither reference is provided in MSFC-STD-1249. The flaw size under these same conditions for an aspect ratio of 5 is 0.200 inch long by 0.040 inch deep, which appears to be interpolated between the $a/2c = 0.1$ and 0.5 aspect ratios on the straight-line boundary in OFCP that suggests a flaw size of 0.215 inch long by 0.043 inch deep.

Standard NDE flaw sizes for $t < 0.075$ inch are the same as $t \geq 0.075$ inch, except at an aspect ratio of 5, which is a longer detectable length. Recall, the thinnest specimens in the Bishop study were 0.060 inch thick, however Bishop's flaw sizes appear to better correlate with $t \geq 0.075$ inch. The rationale for introducing part thickness categories is not provided.

The Special NDE flaw sizes for penetrant in Figure 2.3-1a differs from the OFCP. For example, $t \geq 0.075$ inch, PTC, $a/2c = 0.5$ reports a Special NDE flaw size of 0.075 inch long by 0.038 inch deep, while the OFCP reported a 0.050-inch-long by 0.025-inch-deep flaw. No reference was found to support these Special NDE flaw sizes. However, by inspection it is peculiar that they are exactly half the length of the Standard NDE for most entries, which may simply explain their derivation.

[3] MSFC-STD-1249 defines aspect ratio as depth/length, and lists $a/2c = 0.1, 0.2, 0.5$.

In the middle section of Figure 2.3-1a, the table includes flaw sizes for other crack geometries (e.g., “Surface Edges, and Around Drilled or Reamed Holes”), and it provides similar figures describing these geometries as OFCP for parts without and with holes. The flaw sizes and category ranges are similar to the SSP OFCP discussion. However, a confident one-to-one mapping rationale could be inferred. Overall, as with the OFCP, the source of these flaw sizes for other crack geometries is unknown.

In Figure 2.3-1b and 2.3-1c, standard flaw sizes for radiography are provided at 0.7t or 70% depth of penetration flaw, which is most likely the a90/95/95 flaw size reported by Bishop and cited in the SSP OFCP. For Special radiography, 0.6t is reported, which is most likely the inspector average a90/95 reported by Bishop and cited in the OFCP.

It is speculated that the flaw sizes for eddy current and ultrasonic are based on Bishop (1973), but references that mention analysis of POD data were not found, and NESC efforts to reproduce those table entries were unsuccessful.

Overall, the references and/or rationale for the majority of the entries in the MSFC-STD-1249 table are not cited and remain unknown. While the philosophy of the Standard and Special NDE were adopted from the OFCP, there are few table entries that can be directly traced to the OFCP. As will be shown, the Standard NDE flaws sizes reported in MSFC-STD-1249 are nearly identical to what appears in NASA-STD-5009B Table 1.

Initial Flaw Size (Minimum) Detectability Assumptions
for Structures and Pressure Vessels

Area	NDE Method	Part Thickness	Crack Type	Aspect Ratio (a/2c)	Crack Depth	Crack Length
Open Surface	PT-STD	t<0.075	TC		t	0.200
			PTC	0.1		0.250
				0.2		0.200
				0.5	(0.075 max.)	0.175
		t≥0.075	TC		t	0.150
			PTC	0.1		0.250
				0.2		0.200
				0.5		0.150
	PT-SPCL	t<0.075	TC		t	0.100
			PTC	0.1		0.125
				0.2		0.100
				0.5		0.100
		t≥0.075	TC		t	0.075
			PTC	0.1		0.125
				0.2		0.100
				0.5		0.075
Surface Edges, and Around Drilled or Reamed Holes	PT-STD	t<0.075	TC		t	0.100
			CC		t	0.125
		t≥0.075	TC		t	0.100
			CC		0.075	0.100
	PT-SPCL	t<0.075	TC		t	0.075
			CC		t	0.075
		t≥0.075	TC		t	0.075
			CC		0.075	0.075
Open Surface	ET-STD	t≥0.020	TC		t	0.100
			PTC	0.1		0.100
				0.2		0.100
				0.5		0.100
	ET-SPCL	t≥0.020	TC		t	0.050
			PTC	0.1		0.075
				0.2		0.050
				0.5		0.050
						Appendix B

a) For penetrant and eddy current.

Initial Flaw Size (Minimum) Detectability Assumptions
for Structures and Pressure Vessels

Area	NDE Method	Part Thickness	Crack Type	Aspect Ratio (a/2c)	Crack Depth	Crack Length
Surface Edges, and Around Drilled or Reamed Holes	ET-STD	t≥0.020	TC CC		t 0.020	0.050 0.050
	ET-SPCL	t≥0.020	TC CC		t 0.020	0.025 0.025
Open Surface	MT-STD	t≥0.070	TC PTC	 0.1 0.2 0.5	t	0.250 0.375 0.275 0.250
	MT-SPCL	t≥0.070	TC PTC	 0.1 0.2 0.5	t	0.150 0.225 0.175 0.150
Surface Edges, and Around Drilled or Reamed Holes	MT-STD	t≥0.070	TC CC		t 0.070	0.250 0.250
	MT-SPCL	t≥0.070	TC CC		t 0.070	0.150 0.150
Raw Stock, and Machined Product	UT-STD (L-Wave)	t≥0.300	Embedded or PTC, TC, CC	Class B Class A	0.200 dia. (Equiv. Area) 0.130 dia. (Equiv. Area)	
	UT-SPCL (L-Wave)	t≥0.200	Embedded or PTC, TC, CC	Class AA	0.080 dia. (Equiv. Area)	
	UT-STD (S-Wave)	t≥0.300	Embedded or PTC, TC, CC	Class B Class A	0.200 dia. (Equiv. Area) 0.130 dia. (Equiv. Area)	
	UT-SPCL (S-Wave)	t≥0.150	Embedded or PTC, TC, CC	Class AA	0.080 dia. (Equiv. Area)	
Raw Stock, and Machined Product	RT-STD	t≥0.050	Embedded PTC, TC, CC	Ellipse 1/2 Ellipse	0.7t 0.7t	t (0.150 min.) t (0.150 min.)
	RT-STD	t<0.050	Embedded	Ellipse	0.7t (0.025 min.)	0.150
			PTC, TC, CC	1/2 Ellipse	0.7t (0.025 min.)	0.150

b) For eddy current, ultrasonic, and radiographic.

Initial Flaw Size (Minimum) Detectability Assumptions
for Structures and Pressure Vessels

Area	NDE Method	Part Thickness	Crack Type	Aspect Ratio (a/2c)	Crack Depth	Crack Length
Raw Stock, and Machined Product	RT-SPCL	t≥0.050	Embedded	Ellipse	0.6t	t (0.100 min.)
			PTC, TC, CC	1/2 Ellipse	0.6t	t (0.100 min.)
	RT-SPCL	t<0.050	Embedded	Ellipse	0.6t (0.025 min.)	0.100
			PTC, TC, CC	1/2 Ellipse	0.6t (0.025 min.)	0.100

c) For radiographic.

Figure 2.3-1. Initial flaw size (minimum) detectability assumptions for structures and pressure vessels.

2.3.1 Summary of MSFC-STD-1249 (1985)

The significance of MSFC-STD-1249 is that it presents the first tabulation of Standard and Special NDE flaws sizes for the methods of penetrant, eddy current, ultrasonic, radiographic, and magnetic particle for multiple specimen thicknesses, and flaw aspect ratios and geometries. These tabulated values are almost identical to NASA-STD-500B, as will be discussed in the next section. MSFC-STD-1249's influence beyond NASA is evidenced by its citation in the Air Force Structures Bulletin: In-Service Inspection Crack Size Assumptions for Metallic Structures (EN-SB-08-012, Revision D (2018)). While a few table entries in MSFC-STD-1249 indicate a linkage to the SSP OFCP, derived from Bishop (1973), regrettably, the source of most entries in the table was not identified. The following list highlights contributions of MSFC-STD-1249.

- Penetrant:
  - Tabulated Standard NDE flaw sizes for open surface, PTC at aspect ratios of 2, 5, and 10, and introduced a part thickness restriction for $t < 0.075$ inch and $t \geq 0.075$ inch.
    - Adopted SSP OFCP's flaw sizes for $2c/a = 2$ and 10, and $2c/a = 5$ was derived from the OFCP boundary, not adhering to equivalent area.
- Penetrant:
  - Tabulated Standard NDE flaw sizes for open surface, TC with a part thickness restriction for $t < 0.075$ inch and $t \geq 0.075$ inch.
  - Tabulated Standard NDE flaw sizes for TCs and corner cracks for surface edges and around drilled and reamed holes with a part thickness restriction for $t < 0.075$ inch and $t \geq 0.075$ inch.
- Eddy Current:
  - Tabulated Standard NDE flaw sizes for open surface, PTC at aspect ratios of 2, 5, and 10, and introduced a part thickness restriction $t \geq 0.020$ inch.
  - Tabulated Standard NDE flaw sizes for open surface, TC with a part thickness restriction $t \geq 0.020$ inch.

    - Tabulated Standard NDE flaw sizes for TCs and corner cracks for surface edges and around drilled and reamed holes with a part thickness restriction $t \geq 0.020$ inch.
- Magnetic Particle:
    - Tabulated Standard NDE flaw sizes for open surface, PTC at aspect ratios of 2, 5, and 10, and introduced a part thickness restriction $t \geq 0.070$ inch.
    - Tabulated Standard NDE flaw sizes for open surface, TC with a part thickness restriction $t \geq 0.070$ inch.
- Ultrasonic (L-Wave):
    - Tabulated Standard NDE flaw sizes for embedded, open surface, PTC, TC, corner flaw diameter with a part thickness restriction $t \geq 0.300$ inch at Class B and A, or equivalent area.
- Ultrasonic (S-Wave):
    - Tabulated Standard NDE flaw sizes for embedded, open surface, PTC, TC, corner flaw diameter with a part thickness restriction $t \geq 0.300$ inch at Class B and A, or equivalent area.
- Radiographic:
    - Tabulated Standard NDE flaw sizes for embedded, open surface, part through, through, corner crack, ellipse and ½ ellipse with a part thickness restriction of $t \geq 0.050$ inch and $t < 0.050$ inch for Raw Stock and Machined Product.
        - Adopted SSP OFCP's 0.7t and a minimum crack length of 0.150 inch.

2.4 Review of NASA-STD-5009 (2008)

NASA-STD-5009B serves as the Agency standard for fracture critical human spaceflight systems. The initial release of NASA-STD-5009 was published in 2008, and the latest version, NASA-STD-5009B, was published in 2019. The broad scope, significance, and lineage of NASA-STD-5009B is articulated in the Forward, provided in the excerpt:

> "This NASA Technical Standard is published by the National Aeronautics and Space Administration (NASA) to provide uniform engineering and technical requirements for processes, procedures, practices, and methods that have been endorsed as standard for NASA programs and projects, including requirements for selection, application, and design criteria of an item.
>
> NASA-STD-5009B supersedes NASA-STD-5009A, Nondestructive Evaluation Requirements for Fracture Critical Metallic Components, and MSFC-STD-1249, Standard NDE Guidelines and Requirements for Fracture Control Programs.
>
> This NASA Technical Standard is approved for use by NASA Headquarters and NASA Centers and Facilities, and applicable technical requirements may be cited in contract, program, and other Agency documents. It may also apply to the Jet Propulsion Laboratory (a Federally Funded Research and Development Center (FFRDC)), other contractors, recipients of grants and cooperative agreements, and parties to other agreements only to the extent specified or referenced in applicable contracts, grants, or agreements.
>
> This NASA Technical Standard establishes the nondestructive evaluation (NDE) requirements for any NASA system or component, flight or ground, where fracture control is a requirement. This NASA Technical Standard specifically defines requirements for

nondestructive evaluation in support of NASA-STD-5019A, Fracture Control Requirements for Spaceflight Hardware."

The breadth and impact of this important standard warranted the comprehensive review presented herein that has focused specifically on the Standard NDE flaw sizes contained in NASA-STD-5009B and routinely in the majority of spaceflight fracture analysis. As seen in the forward section, MSFC-STD-1249 is cited as its predecessor. It's noteworthy that neither the SSP OFCP nor Bishop (1973) are referenced in NASA-STD-5009B. However, as the tracing of the lineage has shown, they are primary references.

Standard NDE flaws are defined to be statistically based, implying that they are estimated from experimental POD studies, as noted in the definition:

> "Standard NDE: NDE methods of metallic materials for which a statistically based flaw detection capability has been established. Standard NDE methods addressed by this document are limited to the fluorescent penetrant, radiographic, ultrasonic, eddy current, and magnetic particle methods employing techniques with established capabilities."

More details on the statistical nature of Standard NDE are included in the first NDE requirement in "Section 4.2.2," as:

> **"4.2.2 Standard NDE Crack Sizes**
>
> **4.2.2.1** [NER 23] Nondestructive inspections of fracture-critical hardware shall detect the initial crack sizes used in the damage tolerance fracture analyses with a capability of 90/95 (90 percent probability of detection at a 95 percent confidence level).
>
> *The minimum detectable crack sizes for the Standard NDE methods shown in Table 1 and Table 2 are based principally on an NDE capability study that was conducted on flat, fatigue-cracked 2219-T87 aluminum panels early in the Space Shuttle program, and meet the 90/95 capability requirement. Although many other similar capability studies and tests have been conducted since, in our estimation, none have universal application, neither individually nor in combination. Conducting an ideal NDE capability demonstration where all of the variables are tested is obviously unmanageable and impractical. In order to make the broadest use of NDE flaw detectability data in Table 1 or Table 2, good engineering judgment needs to be applied and should be supported by specific documented analysis of the applicability or variance. For example, a flat panel is representative of a component with a large diameter curvature. It is also reasonable to use the Table 1 or Table 2 data values for most aerospace structural alloys such as titanium or stainless steel."*

Consistent with NASA-STD-5009B's convention, italicized portions indicate a comment to distinguish them from requirements. In [NER 23] the 90/95 detection capability required by NASA-STD-5019A is cited. However, there is no mention of the expectation that most certified inspectors would possess this capability, and no coverage probability (e.g., 95% inspector coverage) is cited. In the following italicized paragraph (denoting a comment and not a requirement) the Standard NDE flaw sizes provided in Table 1 and Table 2 (a conversion of Table 1 into SI units) are implied to support [NER 23] and thereby represent 90/95 capability. Table 1 is reproduced in Figure 2.4-1. Furthermore, this paragraph describes the POD study from Bishop (1973), although not explicitly referenced in the standard. It also states "many other similar capability studies and tests have been conducted since, in our estimation, none have universal

application, neither individually nor in combination." However, no POD studies are referenced in NASA-STD-5009B.

NASA-STD-5009B

Table 1—Minimum Detectable Crack Sizes for Fracture Analysis Based on Standard NDE Methods (See "Conditional Notes," section 4.2.3 for applicability.)

U. S. CUSTOMARY UNITS (inches)

Crack Location	Part Thickness, t	Crack Type	Crack Dimension, a*	Crack Dimension, c*
Eddy Current NDE				
Open Surface	t □ 0.050 t > 0.050	Through PTC[1]	t 0.020 0.050	0.050 0.100 0.050
Edge or Hole	t □ 0.075 t > 0.075	Through Corner	t 0.075	0.100 0.075
Penetrant NDE				
Open Surface	t □ 0.050 0.050<t <0.075 t > 0.075	Through Through PTC	t t 0.025 0.075	0.100 0.150 - t 0.125 0.075
Edge or Hole	t □ 0.100 t > 0.100	Through Corner	t 0.100	0.150 0.150
Magnetic Particle NDE				
Open Surface	t □ 0.075 t > 0.075	Through PTC	t 0.038 0.075	0.125 0.188 0.125
Edge or Hole	t □ 0.075 t > 0.075	Through Corner	t 0.075	0.250 0.250
Radiographic NDE				
Open Surface	t □0.107 t > 0.107	PTC PTC Embedded	0.7t 0.7t 2a=0.7t	0.075 0.7t 0.7t
Ultrasonic NDE Comparable to a Class A Quality Level (ASTM-E-2375)				
Open Surface	t □ 0.100	PTC Embedded**	0.030 0.065 0.017 0.039	0.150 0.065 0.087 0.039

[1] PTC - Partly through crack (Surface Crack)

* See Figure 1 for definitions of "a" and "c" for different geometries.

** Equivalent area is acceptable, ASTM-E-2375 Class A.

APPROVED FOR PUBLIC RELEASE – DISTRIBUTION IS UNLIMITED

29 of 55

Figure 2.4-1. NASA-STD-5009B Table 1 – minimum detectable crack sizes for fracture analysis based on standard NDE methods.

Standard NDE flaw sizes have traditionally been assumed to represent the capability of a large proportion (e.g., 95%) of inspectors that are qualified and certified according to NAS 410, as:

> **"4.5.1 Standard NDE Qualification and Certification**
>
> [NER 92] Personnel performing Standard NDE of fracture-critical hardware shall be, at a minimum, qualified and certified Level II in accordance with NAS 410, NAS Certification and Qualification of Nondestructive Test Personnel."

Therefore, there is no requirement in NASA-STD-5009B for individual inspectors to demonstrate POD detection capability of Standard NDE flaw sizes.

In a subsequent section, it is acknowledged that the Standard NDE flaw sizes were derived for a single material and alloy (2219 aluminum alloy), a flat specimen geometry, open surface fatigue crack flaw type (PTC), and therefore their generalization requires that "transferability or similarity" be established by documented evidence (e.g., POD demonstration or other engineering rationale) as:

> **"4.2.3 Table 1 (or Table 2) —Minimum Detectable Flaw Sizes Conditional Notes**
>
> *Since the Table 1 or Table 2 crack sizes were derived from a limited set of specimens of simple geometry, applying the crack sizes to complex geometries, other materials, material forms, material processes, and nonstandard NDE applications should be done with caution. Where the real inspection conditions deviate significantly from the concept of flat fatigue-cracked panel inspections, the transferability or similarity of the application of the Table 1 or Table 2 crack sizes to real inspection situations should be evaluated and verified by documented evidence, such as experimental data or other available test data documentation; for example, a demonstration using penetrant, where capillary action is compared using penetrant on a curved part and then a flat part. Similarity can be established by other studies, data, or by supportable rationale. Similarity considerations should meet the intent of MIL-HDBK-1823, Nondestructive Evaluation System Reliability Assessment.*
>
> *If similarity cannot be established, additional tests may be required, including Standard or Special NDE demonstration tests (see section 4.3). The values listed in Table 1 and Table 2 may not apply to thick-section components; threaded parts; weldments; compressively loaded structures; double wall radiography; and other unique material, structural, or inspection applications."*

NASA-STD-5009B does not provide a methodology for establishing "transferability or similarity". However, the NESC published a Technical Memorandum in 2022 (NASA/TM–20220003648) entitled "Guidebook for Assessing Similarity and Implementing Empirical Transfer Functions for Probability of Detection Demonstrations for Signal Based Nondestructive Evaluation Methods" (Koshti, et al. 2022) to provide a quantitative methodology and offer practitioner guidance that will be incorporated by reference in the forthcoming revision of NASA-STD-5009C.

A modified version of NASA-STD-5009B's "Table 1" is shown in Figure 2.4-2 to correlate the Standard NDE flaw size changes from MSFC-STD-1249, in some cases requiring a choice about the best alignment of the tables. Only entries that differ are shown in the MSFC-STD-1249 shaded region of the table (i.e., a blank entry indicates the value was inherited from this standard).

Limiting part thickness changes were noted for all methods which were small, except in the case of the ultrasonic method, for which a much larger thickness change was documented. For open surface TC and PTC, the flaw size changes were relatively small, with the exception of the eddy current flaw length at an aspect ratio of 10, which changed by doubling in length from 0.050 to 0.100 inch. Ultrasonic displays the most substantial changes in the manner in which the standard flaw sizes are specified.

Overall, the majority of the flaw size changes are related to the specification of edge or hole flaw sizes across the methods, which have been considered as subjective entries since their supporting POD studies have not been found. Furthermore, MSFC-STD-1249 definition of edge and corner flaws included PTCs, which was omitted in NASA-STD-5009 flaw geometries, and this change may partially explain the flaw size modifications. Overall based on interviews with key personnel, it is accepted that most of the flaw sizes and flaw sizes changes in NASA-STD-5009 were based on engineering judgment and fracture analysis computational simulation and are not considered to have been demonstrated by POD studies. Therefore, they are not statistically based, as believed at the beginning of this review.

Linking to Bishop (1973), Figure 2.4-1 denotes the four flaw sizes for penetrant and radiography that are traceable to the OFCP standard flaw sizes that were derived from Bishop's analysis and interpreted from Bishop's inspection dataset. The NESC's independent analyses of Bishop's dataset have shown support for other entries of open surface PTCs for eddy current and ultrasonic. However, the coverage probability across the population of inspectors varies by method and aspect ratio, and it is generally less than 95% as traditionally asserted that Standard NDE flaw sizes represent, which was shown in Tables 2.1-3 through 2.1-6.

	MSFC-STD-1249	NASA-STD-5009		MSFC-STD-1249		NASA-STD-5009	
Crack Location	Part Thickness	**Part Thickness, t**	**Crack Type**	Depth (a)	½ Length (c)	**Crack Dimension, a***	**Crack Dimension, c***
			Eddy Current				
Open Surface	t ≥ 0.020	t ≤ 0.050 t > 0.050	Through PTC[1]		0.050	t 0.020 0.050	0.050 0.100 0.050
Edge or Hole	t ≥ 0.020	t ≤ 0.075 t > 0.075	Through Corner	0.020	0.025 0.025	t 0.075	0.100 0.075
			Penetrant				
Open Surface	t < 0.075 t < 0.075 0.075 ≤ t < 0.075	t ≤ 0.050 0.050<t <0.075 t > 0.075	Through Through PTC		0.100	t t 0.025 0.075	0.100 0.150 - t 0.125 0.075
Edge or Hole	0.075 ≤ t < 0.075 0.075 ≤ t < 0.075	t ≤ 0.100 t > 0.100	Through Corner	0.075, t	0.050 0.050, 0.062	t 0.100	0.150 0.150
			Magnetic Particle				
Open Surface	t ≥ 0.070	t ≤ 0.075 t > 0.075	Through PTC	0.062		t 0.038 0.075	0.125 0.188 0.125
Edge or Hole	t ≥ 0.070	t ≤ 0.075 t > 0.075	Through Corner	0.070	0.125 0.125	t 0.075	0.250 0.250
			Radiographic				
Open Surface	t < 0.050 t ≥ 0.050	t ≤0.107 t > 0.107	PTC PTC Embedded	0.7t (0.025 min.) 0.7t	t (0.075 min.) t (0.075 min.)	0.7t 0.7t 2a=0.7t	0.075 0.7t 0.7t
			Ultrasonic				
Open Surface	t ≥ 0.300	t ≥ 0.100	PTC Embedded**	Class B, 0.200 dia. (Equiv. Area) Class 1, 0.130 dia. (Equiv. Area)		0.030 0.065 0.017 0.039	0.150 0.065 0.087 0.039

Orbiter Fracture Control Plan

Figure 2.4-2. NASA-STD-5009B Table 1 modified to compare flaw sizes to MSFC-STD-1249 and the SSP OFCP (Note all dimensions are in inches).

The Standard NDE flaw sizes in NASA-STD-5009B Table 1 have remained unchanged since the original 2008 release of NASA-STD-5009, which is confirmed by the lack of change entries in the "History Log" of revisions.

A significant difference between the tabulation of detectable flaw sizes from MSFC-STD-1249 compared to NASA-STD-5009 is the omission of Special NDE flaw sizes. Recall in MSFC-STD-1249, "Special" referred to a level of NDE practice that reliably detected smaller flaws. In NASA-STD-5009, Special NDE denotes demonstrated capability for each individual inspector, and while it may typically be performed to detect flaws smaller than Standard NDE, it could be required for complex geometries, materials, and inspection access that is deemed to be 'sufficiently' different from the conditions in which the Standard NDE flaws are intended to apply. Special practice would be required for these unique inspection situations, so the usage of the term "special" is not contradictory. In the specific application of NDE to metallic liners for composite overwrap pressure vessels and metallic tanks, the Special NDE flaw size of 0.050 inch long by 0.025 inch deep from the OFCP remains as a common demonstration flaw size. This case demonstrates a mixture of Special NDE referring to a specific flaw size and individual inspector demonstration for specific applications.

A significant finding of this NESC review was that the cracks in Bishop (1973) were etched prior to inspection and the individual inspector a90/95 and subsequent a90/95/95 flaw sizes were based on this surface condition. The influence of etching has been known for penetrant, and NASA-STD-5009 introduces a specification for the amount of etching based on the material, as:

> "[NER 39] The etching procedure shall specify the minimum amount of material to be removed to ensure that smeared metal does not mask cracks.
>
> (1) [NER 40] Non-ferrous materials such as aluminum and titanium alloys shall be etched to remove a minimum of 0.0004 in (0.01 mm) of material.
> (2) [NER 41] Corrosion resistant steel and nickel-based alloys shall be etched to remove a minimum of 0.0002 in (0.005 mm) of material.
>
> *Care must be taken to use an etchant which will preserve the surface finish (likely a buffered etch).*
>
> [NER 42] If etching is not feasible or the minimum depths are not attainable, it shall be demonstrated and documented that the required flaw size can be reliably detected following current machining processes."

The etching level specified is significantly less than the estimated 0.002- to 0.0008-inch that was performed on the Bishop study flaws. Experimental validation of the impact of lighter etching on the Standard NDE flaw sizes is not referenced in NASA-STD-5009. Related to the relationship between etching level and POD, [NER 42] indicates that the effect on POD by deviating from the specified minimum levels etching shall be demonstrated.

More importantly, etching was suggested to increase the detection capability of the other methods in Bishop's POD study by Rummel et al. (1974). In particular, the Standard NDE flaw size for radiography of 0.7t was based on etched cracks. Analyses of the as-machined condition compared to after-etch condition contained in Rummel et al. (1974) and the NTIAC Databook shows that etching, albeit "heavy" etching to 0.002 inch, significantly increased the crack detection capability of radiography. There is ongoing work to investigate the effect of etching on the detectability of cracks by radiography, including at reduced levels of etching depth that is more representative of the level of etching required by NASA-STD-5009B for penetrant inspections. Additionally, computational modeling is being used to understand the reason for increased detectability after etching. The current theory for the cause of this increased detectability is the opening or widening of the cracks near the surface caused by etching that results in a more volumetric type of flaw (to a limited depth) that might be more observable in radiographic images.

As a final note, magnetic particle Standard NDE flaw sizes in NASA-STD-5009B could not be corroborated in this review. Rummel et al. (1976) has traditionally been attributed to be the source POD study. This report contains three inspectors from Martin Marietta performing magnetic particle inspections on steel specimens. Inspections were performed in the as-machined and after-etch-and-proof condition. However, no inspections in the after-etch condition before proof loading condition were included in the dataset. The magnetic particle inspection dataset reported in Rummel et al. (1976) was reanalyzed by the NESC, and the results are significantly different than the Standard NDE values in NASA-STD-5009B. The NESC results are consistent with the analysis results provided in the NTIAC Databook. For all inspectors, the a90/95 flaw sizes could not be estimated in the as-machined condition. However, the a90/95 flaw size can be estimated in the after-etch-and-proof. The Rummel et al. (1976) report confirms this finding stating, "Detection by

the magnetic particle method is also believed to be affected by the cold worked surface layer on specimens in the as-machined condition. An improvement in detection was obtained after etching and proof loading."

2.4.1 Summary of NASA-STD-5009 Review

NASA-STD-5009B's Table 1 inherited the majority of the Standard NDE portion of MSFC-STD-1249 with the following revisions delineated as:

- MSFC-STD-1249 provided crack length (2c) in the flaw size table, and NASA-STD-5009B provides one-half crack length (c). The crack geometry diagrams defined "c" consistently, it was only presented differently in the tables. The changes in length are expressed consistently as crack length (2c).
- MSFC-STD-1249 provided aspect ratio[4] and crack length, but it did not explicitly provide crack depth for PTC, which can be calculated from length and aspect ratio. NASA-STD-5009 omitted aspect ratio and provided a column for crack depth.
- MSFC-STD-1249 provided crack geometries for PTC on an edge and in a hole that were removed in NASA-STD-5009. NASA-STD-5009 added a crack geometry of an embedded flaw not shown in MSFC-STD-1249.
- Penetrant, eddy current, and magnetic particle: Standard flaw size at an aspect ratio of 5 was omitted in NASA-STD-5009B.
- Penetrant:
  - Part thickness for open surface PTC was changed from $t < 0.075$ inch and $t \geq 0.075$ inch to $t > 0.075$ inch.
  - Part thickness for open surface TCs was changed from $t < 0.075$ inch and $t \geq 0.075$ inch to $t \leq 0.050$ inch and $0.050 \text{ inch} < t < 0.075$ inch.
  - Part thickness for edge or hole cracks was changed from $t < 0.075$ inch and $t \geq 0.075$ inch to $t \leq 0.100$ inch and $t > 0.100$ inch.
  - Flaw length was changed from 0.100 and 0.125 inch to 0.300 inch for TCs and corner cracks. The depth for a corner crack was changed from 0.075 to 0.100 inch.
- Eddy Current:
  - Part thickness was changed from $t \geq 0.020$ inch to $t \leq 0.050$ inch and $t > 0.050$ inch for open surface TCs and PTCs and changed to $t \leq 0.075$ inch and $t > 0.075$ inch for edge or hole cracks.
  - Flaw length at an aspect ratio of 10 was increased from 0.100 to 0.200 inch for open surface PTCs, but it remained at 0.100 inch for $2c/a = 2$.
  - Flaw length for edge or hole corner crack was changed from 0.020 inch deep by 0.050 inch long to 0.075 inch deep by 0.150 inch long
- Magnetic Particle:
  - Part thickness was revised from $t \geq 0.070$ inch to $t \leq 0.075$ inch and $t > 0.075$ inch.
  - Flaw at aspect ratio of 2 was changed to an aspect ratio of 3.33, which changed the flaw depth from 0.062 to 0.075 inch at the same length of 0.250 inch.
  - Flaw length for TC and corner crack at an edge and hole was increased from 0.250 to 0.500 inch. The flaw depth for corner crack was increased from 0.070 to 0.075 inch.
- Ultrasonic:

[4] MSFC-STD-1249 defines aspect ratio as depth over length, a/2c.

- The method specifications of L-Wave and S-Wave were removed. The flaw sizes for these specifications were the same in MSFC-STD-1249.
- Part thickness was revised from $t \geq 300$ inch to $t \geq 0.100$ inch.
- Class A and B were specified as 0.130 inch and 0.200-inch diameter, respectively, and was changed to four specific depth-by-length flaws with PTCs and embedded flaws at aspect ratios of 2 and 10.
- Added a table subtitle of "Comparable to as Class A Quality Level (ASTM-E-2375)"
- Added a footnote for embedded flaws of "Equivalent area is acceptable, ASTM-E-2375 Class A."

- Radiographic:
  - Part thickness was revised from $t < 0.050$ inch and $t \geq 0.050$ inch to $t \leq 0.107$ inch and $t > 0.107$ inch.
    - The source of 0.107-inch thickness appears to be derived from the flaw length for $t > 0.107$ inch set to 0.7t, which maintains the minimum one-half flaw length of 0.7*0.107 = 0.075 inch that is traceable to the SSP OFCP minimum flaw length of 0.150 inch.
  - Flaw depth for $t < 0.050$ inch included a minimum of 0.025 inch, which was the limit of a PTC within the thickness.
  - Embedded flaw depth was decreased from 0.7t to 2a = 0.7t, which implies that a = (0.7/2)t.

2.4.2 NESC Independent Analyses of Standard NDE Flaw Sizes in NASA-STD-5009

In this section, additional analyses are presented to estimate the representative inspector coverage probability of the NASA-STD-5009B flaw sizes. In the previous NESC independent analysis MIL-HDBK-1823A analysis methods were applied to the Bishop (1973) POD dataset to compare individual inspector a90/95 flaw sizes, and the Standard NDE a90/95/95 flaw size to Bishop's results. It has been shown that Bishop's original results underwent significant translation and extrapolation throughout the evolution of NASA Standard NDE flaw sizes in NASA-STD-5009B. The purpose of this analysis is to provide insights on the detection capability represented by the current Standard NDE flaw sizes based on Bishop's POD dataset. This analysis is not intended as a rigorous approach to propose updating the flaw sizes or to change the description of Standard NDE flaw size in NASA-STD-5009B.

It was shown that the primary differences in a90/95/95 flaw sizes between the NESC analysis and Bishop's original analysis occurred at the individual inspector a90/95 level, not in the approach to estimate the proportion of the population of inspectors possessing a specified detection capability. These individual inspector a90/95 differences represent differences in the POD (i.e., 90%) and/or the confidence (i.e., 95%) level. At the individual inspector level, an alternative analysis could be performed to estimate an adjusted POD with 95% confidence of Bishop's reported flaw sizes based on the NESC independent analysis. As an example, to clarify, Bishop's reported a90/95 for an individual inspector may better represent a70/95 using MIL-HDBK-1823A methods. However, since NASA-STD-5019A specifies 90/95 detection, it was decided that it would be more appropriate to adjust only the inspector coverage probability, even though it is not the primary source of the flaw size discrepancy. This is an important distinction since the NASA/TM–20220013822 (2022) adopts the same conceptual analysis framework as Bishop to estimate Standard NDE flaw sizes. Without this clarification of the discrepancy source, inappropriate

criticism of the method could be levied based on a misinterpretation of the approach taken in the present analysis. The analysis objective is to estimate adjusted, representative inspector coverage probability of the NASA-STD-5009B Standard NDE flaw sizes based on an analysis of the Bishop (1973) dataset.

As discussed in Section 2.1.5 the NESC analysis chose to use the same flaw characteristic as Bishop (1973) used for estimating individual inspector a90/95 flaw sizes. However, for some methods, NASA-STD-5009B reports alternative expressions of these Standard flaw sizes. As an example, for penetrant and ultrasonic, Bishop reported a90/95 elliptical projected area that was not a function of aspect ratio. However, NASA-STD-5009B reports Standard NDE flaw length and depth at aspect ratios of 2 and 10 for open surface PTCs. The different parameterizations of the detectable flaw sizes are not directly comparable. Therefore, for penetrant and ultrasonic, the approach takes estimates representative of inspector coverage probability for flaw area and compares it to the computed elliptical flaw area for the flaws reported in terms of length and depth in NASA-STD-5009B. For completeness, the estimated a90/95/95 flaw length and depth from Bishop and the NESC's analysis area are provided. Note while penetrant POD is routinely analyzed as a function of flaw length, if the NESC analysis used length as the flaw characteristic for POD analysis it would be inconsistent with Bishop's result. This analysis approach is not to be misconstrued as suggesting the best or most appropriate flaw characteristic for POD modeling of a method, rather it was chosen to make a direct comparison possible.

Table 2.4-1 shows the results of the methods comparison included in Bishop's POD study (i.e., radiographic, penetrant, ultrasonic, and eddy current). The results of the Bishop (1973) and the NESC analyses that provided the Standard NDE flaw sizes (i.e., a90/95/95 were provided in Tables 2.1-3 through 2.1-6). The Bishop and NESC Standard NDE flaw sizes are compared to those reported in NASA-STD-5009B as open surface, PTC, and engineering judgement was required to identify the appropriate part thickness that correlates with the Bishop POD study.

Table 2.4-1. Comparison of Bishop (1973), NESC (2022), and NASA-STD-5009B Standard Flaw Sizes for Open Surface PTCs with an Estimated Representative Inspector Coverage Probability.

		Standard NDE Flaw Size, a90/95/95				Length at Aspect Ratio		5009 Inspector Coverage
NDE Technique	Aspect Ratio (2c/a)	Bishop (1973)	NESC (2022)	STD-5009		NESC	5009	a90/95/XX%
Radiography		70%	84%	70%	a/t, %			50%
Penetrant	2	0.0096	0.0087	0.0088	Area, in^2	0.149	0.150	95%
	10	0.0096	0.0087	0.0049		0.332	0.250	51%
Ultrasonic	2	0.0071	0.0185	0.0066	Area, in^2	0.217	0.130	42%
	10	0.0071	0.0185	0.0071		0.485	0.300	45%
Eddy Current	2	0.038	0.057	0.050	Depth, in			85%
	10	0.038	0.057	0.020				17%

Table 2.4-1 shows that the NASA-STD-5009B Standard NDE flaw size of 0.70t for radiography represents 50% inspector coverage, rather than 95% (i.e., 50% of certified inspectors would be expected to demonstrate 90/95 detection of a 0.70t flaw). As discussed, this result is particularly troublesome since the cracks in the Bishop POD study were etched before radiographic inspection, which is not stipulated as a requirement in NASA-STD-5009B. The level of etching used in Rummel et al. (1974) showed an improvement in POD detection capability of radiographic

inspection compared to as-machined cracks. This implies that the inspector coverage probability could be lower than 50%.

For penetrant, 95% of the inspectors are expected to demonstrate 90/95 detection of an aspect ratio of 2 flaw with a 0.0087 in^2 elliptical flaw area, which can be expressed as length of 0.150 inch. This result was discussed as being an artifact of a miscalculated square root in Bishop's analysis, rather than being supportive of Bishop's POD analysis methodology. Furthermore, for penetrant, only 50% of the inspectors would be expected to demonstrate 90/95 detection capability of an aspect ratio of 10 flaw with a length of 0.250 inch. Recall from Section 2.2 this flaw size was chosen based on a qualitative analysis of a concentration of detected flaws with higher aspect ratio, and it deviated from the equivalent area assumption and reporting of Bishop's results during the SSP OFCP development. This partially explains the discrepancy between the representative inspector coverage for an aspect ratio of 2 and 10.

For ultrasonic, less than 50% of the certified inspectors would be expected to demonstrate 90/95 detection of the Standard NDE flaw sizes at an aspect ratio of 2 or 10. While this low inspector coverage is concerning, ultrasonic is frequently considered as a method that includes a wide variety of implementations, and it is fundamentally not recommended to attempt reporting an overall, average ultrasonic detection capability.

For eddy current, 85% of certified inspectors would be expected to demonstrate 90/95 detection of a 0.050-inch-deep flaw at an aspect ratio of 2, while 17% of the inspectors would be expected to demonstrate 90/95 detection of a 0.020-inch-deep flaw at an aspect ratio of 10. As a comment, eddy current featured 5 inspectors in Bishop's POD study, and as discussed, one inspector provided questionable results that the NESC removed from its analysis. As a result, the Standard NDE flaw size estimate is based on 4 inspectors. NASA/TM–20220013822 (2022) discusses the considerations for choosing the number of inspectors in a Standard NDE study and recommends a minimum of 10. Therefore, with 4 inspectors there is conservatism in estimating the Standard NDE flaw size, which may explain the low representative inspector coverage. In addition, Bishop's analysis did not consider detectable depth as a function of aspect ratio, as discussed in Section 2.1.4. While the NESC explored modeling the POD as a function of depth and aspect ratio, the results were inconclusive, and for consistency it adopts Bishop's approach of modeling the average a90/95 flaw depth over the collection of specimens with varying aspect ratio. This is an additional reason why the NESC's a90/95/95 estimate of 0.057 inch depth may be conservative.

Overall, this comparison shows the Standard NDE flaw sizes in NASA-STD-5009B do not consistently represent 95% inspector coverage. In general, they could be said to represent the typical inspector a90/95 detection capability. NASA-STD-5019A does not require an inspector coverage probability for Standard NDE flaw sizes, only that an inspector is expected to achieve 90/95 detection capability. Therefore, these results do not show a violation of requirements for NASA fractural critical components in human spaceflight, rather it represents a refutation of accepted belief that the Standard NDE flaw sizes represent 95% inspector coverage.

Admittedly, Bishop's study is 50 years old, and it has been argued that inspection methods have enjoyed significant technical improvements, and the argument then asserts that analysis based on Bishop's inspection technology is not representative of current technology. Granted, the technological advancement argument may apply to some methods (e.g., ultrasonic). However, it is hard to argue that much has substantially changed for other methods (e.g., penetrant). Nevertheless, while this technology argument is somewhat persuasive, is has not been shown to

be statistically based through a Standard NDE POD study, since a comprehensive study similar to Bishop has not been found.

3.0 Conclusion

A retrospective review of NASA Standard NDE has been presented that traces the evolution Standard NDE flaw sizes. The genesis of these flaw sizes were traced from Bishop (1973) that conducted the first multi-facility, multi-inspector POD study with the NDE methods of radiographic, penetrant, ultrasonic, and eddy current, and introduced the concept of sampling from a population of inspectors to make statements about the proportion of inspectors that were expected to demonstrate 90/95 detection of a specified flaw size. This seminal study supported the development of the SSP OFCP (1974) that translated and extrapolated Bishop's results primarily for the usage of fracture analysts. It provided the first definition of Standard and Special NDE, and it made the first implicit suggestions regarding detection capability primarily depending on flaw area that has been adopted and ingrained in the fracture analysis community (i.e., equivalent area assumption). Expanding on the conceptual framework proposed in the OFCP, MSFC-STD-1249 (1985) provided the first detailed tabulation of Standard NDE and Special NDE flaw sizes for multiple flaw geometries and included the magnetic particle method. NASA-STD-5009 (2008) extracted the Standard NDE flaw sizes from MSFC-STD-1249's table, with relatively minor modifications to the flaw sizes, and defined Special NDE as denoting a required process of demonstrating the detection capability of individual inspectors for flaw sizes, inspection conditions, or methods that deviated from the Standard NDE table, rather than a Special NDE flaw size. It is interesting to note that the two flaw sizes for open surface PTCs for penetrant and flaw aspect ratio for radiography contained in NASA-STD-5009B are directly traceable to Bishop's POD study analysis and dataset. While there are a significant number of Standard NDE flaw sizes that could not be traced, the analysis presented in Section 2.4.2 indicates that the representative inspector coverage of NASA-STD-5009B's flaw sizes based on Bishop's POD dataset is less than 95%. With the increased understanding gained throughout this review, the forthcoming revision C of NASA-STD-5009 has incorporated significant revisions in describing the Standard NDE flaw sizes, and the review serves as a reference of their origin. The lineage of NASA Standard NDE spans nearly 50 years, and the Standard NDE flaw sizes have served numerous NASA programs without a known, attributable failure due to the application of Standard NDE flaw sizes in fracture control plans.

This review has provided numerous insights and lessons learned for planning, conducting, and analyzing NASA Standard NDE POD studies. Moreover, this review has motivated the development of the first documented methodology to conduct a NASA Standard NDE study in NASA/TM–20220013822 (2022) that will be referenced in NASA-STD-5009C. This methodology will enable the updating the Standard NDE flaw sizes and specification of Standard NDE flaw sizes for methods not included in NASA-STD-5009B. This detailed retrospective review serves as benchmark for evaluating the historical consistency of NASA Standard NDE as it continues to evolve to provide enhanced NDE detection capabilities and emerging methods.

4.0 References

Anderson, R. T.; DeLacy, T. J.; and Stewart, R. C. (1973): "Detection of Fatigue Cracks by Nondestructive Testing Methods," General Dynamics, Convair Division, GDCA-DGB73-02, March 1973.

Berens and Hovey (1981): "Evaluation of NDE Reliability Characterization," University of Dayton Research Institute, AFWAL-TR-81-4160, 1981.

Bishop, C. R. (1973): "Nondestructive Evaluation of Fatigue Cracks," Space Division Rockwell International, SD 73-SH-0219, NASA Contractor Report NAS9-14000, 1973.

EN-SB-08-012, Revision D (2018): In-Service Inspection Crack Size Assumptions for Metallic Structures, Air Force Structures Bulletin, February 2018.

Forsyth, D. S. (2018): "Experiences in Practicing the Assessment of Nondestructive Testing Performance," *44th Annual Review of Progress in Quantitative Nondestructive Evaluation*, Volume 37, AIP Conference Proceedings, 2018.

King, J. P.; and Johnson, K. R. (1974): "Space Shuttle Orbiter Fracture Control Plan," Space Division Rockwell International SD73-SH-0082A, 1974.

Koshti, Ajay; Parker, Peter A.; Forsyth, David S.; Suits, Michael W.; Walker, James L.; and Prosser, William H. (2022): *Guidebook for Assessing Similarity and Implementing Empirical Transfer Functions for Probability of Detection (POD) Demonstrations for Signal Based Nondestructive Evaluation (NDE) Methods*, NASA/TM–20220003648, March 2022.

Lewis, W. H.; Sproat, W. H.; Dodd, B. D.; and Hamilton, J. M. (1978): "Reliability of Nondestructive Inspections," United States Air Force contractor report SA-ALC/MME 76-6-38-1, prepared by The Lockheed-Georgia Company, 1978.

MIL-HDBK-1823A (2009): "Nondestructive Evaluation System Reliability Assessment," 2009.

MIL-STD-410 (1991): "Nondestructive Testing Personnel Qualification and Certification," 1991.

MSFC-STD-1249 (1985): "Standard NDE Guidelines and Requirement for Fracture Control Programs," 1985.

NASA (1988) "Fracture Control Requirements for Payloads Using the National Space Transportation System (NSTS)," National Aeronautics and Space Administration, NHB8071.1, September 1988.

NASA Standard 5009 (2008): "Nondestructive Evaluation Requirements for Fracture-Critical Metallic Components," 2008.

NASA Standard 5009B (2019): "Nondestructive Evaluation Requirements for Fracture-Critical Metallic Components," 2019.

NASA Standard 5019A (2016): "Fracture Control Requirements for Spaceflight Hardware," 2016.

Parker, P.; Koshti, A.; Forsyth, D.; Suits, M.; Walker, J.; and Prosser, W. (2022): "Guidebook for Planning and Analyzing NASA Standard Nondestructive Evaluation (NDE) Probability of Detection (POD) Studies," NASA TM-20220013822, 2022.

Rummel, W. D. (1982): “Recommended Practice for a Demonstration of Nondestructive Evaluation (NDE) Reliability on Aircraft Production Parts,” *Materials Evaluation*, 40, pp. 922-932, 1982.

Rummel, W. D. (2010): “Nondestructive Inspection Reliability – History, Status, and Future Path,” *18th World Conference on Nondestructive Testing*, 16-20 April 2010, Durban, South Africa, 2010.

Rummel, W. D.; Rathke, R. A.; Todd, P. H.; Tedrow, T. L.; and Mullen, S. J. (1976): *Detection of Tightly Closed Flaws by Nondestructive Testing Methods in Steel and Titanium*, NASA CR-151098.

Rummel, W. D.; Todd, P. H.; Frecska, S. A.; and Rathke, R. A. (1974): “The Detection of Fatigue Cracks by Nondestructive Testing Methods,” NASA CR-2369, 1974.

Salkowski, C. (1995): “Nondestructive Inspection Reliability Assumptions for Critical Aerospace Components,” Proceedings SPIE 2455, Nondestructive Evaluation of Aging Aircraft, Airport, Aerospace Hardware, and Materials, 1995.

Spencer, F. W. (2020): “Recommendations on Inspector Numbers for a Standard Methodology of NDE Characterization,” 2020. informal correspondence.

Appendix A – Bishop (1973) Dataset, Sorted by Ascending Flaw Depth

Specimen Characteristics											Radiographic Inspections							Penetrant Inspections							Ultrasonics Inspections					Eddy Current Inspections				
Specimen No.	Surface Finish (microinch)	Location	Incld Angle (degree)	Thick (t) (inch)	Length (2c) (inch)	Depth (a) (inch)	Area (inch^2)	a/2c	a/t	2c/a	A	B	C	D	E	F	G	H	I	J	K	L	M	N	O	P	Q	R	S	T	U	V	W	X
CO18A	50	D6	0.0	0.061	0.007	0.001	5.498E-06	0.143	1.6	7.0	0	0	0	0	0	0	0	0	0	0	0	0	0	0	0	0	0	0	0	0	0	0	0	0
CO25A	45	BC14	2.4	0.061	0.031	0.002	4.869E-05	0.065	3.3	15.5	0	0	0	0	0	0	0	0	0	0	0	1	1	0	1	1	1	1	1	0	0	0	0	0
CO41A	260	E11	5.9	0.060	0.015	0.003	3.534E-05	0.200	5.0	5.0	0	0	0	0	0	0	0	0	0	0	0	0	0	0	0	0	0	1	0	0	0	0	0	0
C014A	40	DE12	4.8	0.061	0.017	0.003	4.006E-05	0.176	4.9	5.7	0	0	0	0	0	0	0	0	0	0	0	0	0	0	1	0	0	0	0	0	0	0	0	0
CO41A	260	D7	1.2	0.060	0.018	0.003	4.241E-05	0.167	5.0	6.0	0	0	0	0	0	0	0	0	0	0	0	0	0	0	1	0	0	1	0	0	0	0	0	0
C018A	50	B14	2.4	0.061	0.025	0.003	5.890E-05	0.120	4.9	8.3	0	0	0	0	0	0	0	0	1	0	1	1	0	0	1	1	0	1	1	0	0	0	0	0
C044A	140	C6	0.0	0.060	0.025	0.003	5.890E-05	0.120	5.0	8.3	0	0	0	0	0	0	0	0	0	0	0	0	0	0	1	0	0	0	0	0	0	0	0	0
C021A	55	C7	1.2	0.059	0.010	0.004	3.142E-05	0.400	6.8	2.5	0	0	0	0	0	0	0	1	0	1	0	0	0	0	1	0	0	0	0	0	0	0	0	0
C042A	55	D11	5.9	0.069	0.011	0.004	3.456E-05	0.364	5.8	2.8	0	0	0	1	0	0	0	1	0	0	1	0	1	1	0	1	1	1	1	1	0	0	1	0
C053A	240	E11	5.9	0.061	0.021	0.004	6.597E-05	0.190	6.6	5.3	0	0	0	0	0	0	1	1	0	1	1	0	1	0	1	1	0	1	1	0	0	0	0	0
C018B	50	BC14	2.4	0.061	0.021	0.004	6.597E-05	0.190	6.6	5.3	0	0	0	0	0	0	0	0	0	0	1	1	0	0	0	1	0	1	1	0	0	0	0	0
C019A	60	B8	2.4	0.058	0.030	0.004	9.425E-05	0.133	6.9	7.5	1	1	0	0	0	0	0	1	1	0	1	1	0	1	0	1	0	1	1	0	0	0	0	0
C077B	45	C13	3.6	0.206	0.020	0.005	7.854E-05	0.250	2.4	4.0	0	0	0	0	0	0	0	0	0	0	0	0	0	0	0	0	0	0	0	0	0	0	0	0
C054A	300	CD11	5.9	0.061	0.020	0.005	7.854E-05	0.250	8.2	4.0	0	0	0	0	0	0	0	0	0	0	0	0	0	0	0	0	0	0	0	0	0	0	0	0
A003	32	EF11	5.9	0.054	0.027	0.005	1.060E-04	0.185	9.3	5.4	0	0	0	0	0	0	0	0	0	0	0	0	0	0	0	0	0	0	0	0	0	0	0	0
C052A	180	EF10	4.8	0.061	0.035	0.005	1.374E-04	0.143	8.2	7.0	0	0	0	0	0	0	0	1	0	1	1	0	1	1	1	1	1	1	1	0	0	0	1	1
C018B	50	CD13	3.6	0.061	0.035	0.006	1.649E-04	0.171	9.8	5.8	0	0	0	1	0	1	0	0	0	0	0	1	1	1	0	0	1	1	1	1	0	0	1	0
C045A	145	DE14	2.4	0.064	0.041	0.006	1.932E-04	0.146	9.4	6.8	0	0	0	0	1	0	1	1	1	0	1	1	1	1	1	1	1	1	1	0	0	0	1	0
C052A	180	CD11	5.9	0.061	0.049	0.006	2.309E-04	0.122	9.8	8.2	0	0	0	0	0	0	0	1	1	0	1	0	1	1	1	1	1	1	1	1	0	0	1	1
A004	30	EF6	0.0	0.063	0.022	0.007	1.210E-04	0.318	11.1	3.1	0	0	0	0	0	1	1	1	0	0	0	0	1	1	1	0	0	1	1	1	0	0	1	1
C084A	45	E6	0.0	0.210	0.028	0.007	1.539E-04	0.250	3.3	4.0	0	0	0	0	0	0	0	1	0	1	0	0	1	1	0	1	1	0	1	1	0	1	0	0
A016	125	BC3	3.6	0.058	0.034	0.007	1.869E-04	0.206	12.1	4.9	0	0	0	0	0	0	0	0	0	0	0	0	0	0	0	0	0	0	0	0	0	0	0	0
C073B	45	B11	5.9	0.209	0.035	0.007	1.924E-04	0.200	3.3	5.0	0	0	0	0	0	0	0	1	1	0	0	1	0	0	0	1	0	0	1	0	0	0	0	0
C052A	180	EF12	4.8	0.061	0.041	0.007	2.254E-04	0.171	11.5	5.9	0	0	0	0	0	0	0	1	1	1	1	0	1	1	1	1	1	1	1	0	0	0	1	1
C011A	40	D6	0.0	0.062	0.044	0.007	2.419E-04	0.159	11.3	6.3	0	0	0	0	0	0	0	1	1	0	1	1	1	1	1	1	1	1	1	0	1	0	1	0
C045A	145	CD12	4.8	0.064	0.045	0.007	2.474E-04	0.156	10.9	6.4	0	0	0	0	0	0	0	1	1	0	0	1	1	1	1	1	1	1	1	0	0	0	1	0
C103B	140	BC9	3.6	0.208	0.017	0.008	1.068E-04	0.471	3.8	2.1	0	0	0	0	0	0	0	1	0	1	0	1	1	0	0	1	1	0	0	0	0	0	0	0
C068A	45	C7	1.2	0.209	0.030	0.008	1.885E-04	0.267	3.8	3.8	0	0	0	0	0	0	0	1	1	1	0	1	1	0	1	1	0	1	1	0	0	0	0	0
C028A	50	D15	1.2	0.059	0.032	0.008	2.011E-04	0.250	13.6	4.0	0	0	0	1	0	0	0	0	1	1	1	1	1	0	1	1	0	0	0	1	0	0	0	0
C030A	160	C6	0.0	0.060	0.045	0.008	2.827E-04	0.178	13.3	5.6	0	0	0	0	0	0	0	1	1	1	1	1	1	1	1	1	1	1	1	0	0	1	1	0
A023	230	FG3	3.6	0.059	0.048	0.008	3.016E-04	0.167	13.6	6.0	0	0	0	0	0	0	0	0	0	0	0	0	0	0	0	0	0	0	0	0	0	0	0	0
C020A	40	E7	1.2	0.059	0.032	0.009	2.262E-04	0.281	15.3	3.6	0	0	0	0	0	0	0	1	1	0	1	1	1	0	1	1	1	1	1	0	1	0	0	0
C025A	45	B10	4.8	0.061	0.030	0.010	2.356E-04	0.333	16.4	3.0	0	0	0	0	0	0	0	1	0	0	0	1	1	0	1	1	1	1	1	0	0	0	0	0
C017A	60	B15	1.2	0.057	0.040	0.010	3.142E-04	0.250	17.5	4.0	0	0	0	0	0	0	0	0	1	0	0	1	1	1	1	1	0	1	0	0	0	0	1	1
Cl00A	205	F6	0.0	0.208	0.040	0.010	3.142E-04	0.250	4.8	4.0	0	0	0	0	0	1	1	1	1	1	0	0	1	1	1	0	0	1	0	1	1	0	1	1
C042B	55	BC8	2.4	0.069	0.055	0.010	4.320E-04	0.182	14.5	5.5	0	1	0	0	0	0	0	1	1	1	1	1	1	1	1	1	1	1	1	0	0	1	1	1
C045B	145	D9	3.6	0.064	0.061	0.010	4.791E-04	0.164	15.6	6.1	0	0	0	0	0	1	1	0	1	1	0	1	0	1	1	1	1	1	1	0	1	0	1	0
C068A	45	CD15	1.2	0.209	0.038	0.011	3.283E-04	0.289	5.3	3.5	0	0	0	0	0	0	0	1	1	0	1	1	1	0	1	1	0	1	1	0	0	0	0	0
C055A	300	B15	1.2	0.054	0.041	0.011	3.542E-04	0.268	20.4	3.7	0	0	0	0	0	0	0	1	1	1	1	0	1	0	1	1	1	1	0	0	1	0	1	0
C100A	205	B8	2.4	0.208	0.041	0.011	3.542E-04	0.268	5.3	3.7	0	0	0	0	0	0	0	1	1	0	0	0	0	0	0	0	0	0	0	0	0	0	0	0
C077A	45	E9	3.6	0.206	0.045	0.011	3.888E-04	0.244	5.3	4.1	0	0	0	0	0	0	0	0	0	0	1	1	1	1	1	1	1	1	1	0	1	1	1	1
C044B	140	CD8	2.4	0.060	0.052	0.011	4.492E-04	0.212	18.3	4.7	0	0	0	1	1	1	0	1	0	1	1	1	1	1	1	1	1	1	1	0	0	1	1	0
C044B	140	BC12	4.8	0.060	0.058	0.011	5.011E-04	0.190	18.3	5.3	0	0	0	0	0	0	0	1	0	0	0	1	1	1	1	0	1	1	1	1	0	0	1	0
C003B	45	D10	4.8	0.059	0.058	0.011	5.011E-04	0.190	18.6	5.3	0	0	0	0	0	0	0	1	1	1	1	1	1	1	1	1	1	1	1	0	1	0	1	0
C030A	160	C12	4.8	0.060	0.061	0.011	5.270E-04	0.180	18.3	5.5	0	0	0	0	0	0	0	1	1	1	1	1	1	1	1	1	1	1	1	1	1	1	1	1
C011A	40	D12	4.8	0.062	0.062	0.011	5.356E-04	0.177	17.7	5.6	0	0	0	0	0	1	0	0	1	1	0	1	1	1	1	1	1	1	1	0	1	1	1	1
C039B	173	F12	4.8	0.061	0.065	0.011	5.616E-04	0.169	18.0	5.9	0	0	0	0	0	0	0	1	1	1	1	0	1	1	1	1	1	1	1	1	1	1	1	1
C030A	160	BC13	3.6	0.060	0.077	0.011	6.652E-04	0.143	18.3	7.0	0	0	0	0	0	0	0	1	1	1	1	1	1	1	1	1	1	1	1	1	1	1	1	1
C003A	45	EF12	4.8	0.059	0.079	0.011	6.825E-04	0.139	18.6	7.2	1	1	0	0	0	1	0	1	1	0	1	1	1	1	1	0	1	1	1	1	1	1	1	1
C015B	45	BC13	3.6	0.061	0.051	0.012	4.807E-04	0.235	19.7	4.3	1	0	0	0	0	0	1	1	1	1	1	1	1	0	0	1	0	1	1	1	1	1	0	1	1
C014A	40	CD15	1.2	0.061	0.068	0.012	6.409E-04	0.176	19.7	5.7	1	0	0	0	1	0	0	0	1	1	1	1	1	1	1	1	1	1	1	1	1	1	1	1	0
A021	230	EF8	2.4	0.051	0.197	0.012	1.857E-03	0.061	23.5	16.4	1	0	0	0	1	1	1	1	1	0	0	1	1	1	1	0	1	1	1	1	1	1	1	1	1
C027A	50	B15	1.2	0.059	0.048	0.013	4.901E-04	0.271	22.0	3.7	0	0	0	0	0	1	1	0	1	1	1	1	1	1	1	1	1	1	1	1	0	1	1	1	0
C116A	180	B6	0.0	0.207	0.057	0.013	5.820E-04	0.228	6.3	4.4	0	0	0	0	0	0	0	0	1	1	1	1	0	1	1	1	1	0	0	0	1	0	1	1
A012	60	DE6	0.0	0.056	0.062	0.013	6.330E-04	0.210	23.2	4.8	0	0	0	0	0	0	0	0	0	0	0	0	1	1	0	0	1	0	0	0	1	1	0	1	1
C015B	45	EF9	3.6	0.061	0.062	0.013	6.330E-04	0.210	21.3	4.8	0	0	0	0	0	0	1	0	1	1	1	1	0	0	1	0	1	1	1	1	1	1	1	1	1
C039B	173	C11	5.9	0.061	0.063	0.013	6.432E-04	0.206	21.3	4.8	0	1	0	1	1	1	1	1	1	1	1	1	1	1	1	1	1	1	1	1	1	1	1	1	1
A017	130	DE11	5.9	0.061	0.064	0.013	6.535E-04	0.203	21.3	4.9	0	0	0	0	0	0	0	0	0	0	0	0	0	1	0	0	0	1	1	1	0	1	0	1	1
C011A	40	D9	3.6	0.062	0.065	0.013	6.637E-04	0.200	21.0	5.0	0	0	0	0	0	0	0	1	1	1	1	1	1	1	1	1	1	1	1	1	1	1	1	1	1
C039B	173	B8	2.4	0.061	0.067	0.013	6.841E-04	0.194	21.3	5.2	1	1	0	0	1	1	1	1	1	1	1	1	1	1	1	1	1	1	1	1	1	0	1	0

Specimen Characteristics											Radiographic Inspections							Penetrant Inspections							Ultrasonics Inspections					Eddy Current Inspections				
	Surface Finish		Incld Angle	Thick (t)	Length (2c)	Depth (a)	Area				A	B	C	D	E	F	G	H	I	J	K	L	M	N	O	P	Q	R	S	T	U	V	W	X
Specimen No.	(microinch)	Location	(degree)	(inch)	(inch)	(inch)	(inch^2)	a/2c	a/t	2c/a																								
C039B	173	E9	3.6	0.061	0.068	0.013	6.943E-04	0.191	21.3	5.2	1	0	0	0	1	1	1	1	1	1	1	0	1	1	1	1	1	1	1	1	1	1	1	1
C047B	160	C8	2.4	0.059	0.036	0.014	3.958E-04	0.389	23.7	2.6	0	0	0	0	0	1	0	1	1	1	1	1	1	1	0	1	1	1	1	0	1	0	1	0
C116A	180	F6	0.0	0.207	0.042	0.014	4.618E-04	0.333	6.8	3.0	0	0	0	0	0	0	0	1	1	1	0	0	0	0	1	1	1	0	1	0	1	0	1	1
C073A	45	F9	3.6	0.209	0.046	0.014	5.058E-04	0.304	6.7	3.3	0	0	0	0	0	0	0	1	1	0	0	1	1	1	1	1	0	1	1	0	0	1	0	0
A018	130	FG7	1.2	0.061	0.055	0.014	6.048E-04	0.255	23.0	3.9	0	0	0	0	0	0	0	0	1	0	0	1	1	1	0	0	1	1	1	0	1	1	1	1
C015A	45	D11	5.9	0.061	0.056	0.014	6.158E-04	0.250	23.0	4.0	1	0	0	1	1	1	1	1	1	1	1	0	0	1	1	1	1	1	0	1	1	0	1	1
A024	230	BC7	1.2	0.057	0.064	0.014	7.037E-04	0.219	24.6	4.6	0	0	0	0	0	0	0	0	0	0	1	0	1	1	0	1	1	1	1	1	1	0	0	0
C002A	60	EF11	5.9	0.058	0.067	0.014	7.367E-04	0.209	24.1	4.8	0	0	0	0	0	1	1	1	1	1	1	1	1	1	1	1	0	1	1	0	1	0	1	1
C012A	35	F6	0.0	0.062	0.077	0.014	8.467E-04	0.182	22.6	5.5	1	0	0	1	0	0	0	1	1	0	1	1	1	1	1	1	1	1	1	1	1	1	1	1
C013A	35	E9	3.6	0.059	0.077	0.014	8.467E-04	0.182	23.7	5.5	0	1	0	0	1	1	1	1	1	1	1	1	1	0	1	1	1	1	1	1	1	1	1	1
C020A	40	BC11	5.9	0.059	0.047	0.015	5.537E-04	0.319	25.4	3.1	1	1	1	0	1	1	1	1	1	1	1	1	1	1	1	1	1	1	1	0	1	1	1	0
C074B	45	C13	3.6	0.208	0.054	0.015	6.362E-04	0.278	7.2	3.6	0	0	0	0	0	0	0	1	0	0	1	1	1	1	1	1	0	1	1	1	1	0	0	1
A015	125	EF5	1.2	0.059	0.059	0.015	6.951E-04	0.254	25.4	3.9	0	0	0	0	0	0	0	0	0	0	0	1	1	0	0	0	1	1	1	1	1	1	0	0
C045B	145	EF14	2.4	0.064	0.067	0.015	7.893E-04	0.224	23.4	4.5	0	0	0	0	0	0	1	1	1	0	1	1	1	1	0	1	1	1	1	0	1	0	1	1
C053A	240	B8	2.4	0.061	0.069	0.015	8.129E-04	0.217	24.6	4.6	0	0	0	1	1	1	1	1	1	1	1	1	1	1	1	1	1	1	1	0	1	0	1	1
A012	60	EF9	3.6	0.056	0.069	0.015	8.129E-04	0.217	26.8	4.6	0	0	0	0	0	0	1	0	0	0	0	0	1	0	0	1	1	0	1	1	1	1	1	1
C003B	45	D14	2.4	0.059	0.074	0.015	8.718E-04	0.203	25.4	4.9	0	0	0	0	0	1	0	0	1	1	1	1	1	1	1	1	1	1	1	1	1	1	0	1
C014A	40	F7	1.2	0.061	0.077	0.015	9.071E-04	0.195	24.6	5.1	0	0	0	0	0	0	0	1	1	1	1	1	1	1	1	1	1	1	1	0	1	1	1	0
C019B	60	E10	4.8	0.058	0.079	0.015	9.307E-04	0.190	25.9	5.3	1	1	1	1	1	1	1	1	1	0	1	1	1	1	1	1	1	1	1	1	1	1	1	1
C019B	60	F15	1.2	0.058	0.083	0.015	9.778E-04	0.181	25.9	5.5	1	0	0	1	1	1	1	1	1	0	1	1	1	1	1	1	1	1	1	1	1	1	1	1
C084A	45	C8	2.4	0.210	0.049	0.016	6.158E-04	0.327	7.6	3.1	0	0	0	0	0	0	1	1	1	0	1	1	1	0	1	1	0	1	1	0	1	0	0	1
C101A	300	CD14	2.4	0.210	0.055	0.016	6.912E-04	0.291	7.6	3.4	0	0	0	1	0	0	0	1	0	1	1	1	1	0	1	1	0	0	1	0	1	0	1	1
A002	30	CD13	3.6	0.059	0.068	0.016	8.545E-04	0.235	27.1	4.3	0	0	0	0	0	0	0	1	1	0	1	1	1	0	0	0	1	1	1	0	1	1	0	1
C019B	60	E12	4.8	0.058	0.070	0.016	8.796E-04	0.229	27.6	4.4	0	0	0	0	0	1	1	1	1	0	1	1	1	1	1	1	1	1	1	1	1	1	1	0
C018A	50	C11	5.9	0.061	0.072	0.016	9.048E-04	0.222	26.2	4.5	0	0	0	0	0	1	1	1	1	1	1	1	1	1	0	1	1	1	1	1	1	1	1	0
C044A	140	BC10	4.8	0.060	0.026	0.017	3.471E-04	0.654	28.3	1.5	0	0	0	0	0	1	1	1	0	0	1	0	1	1	1	1	1	1	1	1	0	1	1	1
C044A	140	B14	2.4	0.060	0.033	0.017	4.406E-04	0.515	28.3	1.9	0	0	0	0	0	0	0	1	0	0	1	0	1	1	1	1	1	1	0	0	1	0	0	0
C047A	160	DE15	1.2	0.059	0.047	0.017	6.275E-04	0.362	28.8	2.8	0	0	0	0	0	1	0	1	1	0	0	1	1	1	1	1	1	1	1	0	1	1	1	0
C033A	150	DE14	2.4	0.059	0.049	0.017	6.542E-04	0.347	28.8	2.9	0	0	0	0	0	0	0	1	0	0	0	0	0	1	1	1	0	1	1	0	0	1	1	0
C100A	205	EF9	3.6	0.208	0.055	0.017	7.343E-04	0.309	8.2	3.2	0	0	0	0	0	0	0	1	0	0	0	0	0	0	0	0	0	0	0	0	1	0	0	0
A017	130	EF7	1.2	0.061	0.065	0.017	8.679E-04	0.262	27.9	3.8	0	0	0	0	0	0	0	0	0	0	0	0	0	1	0	0	0	1	1	1	0	1	1	1
C036A	140	BC12	4.8	0.061	0.073	0.017	9.747E-04	0.233	27.9	4.3	1	0	0	1	1	1	1	1	1	1	1	1	1	1	1	1	1	1	1	1	1	1	1	1
C019A	60	C13	3.6	0.058	0.086	0.017	1.148E-03	0.198	29.3	5.1	1	1	1	1	1	1	1	1	1	0	1	1	1	1	0	1	1	1	1	1	0	1	1	1
C052A	180	BC14	2.4	0.061	0.090	0.017	1.202E-03	0.189	27.9	5.3	1	1	0	1	1	1	1	1	1	1	1	1	1	1	1	1	1	1	1	1	1	1	1	1
C048A	160	B10	4.8	0.059	0.045	0.018	6.362E-04	0.400	30.5	2.5	1	0	0	1	0	0	1	1	1	1	1	1	1	1	1	1	1	1	1	0	1	1	1	0
C109B	160	EF12	4.8	0.208	0.066	0.018	9.331E-04	0.273	8.7	3.7	0	0	0	0	0	1	0	0	1	0	1	1	0	0	0	1	1	1	1	0	1	1	1	1
A023	230	CD5	1.2	0.059	0.069	0.018	9.755E-04	0.261	30.5	3.8	0	0	0	0	0	0	0	1	0	1	1	1	1	1	0	0	0	0	0	0	1	1	1	1
C025A	45	D8	2.4	0.061	0.079	0.018	1.117E-03	0.228	29.5	4.4	1	1	0	1	0	1	1	1	1	0	1	1	1	1	1	1	1	1	1	0	1	1	1	1
C007A	50	EF7	1.2	0.059	0.087	0.018	1.230E-03	0.207	30.5	4.8	0	0	1	0	0	1	1	1	0	0	1	1	1	1	1	1	1	1	1	1	1	1	1	1
C068A	45	F9	3.6	0.209	0.061	0.019	9.103E-04	0.311	9.1	3.2	0	0	0	0	0	0	0	1	1	1	0	1	1	1	1	1	0	1	1	1	1	1	1	1
A006	32	DE8	2.4	0.062	0.081	0.019	1.209E-03	0.235	30.6	4.3	0	0	0	0	0	0	0	0	0	0	0	0	0	1	0	0	1	1	1	1	0	1	1	0
A020	230	CD14	2.4	0.060	0.085	0.019	1.268E-03	0.224	31.7	4.5	0	0	0	0	0	1	0	1	1	0	0	1	1	1	0	1	1	1	1	1	1	1	1	1
C019B	60	F7	1.2	0.058	0.086	0.019	1.283E-03	0.221	32.8	4.5	0	0	0	0	1	1	1	1	1	1	0	1	1	1	1	1	1	1	1	1	1	0	1	1
C048A	160	EF9	3.6	0.059	0.026	0.020	4.084E-04	0.769	33.9	1.3	1	0	0	0	0	1	0	1	1	1	1	1	1	1	1	1	1	1	1	1	0	1	1	1
C034A	80	BC8	2.4	0.059	0.058	0.020	9.111E-04	0.345	33.9	2.9	1	0	0	0	1	0	1	1	1	0	1	1	1	1	1	1	1	1	1	1	1	0	1	0
C028B	50	BC11	5.9	0.059	0.059	0.020	9.268E-04	0.339	33.9	3.0	0	0	0	0	0	0	0	1	1	1	1	1	0	0	0	0	1	1	1	0	1	0	1	0
C069A	50	E7	1.2	0.209	0.066	0.020	1.037E-03	0.303	9.6	3.3	0	0	0	0	0	0	0	1	1	1	1	1	1	1	1	1	0	1	1	1	1	1	1	0
C003A	45	EF9	3.6	0.059	0.082	0.020	1.288E-03	0.244	33.9	4.1	0	0	0	0	1	1	1	1	1	1	1	1	1	1	1	1	1	1	1	1	1	1	1	1
C006A	55	E9	3.6	0.059	0.084	0.020	1.319E-03	0.238	33.9	4.2	0	0	0	0	0	0	0	1	1	0	1	0	0	0	0	1	0	0	0	1	1	0	0	0
C052A	180	B9	3.6	0.061	0.086	0.020	1.351E-03	0.233	32.8	4.3	1	1	0	0	1	1	1	1	1	1	1	1	1	1	1	1	1	1	1	1	1	1	1	1
A023	230	DE15	1.2	0.059	0.089	0.020	1.398E-03	0.225	33.9	4.5	0	0	0	0	0	0	0	1	1	1	1	1	1	1	0	1	1	0	0	0	1	1	1	1
C025A	45	FG12	4.8	0.061	0.015	0.021	2.474E-04	1.400	34.4	0.7	0	0	0	0	0	0	0	0	0	0	0	0	0	0	0	0	0	0	0	0	0	0	0	0
C033A	150	EF10	4.8	0.059	0.060	0.021	9.896E-04	0.350	35.6	2.9	0	0	0	0	0	1	0	0	1	1	1	1	1	1	1	1	1	1	1	1	1	0	1	1
C047B	160	B11	5.9	0.059	0.062	0.021	1.023E-03	0.339	35.6	3.0	0	0	0	0	0	0	1	1	1	1	1	1	1	0	1	1	1	1	1	0	1	1	1	0
C054B	300	E17	1.2	0.061	0.063	0.021	1.039E-03	0.333	34.4	3.0	1	1	1	1	0	0	0	1	1	1	1	1	1	1	1	1	1	1	1	1	1	1	1	1
C069A	50	E13	3.6	0.209	0.064	0.021	1.056E-03	0.328	10.0	3.0	0	0	0	0	0	0	0	1	0	1	1	1	1	1	1	1	0	1	1	1	1	1	1	1
C084A	45	A10	4.8	0.210	0.069	0.021	1.138E-03	0.304	10.0	3.3	0	0	0	0	0	1	0	0	0	1	0	1	1	1	1	1	1	1	1	1	0	1	1	1
A022	230	BC13	3.6	0.061	0.069	0.021	1.138E-03	0.304	34.4	3.3	0	0	0	0	0	0	0	0	1	1	1	0	0	0	0	1	1	1	1	1	1	0	0	0
A005	32	BC2	4.8	0.063	0.075	0.021	1.237E-03	0.280	33.3	3.6	0	0	0	0	0	0	0	1	0	1	0	1	1	1	0	0	1	1	1	1	1	1	0	1
A010	60	BC15	1.2	0.060	0.078	0.021	1.286E-03	0.269	35.0	3.7	1	1	0	1	0	0	0	1	1	1	1	1	1	1	0	1	1	1	1	1	1	0	1	1

Specimen Characteristics											Radiographic Inspections							Penetrant Inspections							Ultrasonics Inspections					Eddy Current Inspections				
Specimen No.	Surface Finish (microinch)	Location	Incld Angle (degree)	Thick (t) (inch)	Length (2c) (inch)	Depth (a) (inch)	Area (inch^2)	a/2c	a/t	2c/a	A	B	C	D	E	F	G	H	I	J	K	L	M	N	O	P	Q	R	S	T	U	V	W	X
C041A	260	CD15	1.2	0.060	0.080	0.021	1.319E-03	0.263	35.0	3.8	0	0	0	0	0	1	1	1	1	1	1	1	1	1	1	1	0	1	1	1	1	1	1	1
A024	230	BC2	4.8	0.057	0.084	0.021	1.385E-03	0.250	36.8	4.0	0	0	0	0	0	0	0	0	0	0	0	0	0	0	1	0	1	1	1	1	1	1	0	0
C018A	50	B13	3.6	0.061	0.091	0.021	1.501E-03	0.231	34.4	4.3	1	0	0	1	1	1	1	1	1	1	1	1	1	1	1	1	1	1	1	1	1	1	1	1
C050B	140	E8	2.4	0.063	0.096	0.021	1.583E-03	0.219	33.3	4.6	1	1	0	0	0	1	1	1	1	1	1	1	1	1	1	1	1	1	1	1	1	1	1	1
A024	230	FG7	1.2	0.057	0.104	0.021	1.715E-03	0.202	36.8	5.0	1	0	0	0	0	0	0	1	0	0	1	0	1	1	0	1	1	1	1	1	1	1	1	1
C055B	300	B8	2.4	0.054	0.069	0.022	1.192E-03	0.319	40.7	3.1	0	0	0	1	1	1	1	1	1	1	1	1	1	1	0	1	1	1	1	1	1	1	1	1
C116A	180	B9	3.6	0.207	0.072	0.022	1.244E-03	0.306	10.6	3.3	0	0	0	0	0	0	0	1	1	1	1	1	0	1	1	1	1	1	0	1	1	0	1	1
A009	60	EF5	1.2	0.059	0.073	0.022	1.261E-03	0.301	37.3	3.3	0	0	0	0	0	0	0	1	0	1	1	1	1	0	0	1	1	1	1	1	1	1	1	1
A008	60	EF8	2.4	0.059	0.080	0.022	1.382E-03	0.275	37.3	3.6	0	0	0	0	0	0	0	1	1	1	1	1	1	1	0	1	1	1	1	1	1	1	1	1
C070A	45	BC7	1.2	0.206	0.087	0.022	1.503E-03	0.253	10.7	4.0	0	0	0	0	1	0	0	1	1	1	1	1	1	1	1	1	0	1	1	1	1	1	1	1
A017	130	BC15	1.2	0.061	0.089	0.022	1.538E-03	0.247	36.1	4.0	0	0	0	0	0	0	0	1	1	1	1	0	1	0	0	1	1	1	1	0	1	1	1	1
C039B	173	D6	0.0	0.061	0.091	0.022	1.572E-03	0.242	36.1	4.1	1	0	0	1	1	1	1	1	1	1	1	1	1	1	1	1	1	1	1	1	1	0	1	1
C068A	45	B10	4.8	0.209	0.064	0.023	1.156E-03	0.359	11.0	2.8	0	0	0	0	0	0	0	1	1	1	1	1	1	1	1	1	0	1	1	1	1	0	1	1
C101A	300	C6	0.0	0.210	0.064	0.023	1.156E-03	0.359	11.0	2.8	0	0	0	1	0	0	0	1	1	1	1	1	1	1	1	1	1	1	0	0	1	0	0	1
C108A	150	F11	5.9	0.209	0.070	0.023	1.264E-03	0.329	11.0	3.0	0	0	0	0	0	0	0	1	0	0	0	0	0	0	1	1	0	0	1	1	1	0	0	0
C073A	45	E14	2.4	0.209	0.071	0.023	1.283E-03	0.324	11.0	3.1	0	0	0	0	0	0	0	1	1	0	1	1	1	1	1	1	1	1	1	1	1	1	1	0
A010	60	EF3	3.6	0.060	0.075	0.023	1.355E-03	0.307	38.3	3.3	0	0	0	0	0	0	0	1	1	1	1	1	1	1	0	1	1	1	1	1	1	1	1	1
C033B	150	CD8	2.4	0.059	0.062	0.024	1.169E-03	0.387	40.7	2.6	1	0	0	0	1	1	1	1	1	1	1	1	1	1	0	1	1	1	1	1	1	1	1	0
C034A	80	BC16	0.0	0.059	0.062	0.024	1.169E-03	0.387	40.7	2.6	1	1	0	0	1	1	1	1	1	0	1	1	1	1	1	1	1	1	1	1	1	1	1	0
C109A	160	BC14	2.4	0.208	0.063	0.024	1.188E-03	0.381	11.5	2.6	0	0	0	0	0	0	0	1	1	1	1	1	1	1	1	1	1	1	1	1	0	1	1	0
C009A	50	CD6	0.0	0.057	0.066	0.024	1.244E-03	0.364	42.1	2.8	0	0	0	0	1	0	1	1	1	1	1	1	1	1	1	1	1	1	1	1	1	1	1	1
A006	32	EF13	3.6	0.062	0.067	0.024	1.263E-03	0.358	38.7	2.8	0	0	0	0	1	0	0	0	0	1	1	0	1	1	0	1	1	1	1	0	1	1	1	1
C018A	150	D15	1.2	0.209	0.073	0.024	1.376E-03	0.329	11.5	3.0	0	0	0	0	0	0	0	1	1	1	1	1	1	1	1	1	1	1	1	1	1	1	1	1
A005	32	FG4	2.4	0.063	0.085	0.024	1.602E-03	0.282	38.1	3.5	0	0	0	0	0	0	0	1	1	1	1	1	1	1	0	1	1	1	1	1	1	1	1	1
A009	60	CD10	4.8	0.059	0.090	0.024	1.696E-03	0.267	40.7	3.8	0	0	0	0	0	0	0	1	0	1	1	1	1	1	0	1	1	1	1	1	1	0	1	1
C047A	160	F7	1.2	0.059	0.067	0.025	1.316E-03	0.373	42.4	2.7	1	0	0	0	0	1	1	0	1	1	1	1	1	1	1	1	1	1	1	1	1	1	1	1
C116A	180	F13	3.6	0.207	0.069	0.025	1.355E-03	0.362	12.1	2.8	0	0	0	0	0	0	0	1	1	0	0	0	0	0	1	1	1	0	1	0	1	0	1	1
C069A	50	E15	1.2	0.209	0.071	0.025	1.394E-03	0.352	12.0	2.8	0	0	0	0	0	0	0	1	0	1	1	1	1	0	1	1	0	1	1	1	1	1	1	0
C055A	300	E7	1.2	0.054	0.076	0.025	1.492E-03	0.329	46.3	3.0	0	0	0	0	0	0	1	1	1	1	1	1	1	1	1	1	1	1	1	1	1	1	1	1
C073A	45	EF12	4.8	0.209	0.080	0.025	1.571E-03	0.313	12.0	3.2	0	0	0	0	0	0	0	0	1	0	1	1	1	1	1	1	1	1	1	1	1	1	1	0
C021B	55	E10	4.8	0.059	0.092	0.025	1.806E-03	0.272	42.4	3.7	0	1	0	1	1	1	1	1	1	1	1	1	1	1	1	1	1	1	1	1	1	1	1	1
A017	130	EF3	3.6	0.061	0.096	0.025	1.885E-03	0.260	41.0	3.8	0	0	0	0	0	0	0	1	1	1	1	0	1	0	0	1	1	1	1	0	1	1	1	1
C039B	173	D14	2.4	0.061	0.097	0.025	1.905E-03	0.258	41.0	3.9	1	0	0	1	1	1	1	1	1	1	1	1	1	1	1	1	1	1	1	1	1	1	1	1
C001A	85	D11	5.9	0.052	0.242	0.025	4.752E-03	0.103	48.1	9.7	1	1	1	0	1	1	1	1	1	1	1	1	1	1	0	1	1	1	1	0	1	1	0	1
C106A	160	BC6	0.0	0.209	0.312	0.025	6.126E-03	0.080	12.0	12.5	0	0	0	0	0	1	0	1	1	1	1	1	1	1	1	1	1	1	1	1	1	1	1	1
C007A	50	BC1	5.9	0.059	0.060	0.026	1.225E-03	0.433	44.1	2.3	1	0	0	0	1	1	1	1	0	0	1	1	1	1	1	1	1	1	1	1	1	0	1	0
C002A	60	E7	1.2	0.058	0.060	0.026	1.225E-03	0.433	44.8	2.3	0	0	0	0	0	0	1	0	1	1	1	1	1	1	1	1	1	1	1	1	1	1	1	1
C045A	145	B6	0.0	0.064	0.066	0.026	1.348E-03	0.394	40.6	2.5	0	0	0	0	0	0	0	0	0	1	0	0	0	0	0	0	0	1	0	0	0	0	0	0
C017A	60	E6	0.0	0.057	0.069	0.026	1.409E-03	0.377	45.6	2.7	0	0	0	0	0	1	1	1	1	1	0	1	1	1	1	1	1	1	1	1	1	1	1	1
C013B	140	E13	3.6	0.208	0.073	0.026	1.491E-03	0.356	12.5	2.8	0	0	0	0	0	0	0	0	1	0	1	1	1	1	0	1	1	1	1	1	1	0	1	0
C081A	40	B7	1.2	0.208	0.075	0.026	1.532E-03	0.347	12.5	2.9	0	0	0	0	1	0	0	0	1	1	1	1	1	1	0	1	1	0	1	1	1	1	1	1
C094A	140	EF9	3.6	0.210	0.076	0.026	1.552E-03	0.342	12.4	2.9	0	0	0	0	0	0	0	0	1	1	1	1	1	1	1	0	1	0	0	1	1	1	1	1
A018	130	FG2	4.8	0.061	0.081	0.026	1.654E-03	0.321	42.6	3.1	0	0	0	0	0	0	0	0	1	0	0	1	1	1	0	1	1	1	1	1	1	1	1	1
C045B	145	C07	1.2	0.064	0.102	0.026	2.083E-03	0.255	40.6	3.9	1	1	0	0	1	1	0	1	1	1	1	1	1	1	1	1	1	1	1	1	1	1	1	1
A012	60	DE1	5.9	0.056	0.296	0.026	6.044E-03	0.088	46.4	11.4	1	1	1	1	1	0	1	1	1	1	1	0	1	1	1	1	1	1	1	1	1	0	1	1
C007A	50	C8	2.4	0.059	0.067	0.027	1.421E-03	0.403	45.8	2.5	0	0	0	0	0	0	0	1	0	0	1	1	1	1	1	1	1	1	1	1	1	1	1	1
C034A	80	EF1	5.9	0.059	0.070	0.027	1.484E-03	0.386	45.8	2.6	0	0	0	0	0	0	0	1	0	0	0	1	1	1	1	1	1	1	1	1	1	1	1	1
C110A	145	BC1	4.8	0.209	0.075	0.027	1.590E-03	0.360	12.9	2.8	0	0	0	0	0	0	0	1	1	1	1	1	0	1	1	1	1	1	1	1	1	0	1	1
C068A	45	F14	2.4	0.209	0.084	0.027	1.781E-03	0.321	12.9	3.1	0	0	0	0	0	0	0	1	1	0	1	1	1	1	1	1	1	0	1	1	1	1	1	1
A005	32	EF7	1.2	0.063	0.094	0.027	1.993E-03	0.287	42.9	3.5	0	0	0	0	0	0	1	0	1	1	1	1	1	1	1	0	1	1	1	1	1	1	1	1
C042B	55	EF1	3.6	0.069	0.095	0.027	2.015E-03	0.284	39.1	3.5	0	1	0	1	1	1	1	1	1	1	1	1	1	1	1	0	1	1	1	1	0	1	1	1
B024	230	BC3	3.6	0.211	0.109	0.027	2.311E-03	0.248	12.8	4.0	0	0	0	0	0	0	0	1	0	1	1	1	1	1	0	0	1	1	1	1	1	1	1	1
C117A	220	BC7	1.2	0.208	0.078	0.028	1.715E-03	0.359	13.5	2.8	0	0	0	0	0	1	1	1	1	1	1	0	1	1	1	1	1	1	1	0	1	1	1	1
C033B	150	BC1	4.8	0.059	0.078	0.028	1.715E-03	0.359	47.5	2.8	1	1	1	0	0	1	1	1	1	1	1	1	1	1	0	1	1	1	1	1	1	1	1	0
C084A	45	DE1	2.4	0.210	0.080	0.028	1.759E-03	0.350	13.3	2.9	0	0	0	1	0	0	1	1	1	1	0	1	1	1	1	1	1	1	1	1	1	1	1	1
C086A	35	B11	5.9	0.206	0.097	0.028	2.133E-03	0.289	13.6	3.5	0	0	0	0	0	0	0	1	1	1	1	1	1	1	1	1	1	0	1	1	1	1	1	1
C006A	55	BC1	4.8	0.059	0.150	0.028	3.299E-03	0.187	47.5	5.4	1	1	1	1	0	0	0	1	1	0	1	0	0	0	1	1	0	0	0	1	1	0	0	0
C026A	290	C8	2.4	0.056	0.083	0.029	1.890E-03	0.349	51.8	2.9	0	0	0	0	1	1	1	1	1	1	0	1	1	1	1	1	1	1	1	1	1	1	1	0
C004B	45	F9	3.6	0.060	0.083	0.029	1.890E-03	0.349	48.3	2.9	1	1	1	0	0	1	1	1	1	1	1	1	1	1	1	1	1	1	1	1	1	1	1	1
A022	230	FG3	3.6	0.061	0.085	0.029	1.936E-03	0.341	47.5	2.9	0	0	0	0	0	0	0	1	1	1	1	1	1	1	0	1	1	1	1	1	1	1	1	1

Specimen Characteristics											Radiographic Inspections							Penetrant Inspections							Ultrasonics Inspections					Eddy Current Inspections				
	Surface Finish		Incld Angle	Thick (t)	Length (2c)	Depth (a)	Area				A	B	C	D	E	F	G	H	I	J	K	L	M	N	O	P	Q	R	S	T	U	V	W	X
Specimen No.	(microinch)	Location	(degree)	(inch)	(inch)	(inch)	(inch^2)	a/2c	a/t	2c/a																								
A011	60	BC15	1.2	0.062	0.086	0.029	1.959E-03	0.337	46.8	3.0	0	0	0	0	0	0	0	1	0	1	1	1	1	1	1	1	1	1	1	1	1	1	1	1
C028A	50	D7	1.2	0.059	0.079	0.030	1.861E-03	0.380	50.8	2.6	1	1	0	0	1	0	0	1	1	1	1	1	1	1	1	1	1	1	1	1	1	1	1	1
C034A	80	DE14	2.4	0.059	0.080	0.030	1.885E-03	0.375	50.8	2.7	1	1	1	1	1	1	1	1	1	0	1	1	1	1	1	1	1	1	1	1	1	1	1	1
C027B	50	C7	1.2	0.059	0.083	0.030	1.956E-03	0.361	50.8	2.8	0	1	0	1	1	1	1	1	1	1	1	1	1	1	1	1	1	1	1	1	1	1	1	1
B004	32	BC14	2.4	0.211	0.116	0.030	2.733E-03	0.259	14.2	3.9	0	0	0	0	0	0	0	1	0	1	1	1	1	1	0	1	1	1	1	1	1	0	0	1
C016A	50	E9	3.6	0.059	0.248	0.030	5.843E-03	0.121	50.8	8.3	1	1	1	1	1	1	1	1	1	1	1	1	1	1	1	1	1	1	1	1	1	1	1	1
C048A	160	F12	4.8	0.059	0.079	0.031	1.923E-03	0.392	52.5	2.5	1	0	0	0	1	1	1	1	1	1	1	1	1	1	1	1	1	1	1	1	1	1	1	1
C033A	150	F6	0.0	0.059	0.082	0.031	1.996E-03	0.378	52.5	2.6	0	0	0	1	0	1	0	1	1	1	1	1	1	1	1	1	1	1	1	1	1	1	1	1
C040B	290	CD11	5.9	0.058	0.086	0.031	2.094E-03	0.360	53.4	2.8	1	1	1	1	1	1	1	1	1	1	1	1	1	1	1	1	1	1	1	1	1	1	1	1
C110A	145	F8	2.4	0.209	0.098	0.031	2.386E-03	0.316	14.8	3.2	0	0	0	0	0	1	0	0	1	1	1	1	1	1	1	1	1	1	1	1	1	1	1	1
B024	230	FG3	3.6	0.211	0.118	0.031	2.873E-03	0.263	14.7	3.8	0	0	0	0	0	0	0	1	0	1	1	1	1	0	0	1	1	1	1	1	1	1	1	1
C016A	50	DE5	1.2	0.059	0.253	0.031	6.160E-03	0.123	52.5	8.2	1	1	1	1	1	1	1	1	1	1	1	1	1	1	1	1	1	1	1	1	1	1	1	1
C056A	40	D6	0.0	0.207	0.290	0.031	7.061E-03	0.107	15.0	9.4	0	1	0	0	1	1	1	1	1	1	1	1	1	1	1	1	1	1	1	0	1	1	1	1
C002A	60	EF9	3.6	0.058	0.082	0.032	2.061E-03	0.390	55.2	2.6	0	1	1	0	1	1	1	1	1	1	1	1	1	1	1	1	1	1	1	1	1	1	1	1
C111A	100	EF15	1.2	0.209	0.092	0.032	2.312E-03	0.348	15.3	2.9	0	0	0	0	0	0	0	1	1	1	1	0	1	1	1	1	1	1	1	1	1	1	1	1
C101A	300	BC9	3.6	0.210	0.094	0.032	2.362E-03	0.340	15.2	2.9	0	0	0	1	0	0	0	1	1	1	1	1	1	1	1	1	1	1	1	1	1	1	1	1
C086A	35	CD9	3.6	0.206	0.095	0.032	2.388E-03	0.337	15.5	3.0	0	0	0	0	0	0	0	1	1	1	1	1	1	1	1	1	0	1	0	1	1	1	1	1
C100A	205	B13	3.6	0.208	0.097	0.032	2.438E-03	0.330	15.4	3.0	0	0	0	0	0	0	1	1	1	1	1	1	1	1	1	1	0	1	1	1	1	1	1	1
C022B	55	D14	2.4	0.057	0.241	0.032	6.057E-03	0.133	56.1	7.5	1	1	0	1	1	1	1	1	1	1	1	1	1	1	1	1	1	1	1	1	1	1	1	1
C031A	150	E6	0.0	0.060	0.249	0.032	6.258E-03	0.129	53.3	7.8	1	0	0	1	1	1	1	1	1	1	1	1	1	1	1	1	1	1	1	1	1	1	1	1
A004	30	DE9	3.6	0.063	0.340	0.032	8.545E-03	0.094	50.8	10.6	1	1	1	1	1	0	0	1	1	1	1	0	0	0	1	1	0	0	0	1	1	0	0	0
C109A	160	BC6	0.0	0.208	0.076	0.033	1.970E-03	0.434	15.9	2.3	0	0	0	0	0	0	0	1	1	1	1	0	0	0	1	1	0	0	0	1	1	0	0	0
C048A	160	BC12	4.8	0.059	0.085	0.033	2.203E-03	0.388	55.9	2.6	1	0	1	1	1	1	1	1	1	1	1	1	1	1	1	1	1	1	1	1	1	1	1	1
C020A	40	C8	2.4	0.059	0.085	0.033	2.203E-03	0.388	55.9	2.6	1	0	1	1	1	1	1	1	1	1	1	1	1	1	1	1	1	1	1	1	1	1	1	1
C081A	40	C13	3.6	0.208	0.088	0.033	2.281E-03	0.375	15.9	2.7	0	0	0	1	0	0	0	1	1	1	1	1	1	1	1	1	0	1	1	1	1	1	1	1
C047A	160	E10	4.8	0.059	0.108	0.033	2.799E-03	0.306	55.9	3.3	1	0	0	0	1	0	1	1	1	1	1	1	1	1	1	1	1	1	1	1	1	1	1	1
B017	130	FG10	4.8	0.212	0.123	0.033	3.188E-03	0.268	15.6	3.7	0	0	0	0	0	0	0	1	1	1	1	1	1	1	1	1	1	1	1	1	1	1	1	1
C031A	150	B14	2.4	0.060	0.249	0.033	6.454E-03	0.133	55.0	7.5	1	1	1	1	1	1	1	1	1	1	1	1	1	1	1	1	1	1	1	1	1	1	1	1
C016A	50	DE13	3.6	0.059	0.257	0.033	6.661E-03	0.128	55.9	7.8	1	1	1	1	1	1	1	1	1	1	1	1	1	1	1	1	1	1	1	1	1	1	1	1
C022A	55	C10	4.8	0.057	0.258	0.033	6.687E-03	0.128	57.9	7.8	1	1	1	1	1	1	1	1	1	1	1	1	1	1	1	1	1	1	1	1	1	1	1	1
C043A	160	E9	3.6	0.057	0.260	0.033	6.739E-03	0.127	57.9	7.9	1	1	1	1	1	1	1	1	1	1	1	1	1	1	1	1	1	1	1	1	1	1	1	1
C046B	150	E10	4.8	0.060	0.261	0.033	6.765E-03	0.126	55.0	7.9	1	1	1	1	1	1	1	1	1	1	1	1	1	1	1	1	1	1	1	1	1	1	1	1
C100A	205	D10	4.8	0.208	0.076	0.034	2.029E-03	0.447	16.3	2.2	0	0	0	0	1	1	1	1	1	1	1	1	1	1	1	1	1	1	1	1	1	1	1	1
A004	30	BC12	4.8	0.063	0.111	0.034	2.964E-03	0.306	54.0	3.3	1	0	1	0	0	0	0	1	1	1	1	1	1	1	1	1	1	1	1	1	1	0	1	1
B006	32	BC3	3.6	0.211	0.124	0.034	3.311E-03	0.274	16.1	3.6	0	0	0	0	0	0	0	0	0	0	1	1	1	0	1	1	1	1	1	1	1	1	1	1
C008A	50	C14	2.4	0.058	0.275	0.034	7.343E-03	0.124	58.6	8.1	1	1	1	1	1	1	1	1	1	1	1	1	1	1	1	1	1	1	1	1	1	1	1	1
A016	125	DE7	1.2	0.058	0.288	0.034	7.691E-03	0.118	58.6	8.5	1	1	1	1	1	1	1	1	1	1	1	1	1	1	1	1	1	1	1	1	1	1	1	1
C092B	160	C7	1.2	0.209	0.301	0.034	8.038E-03	0.113	16.3	8.9	0	0	0	0	0	1	1	1	1	1	1	1	1	1	1	1	1	1	1	1	1	1	1	1
C058A	40	DE15	1.2	0.208	0.310	0.034	8.278E-03	0.110	16.3	9.1	0	0	0	0	1	0	1	0	0	1	1	1	1	1	1	1	1	1	1	1	1	1	1	1
C094A	140	D7	1.2	0.210	0.098	0.035	2.694E-03	0.357	16.7	2.8	0	0	1	0	0	1	0	1	1	1	1	1	1	1	0	1	0	0	1	1	1	1	1	1
C081A	40	E11	5.9	0.208	0.100	0.035	2.749E-03	0.350	16.8	2.9	0	0	0	0	1	0	0	1	1	1	1	1	1	1	1	1	1	1	1	1	1	1	1	1
C101A	300	EF11	5.9	0.210	0.103	0.035	2.831E-03	0.340	16.7	2.9	0	0	0	0	1	1	1	1	1	1	1	1	1	1	1	1	1	1	0	1	1	1	1	1
C101A	300	BC12	4.8	0.210	0.106	0.035	2.914E-03	0.330	16.7	3.0	0	0	0	0	1	0	0	1	1	1	1	1	1	1	1	1	1	1	1	1	1	1	1	1
B005	32	BC4	2.4	0.213	0.121	0.035	3.326E-03	0.289	16.4	3.5	0	0	0	0	0	0	0	1	1	1	1	1	0	1	0	0	1	1	1	1	1	1	1	1
C043A	160	DE5	1.2	0.057	0.256	0.035	7.037E-03	0.137	61.4	7.3	1	1	1	1	1	1	1	1	1	1	1	1	1	1	1	1	1	1	1	1	1	1	1	1
C046A	150	C6	0.0	0.060	0.257	0.035	7.065E-03	0.136	58.3	7.3	1	1	1	1	1	1	1	1	1	1	1	1	1	1	1	1	1	1	1	1	1	1	1	1
C043A	160	DE13	3.6	0.057	0.258	0.035	7.092E-03	0.136	61.4	7.4	1	1	1	1	1	1	1	1	1	1	1	1	1	1	1	1	1	1	1	1	1	1	1	1
C005A	45	C10	4.8	0.061	0.258	0.035	7.092E-03	0.136	57.4	7.4	1	1	1	1	1	1	1	1	1	1	1	1	1	1	1	1	1	1	1	1	1	1	1	1
C008A	50	D6	0.0	0.058	0.259	0.035	7.120E-03	0.135	60.3	7.4	1	1	1	1	1	1	1	1	1	1	1	1	1	1	1	1	1	1	1	1	1	1	1	1
C035A	220	D9	3.6	0.061	0.268	0.035	7.367E-03	0.131	57.4	7.7	1	1	0	1	1	1	1	1	1	1	1	1	1	1	1	1	1	1	1	1	1	1	1	1
C108A	150	B11	5.9	0.209	0.095	0.036	2.686E-03	0.379	17.2	2.6	0	0	0	0	0	0	0	1	1	1	1	1	1	1	1	1	1	1	1	1	1	1	1	1
C069A	50	B10	4.8	0.209	0.096	0.036	2.714E-03	0.375	17.2	2.7	0	0	0	0	0	0	0	1	1	1	1	1	1	0	1	1	1	1	1	1	1	1	1	1
A011	60	EF13	3.6	0.062	0.098	0.036	2.771E-03	0.367	58.1	2.7	1	0	0	0	0	0	0	1	1	1	1	1	1	1	1	1	1	1	1	1	1	1	1	1
C074B	45	CD9	3.6	0.208	0.103	0.036	2.912E-03	0.350	17.3	2.9	0	0	0	1	0	0	0	1	1	1	1	1	1	1	0	1	1	1	1	0	1	1	1	1
A018	130	CD2	4.8	0.061	0.123	0.036	3.478E-03	0.293	59.0	3.4	1	0	0	1	0	0	0	0	1	0	0	1	1	1	1	1	1	1	1	1	1	1	1	1
C005A	45	C6	0.0	0.061	0.247	0.036	6.984E-03	0.146	59.0	6.9	1	1	1	1	1	1	1	1	1	1	1	1	1	1	1	1	1	1	1	1	1	1	1	1
C078A	40	C7	1.2	0.207	0.250	0.036	7.069E-03	0.144	17.4	6.9	0	1	0	0	1	1	0	1	1	1	1	1	1	1	1	1	1	1	1	1	1	1	1	1
C029A	120	D10	4.8	0.059	0.252	0.036	7.125E-03	0.143	61.0	7.0	1	1	1	1	1	1	1	1	1	1	1	1	1	1	1	1	1	1	1	1	1	1	1	1
A016	125	EF10	4.8	0.058	0.290	0.036	8.200E-03	0.124	62.1	8.1	1	1	1	1	1	1	1	1	1	1	1	1	1	1	1	1	1	1	1	1	1	0	1	1
C107A	140	EF7	1.2	0.210	0.304	0.036	8.595E-03	0.118	17.1	8.4	0	0	0	0	1	0	0	1	1	1	1	1	1	1	1	1	1	1	1	1	1	1	1	1

Specimen Characteristics											Radiographic Inspections							Penetrant Inspections							Ultrasonics Inspections					Eddy Current Inspections				
	Surface Finish		Incld Angle	Thick (t)	Length (2c)	Depth (a)	Area				A	B	C	D	E	F	G	H	I	J	K	L	M	N	O	P	Q	R	S	T	U	V	W	X
Specimen No.	(microinch)	Location	(degree)	(inch)	(inch)	(inch)	(inch^2)	a/2c	a/t	2c/a																								
A003	32	BC8	2.4	0.054	0.318	0.036	8.991E-03	0.113	66.7	8.8	1	1	1	1	1	1	1	1	1	1	1	1	1	1	1	1	1	1	1	1	1	1	1	1
A012	60	CD7	1.2	0.056	0.340	0.036	9.613E-03	0.106	64.3	9.4	1	1	1	1	0	0	1	1	1	1	1	0	1	1	1	1	1	1	1	1	1	1	1	1
C054A	300	B15	1.2	0.061	0.101	0.037	2.935E-03	0.366	60.7	2.7	1	1	1	1	1	1	1	1	1	1	1	1	1	1	1	1	1	1	1	1	1	1	1	1
C118A	300	B13	3.6	0.209	0.105	0.037	3.051E-03	0.352	17.7	2.8	0	0	0	0	0	0	0	1	1	1	1	1	1	1	1	1	1	1	1	1	1	1	1	1
B018	130	BC4	2.4	0.210	0.134	0.037	3.894E-03	0.276	17.6	3.6	0	0	0	0	0	0	0	0	0	1	1	0	1	0	1	1	0	0	1	1	1	1	1	1
C046A	150	C14	2.4	0.060	0.261	0.037	7.585E-03	0.142	61.7	7.1	1	1	1	1	1	1	1	1	1	1	1	1	1	1	1	1	1	1	1	1	1	1	1	1
C049A	200	DE14	2.4	0.061	0.262	0.037	7.614E-03	0.141	60.7	7.1	1	1	1	1	1	1	1	1	1	1	1	1	1	1	1	1	1	1	1	1	1	1	1	1
C049A	200	CD6	0.0	0.061	0.279	0.037	8.108E-03	0.133	60.7	7.5	1	1	1	0	1	1	1	1	1	1	1	1	1	1	1	1	1	1	1	1	1	1	1	1
C092B	160	D14	2.4	0.209	0.298	0.037	8.660E-03	0.124	17.7	8.1	0	0	0	0	1	1	1	1	1	1	1	1	1	1	1	1	1	1	1	1	1	1	1	1
C070B	45	D11	5.9	0.206	0.106	0.038	3.164E-03	0.358	18.4	2.8	0	0	0	0	0	0	1	1	1	1	1	1	1	1	1	1	1	1	1	1	1	1	1	1
B012	60	BC14	2.4	0.221	0.124	0.038	3.701E-03	0.306	17.2	3.3	0	0	0	0	0	0	0	1	1	1	1	1	1	1	0	1	1	1	1	0	1	1	1	1
C001B	85	D6	0.0	0.052	0.279	0.038	8.327E-03	0.136	73.1	7.3	1	1	0	0	1	1	1	1	1	1	1	1	1	1	1	1	1	1	1	1	1	1	1	1
C022B	55	C6	0.0	0.057	0.287	0.038	8.566E-03	0.132	66.7	7.6	1	1	1	1	1	1	1	1	1	1	1	1	1	1	1	1	1	1	1	1	1	1	1	1
C001B	85	D18	2.4	0.052	0.269	0.039	8.240E-03	0.145	75.0	6.9	1	1	1	1	1	1	1	1	1	1	1	1	1	1	1	1	1	1	1	1	1	1	1	1
C117A	220	BC15	1.2	0.206	0.119	0.040	3.738E-03	0.336	19.4	3.0	0	0	0	0	1	1	1	1	1	1	1	0	1	1	1	1	1	1	1	1	1	1	1	1
C065A	50	BC10	4.8	0.196	0.119	0.040	3.738E-03	0.336	20.4	3.0	0	0	0	0	0	0	1	1	1	1	1	1	1	1	1	1	1	1	1	1	1	1	1	1
C064A	60	F10	4.8	0.209	0.125	0.040	3.927E-03	0.320	19.1	3.1	0	0	0	0	0	1	1	1	1	1	1	1	0	1	1	1	1	1	1	1	1	1	1	1
A006	32	FG3	3.6	0.062	0.129	0.040	4.053E-03	0.310	64.5	3.2	1	0	1	0	0	0	1	1	1	1	1	0	1	1	1	1	1	1	1	0	1	1	1	1
C106A	160	F10	4.8	0.209	0.306	0.040	9.613E-03	0.131	19.1	7.7	1	1	0	0	1	1	1	1	1	1	1	1	1	1	0	1	1	1	1	1	1	0	1	1
A024	230	CD12	4.8	0.057	0.334	0.040	1.049E-02	0.120	70.2	8.4	1	1	1	1	0	0	0	1	1	1	1	0	1	1	1	1	1	1	1	0	1	1	1	1
C084A	45	A11	5.9	0.210	0.105	0.041	3.381E-03	0.390	19.5	2.6	0	0	0	1	1	0	0	1	1	1	1	1	1	1	1	1	1	1	1	1	1	1	1	1
C086A	35	C7	1.2	0.206	0.108	0.041	3.478E-03	0.380	19.9	2.6	0	0	0	0	0	0	0	1	1	1	1	1	1	1	1	1	0	1	1	1	1	1	1	1
C116A	180	D11	5.9	0.207	0.117	0.041	3.768E-03	0.350	19.8	2.9	0	0	0	0	0	0	0	1	1	0	1	1	0	1	1	1	1	1	1	1	1	1	1	1
C008B	50	C10	4.8	0.058	0.342	0.041	1.101E-02	0.120	70.7	8.3	1	1	1	1	1	1	1	1	1	1	1	1	1	1	1	1	1	1	1	1	1	1	1	1
C069A	50	E11	5.9	0.209	0.115	0.042	3.793E-03	0.365	20.1	2.7	0	0	0	0	0	0	0	1	1	1	1	1	1	1	1	1	1	1	1	1	1	1	1	1
C080A	35	E15	1.2	0.206	0.117	0.042	3.859E-03	0.359	20.4	2.8	0	0	0	0	0	0	0	1	1	1	1	1	1	1	1	1	1	1	1	1	1	1	1	1
A011	60	EF6	0.0	0.062	0.352	0.042	1.161E-02	0.119	67.7	8.4	1	1	1	1	1	1	1	1	1	1	1	1	1	1	1	1	1	1	1	1	1	1	1	1
A024	230	DE9	3.6	0.057	0.352	0.042	1.161E-02	0.119	73.7	8.4	1	1	1	1	0	0	1	1	1	1	1	0	1	1	1	1	1	1	1	1	1	1	1	1
B017	130	CD14	2.4	0.212	0.143	0.043	4.829E-03	0.301	20.3	3.3	0	0	0	0	0	0	1	0	0	1	1	0	1	0	0	1	1	1	1	1	1	0	0	1
B012	60	EF11	5.9	0.221	0.143	0.043	4.829E-03	0.301	19.5	3.3	0	0	0	0	0	0	0	1	1	1	1	1	1	0	0	1	1	1	1	1	1	1	1	1
C005B	45	E14	2.4	0.061	0.247	0.043	8.342E-03	0.174	70.5	5.7	1	1	1	1	1	1	1	1	1	1	1	1	1	1	1	1	1	1	1	1	1	1	1	1
C016A	160	BC14	2.4	0.209	0.331	0.043	1.118E-02	0.130	20.6	7.7	0	0	0	0	1	1	1	1	1	1	1	1	1	1	1	1	1	1	1	1	1	1	1	1
C116A	180	B14	2.4	0.207	0.124	0.044	4.285E-03	0.355	21.3	2.8	0	0	0	0	0	1	0	0	1	1	1	1	1	1	1	1	1	1	1	1	0	1	1	1	1	1
C096A	180	BC6	0.0	0.207	0.313	0.044	1.082E-02	0.141	21.3	7.1	1	0	0	0	0	1	1	1	1	1	1	1	1	1	1	1	1	1	1	0	1	1	1	1
C095A	190	C10	4.8	0.208	0.322	0.044	1.113E-02	0.137	21.2	7.3	1	1	0	1	0	1	0	1	1	1	1	1	1	1	1	1	1	1	1	0	1	1	1	0	1	1
C057A	35	DE14	2.4	0.208	0.323	0.044	1.116E-02	0.136	21.2	7.3	0	0	0	0	0	1	1	1	1	1	1	1	1	1	1	1	1	1	1	1	1	1	1	1	1	1
A018	130	CD12	4.8	0.061	0.326	0.044	1.127E-02	0.135	72.1	7.4	1	1	1	1	1	0	1	0	1	1	1	1	1	1	1	1	1	1	1	1	1	1	1	1	1	1
C058A	40	EF11	5.9	0.208	0.331	0.044	1.144E-02	0.133	21.2	7.5	0	0	0	0	1	1	1	1	1	1	1	1	1	1	1	1	1	1	1	1	1	1	1	1	1	1
A014	125	CD14	2.4	0.064	0.342	0.044	1.182E-02	0.129	68.8	7.8	1	1	1	1	1	1	1	1	1	0	1	1	1	1	0	1	1	1	1	1	1	1	1	1	1	1
A011	60	Cd9	3.6	0.062	0.362	0.044	1.251E-02	0.122	71.0	8.2	1	1	1	1	1	1	1	1	1	1	1	1	1	1	1	1	1	1	1	1	1	1	1	1	1	1
C100A	205	B14	2.4	0.208	0.131	0.045	4.630E-03	0.344	21.6	2.9	0	0	0	0	0	1	1	1	1	1	1	1	1	1	1	1	1	0	1	1	0	1	1	1	1	1
B010	60	EF4	2.4	0.224	0.135	0.045	4.771E-03	0.333	20.1	3.0	0	0	0	0	0	0	0	1	1	0	1	0	1	1	0	1	1	1	1	1	1	1	1	1	1	1
C068A	45	C12	4.8	0.209	0.122	0.046	4.408E-03	0.377	22.0	2.7	0	0	0	0	0	0	0	1	1	1	1	1	1	1	1	1	0	1	1	1	1	1	1	1	1	1
C080A	35	D12	4.8	0.206	0.124	0.046	4.480E-03	0.371	22.3	2.7	0	0	0	0	0	0	0	1	1	1	1	1	1	1	1	1	1	1	1	1	1	1	1	1	1	1
A010	60	CD8	2.4	0.060	0.362	0.046	1.308E-02	0.127	76.7	7.9	1	1	1	1	1	0	0	1	1	1	1	1	1	1	1	1	1	1	1	1	1	1	1	1	1	1
A006	32	CD6	0.0	0.062	0.370	0.046	1.337E-02	0.124	74.2	8.0	1	1	1	1	1	1	1	1	1	1	1	0	1	1	1	1	1	1	1	1	1	1	1	1	1	1
A023	230	CD10	4.8	0.059	0.372	0.046	1.344E-02	0.124	78.0	8.1	1	1	1	1	0	0	0	1	1	1	1	0	0	0	1	1	0	0	0	1	1	0	0	0	1	1
A018	130	CD9	3.6	0.061	0.372	0.046	1.344E-02	0.124	75.4	8.1	1	1	1	1	0	1	1	0	1	1	1	1	1	1	1	1	1	1	1	1	1	1	1	1	1	1
A005	32	CD11	5.9	0.063	0.384	0.046	1.387E-02	0.120	73.0	8.3	1	1	1	1	0	1	1	1	1	1	1	1	1	1	1	1	1	1	1	1	1	1	1	1	1	1
C092A	160	E10	4.8	0.209	0.295	0.047	1.089E-02	0.159	22.5	6.3	0	0	0	0	0	1	1	1	1	1	1	1	1	1	1	1	1	1	1	1	1	1	1	1	1	1
C108A	150	D8	2.4	0.209	0.134	0.048	5.052E-03	0.358	23.0	2.8	0	0	0	0	0	0	0	1	1	1	1	1	1	1	1	1	1	1	1	1	1	1	1	1	1	1
B010	60	FG13	3.6	0.224	0.137	0.048	5.165E-03	0.350	21.4	2.9	0	0	0	0	0	0	0	1	1	1	1	1	1	1	0	1	1	1	1	1	1	1	1	1	1	1
C058A	40	E7	1.2	0.208	0.326	0.048	1.229E-02	0.147	23.1	6.8	0	0	0	0	0	0	1	0	1	1	1	1	1	1	1	1	1	1	1	1	1	1	1	1	1	1
A006	32	DB11	5.9	0.062	0.370	0.048	1.395E-02	0.130	77.4	7.7	1	1	1	1	0	1	1	1	1	1	1	0	1	1	1	1	1	1	1	1	1	1	1	1	1	1
C074B	45	E8	2.4	0.208	0.129	0.049	4.965E-03	0.380	23.6	2.6	0	0	0	0	0	0	0	1	1	1	1	1	1	1	0	1	1	1	1	1	1	1	0	1	1	1
C069A	50	E9	3.6	0.209	0.131	0.049	5.041E-03	0.374	23.4	2.7	0	0	0	0	0	0	0	1	1	1	1	1	1	1	1	1	0	1	1	1	1	1	1	1	1	1
C070A	45	EF15	1.2	0.206	0.134	0.049	5.157E-03	0.366	23.8	2.7	0	0	0	0	0	0	1	1	1	1	1	1	1	1	1	1	1	1	1	1	1	1	1	1	1	1
C084A	45	EF13	3.6	0.210	0.136	0.049	5.234E-03	0.360	23.3	2.8	0	0	0	0	1	0	0	0	1	1	1	1	1	1	1	1	1	1	1	1	1	1	1	1	1	1
C088A	150	EF15	1.2	0.197	0.310	0.049	1.193E-02	0.158	24.9	6.3	0	0	0	0	0	1	1	1	1	1	0	1	1	1	1	1	1	1	1	1	1	1	1	1	1	1
C118A	300	D8	2.4	0.209	0.132	0.050	5.184E-03	0.379	23.9	2.6	0	0	0	0	0	0	0	1	1	1	1	1	1	1	1	1	1	1	1	1	1	1	1	1	1	1

Specimen Characteristics											Radiographic Inspections							Penetrant Inspections							Ultrasonics Inspections					Eddy Current Inspections				
	Surface Finish		Incld Angle	Thick (t)	Length (2c)	Depth (a)	Area				A	B	C	D	E	F	G	H	I	J	K	L	M	N	O	P	Q	R	S	T	U	V	W	X
Specimen No.	(microinch)	Location	(degree)	(inch)	(inch)	(inch)	(inch^2)	a/2c	a/t	2c/a																								
C081A	40	F14	2.4	0.208	0.135	0.050	5.301E-03	0.370	24.0	2.7	0	0	0	0	0	0	0	1	1	1	1	1	1	0	1	1	0	1	1	1	1	1	1	1
C086A	35	DE15	1.2	0.206	0.138	0.050	5.419E-03	0.362	24.3	2.8	0	0	0	0	0	0	0	1	1	1	1	1	1	1	1	1	0	1	1	1	1	1	1	1
B011	60	DE10	4.8	0.224	0.144	0.050	5.655E-03	0.347	22.3	2.9	0	0	0	0	1	1	1	1	1	1	1	1	1	1	1	1	1	1	1	1	1	1	1	1
C057A	35	EF10	4.8	0.208	0.362	0.050	1.422E-02	0.138	24.0	7.2	0	0	0	0	0	1	0	1	1	1	1	1	1	1	1	1	1	1	1	1	1	1	1	1
C080A	35	ED7	1.2	0.206	0.129	0.051	5.167E-03	0.395	24.8	2.5	0	0	0	0	0	0	0	1	1	1	1	1	1	1	1	1	1	1	1	1	1	1	1	1
C075B	55	EF15	1.2	0.210	0.317	0.051	1.270E-02	0.161	24.3	6.2	0	0	0	0	0	0	0	1	1	1	1	1	1	0	1	1	1	1	1	1	1	1	1	1
C095A	190	BC14	2.4	0.208	0.328	0.051	1.314E-02	0.155	24.5	6.4	0	0	0	0	0	0	0	1	1	1	1	1	1	1	1	1	1	1	1	1	1	1	1	1
C101A	300	F8	2.4	0.210	0.140	0.052	5.718E-03	0.371	24.8	2.7	0	0	0	1	0	1	0	1	1	1	1	1	1	1	1	1	1	1	1	1	1	1	1	1
B003	32	DE9	3.6	0.223	0.144	0.052	5.881E-03	0.361	23.3	2.8	0	0	0	0	0	0	1	1	0	1	1	1	0	1	1	1	0	0	1	1	1	0	0	0
C059A	35	C14	2.4	0.208	0.318	0.052	1.299E-02	0.164	25.0	6.1	1	1	0	0	0	1	0	1	1	1	1	1	1	1	1	1	1	1	1	1	1	1	1	1
C102A	300	E13	3.6	0.211	0.136	0.053	5.661E-03	0.390	25.1	2.6	0	0	0	1	1	1	0	1	1	0	1	1	1	1	1	1	1	1	1	1	1	1	1	1
B016	130	DE9	3.6	0.225	0.140	0.053	5.828E-03	0.379	23.6	2.6	0	0	0	0	0	0	0	1	1	1	1	0	1	0	1	1	1	1	1	1	1	1	0	1
B002	32	BC10	4.8	0.225	0.145	0.053	6.036E-03	0.366	23.6	2.7	0	0	0	0	0	0	0	1	1	1	1	1	0	1	1	1	1	1	1	1	1	1	1	1
C075B	55	C7	1.2	0.210	0.321	0.053	1.336E-02	0.165	25.2	6.1	1	1	0	0	0	0	0	1	1	1	1	1	1	0	1	1	1	1	1	1	1	1	1	1
C088A	150	E11	5.9	0.197	0.329	0.053	1.369E-02	0.161	26.9	6.2	0	0	0	0	0	1	1	1	1	1	1	1	1	1	1	1	1	1	1	1	1	1	1	1
C057A	35	E6	0.0	0.208	0.330	0.053	1.374E-02	0.161	25.5	6.2	1	0	0	1	1	1	1	1	1	1	1	1	1	1	1	1	1	1	1	1	1	1	1	1
C085A	45	C15	1.2	0.209	0.146	0.054	6.192E-03	0.370	25.8	2.7	0	0	0	0	0	0	0	1	1	1	1	1	1	1	1	1	1	1	1	1	1	1	1	1
B015	125	BC10	4.8	0.225	0.149	0.054	6.319E-03	0.362	24.0	2.8	0	0	0	0	0	0	0	1	1	1	1	1	0	0	1	1	1	1	1	1	1	1	1	1
C064A	60	B13	3.6	0.209	0.153	0.054	6.489E-03	0.353	25.8	2.8	0	0	0	0	0	0	1	1	1	1	1	1	1	1	1	1	1	1	1	1	1	1	1	1
C059B	35	E10	4.8	0.208	0.313	0.054	1.327E-02	0.173	26.0	5.8	0	0	0	0	0	1	1	1	1	1	1	1	1	1	1	1	1	1	1	1	1	1	1	1
A022	230	EF7	1.2	0.061	0.356	0.054	1.510E-02	0.152	88.5	6.6	1	1	1	1	1	1	1	1	1	1	1	1	1	1	1	1	1	1	1	1	1	1	1	1
B017	130	EF5	1.2	0.212	0.426	0.054	1.807E-02	0.127	25.5	7.9	0	0	0	0	0	0	0	1	1	1	1	1	1	1	1	1	1	1	1	1	1	1	1	1
B021	230	ED9	3.6	0.227	0.144	0.055	6.220E-03	0.382	24.2	2.6	0	0	0	0	0	0	0	1	1	1	1	1	1	1	1	1	0	0	1	1	1	1	1	1
B005	32	CD9	3.6	0.213	0.442	0.056	1.944E-02	0.127	26.3	7.9	1	1	1	1	1	0	1	1	1	1	1	0	1	1	1	1	1	1	1	1	1	1	0	1
C097A	145	D10	4.8	0.210	0.126	0.057	5.641E-03	0.452	27.1	2.2	0	0	0	0	0	1	1	1	1	1	1	1	1	1	1	1	1	0	1	1	1	1	1	1
C102A	300	C8	2.4	0.211	0.141	0.057	6.312E-03	0.404	27.0	2.5	0	0	0	0	0	1	0	1	1	1	1	1	1	1	1	1	1	1	1	1	1	0	1	1
C074B	45	DE11	5.9	0.208	0.158	0.057	7.073E-03	0.361	27.4	2.8	0	0	0	0	0	1	0	1	1	1	1	1	1	1	1	1	1	1	1	1	1	1	1	1
C059A	35	D6	0.0	0.208	0.345	0.057	1.544E-02	0.165	27.4	6.1	1	1	1	1	1	1	1	1	1	1	1	1	1	1	1	1	1	1	1	1	1	1	1	1
C117B	220	F9	3.6	0.208	0.129	0.058	5.876E-03	0.450	27.9	2.2	0	0	0	0	1	1	1	1	1	1	1	1	1	1	1	1	1	1	0	1	1	0	1	1
B023	230	EF14	2.4	0.227	0.157	0.058	7.152E-03	0.369	25.6	2.7	0	0	0	0	0	0	0	1	1	1	1	0	1	1	1	1	1	1	1	1	1	1	1	1
C056B	40	D10	4.8	0.207	0.408	0.058	1.859E-02	0.142	28.0	7.0	0	1	0	0	1	1	1	1	1	1	1	1	1	1	0	1	1	1	1	1	1	1	1	1
C109A	160	BC10	4.8	0.208	0.151	0.059	6.997E-03	0.391	28.4	2.6	0	0	0	0	1	1	1	1	1	1	1	1	1	1	1	1	1	1	1	1	1	1	1	1
C056A	40	D14	2.4	0.207	0.336	0.059	1.557E-02	0.176	28.5	5.7	0	1	0	0	0	1	1	1	1	1	1	1	1	1	1	1	1	1	0	1	1	1	1	1
C096A	180	E10	4.8	0.207	0.347	0.059	1.608E-02	0.170	28.5	5.9	1	0	0	0	1	1	1	1	1	1	1	1	1	1	1	1	1	1	0	1	1	1	1	1
C103A	140	D11	5.9	0.208	0.148	0.060	6.974E-03	0.405	28.8	2.5	0	0	0	0	0	1	1	1	1	0	1	1	1	1	1	1	1	0	1	1	1	1	1	1
C094A	140	D12	4.8	0.210	0.153	0.060	7.210E-03	0.392	28.6	2.6	0	0	0	0	0	0	1	1	1	1	1	1	1	1	1	1	1	0	1	1	1	1	1	1
C095A	190	Ey	0.0	0.208	0.338	0.060	1.593E-02	0.178	28.8	5.6	1	1	0	0	0	0	0	1	1	1	1	0	1	0	1	1	1	0	1	1	1	0	0	1
C073B	45	C9	3.6	0.209	0.060	0.061	2.875E-03	1.017	29.2	1.0	0	0	0	0	1	1	1	1	1	1	1	1	1	1	1	1	1	1	1	1	1	1	1	1
C114A	250	BC15	1.2	0.208	0.342	0.062	1.665E-02	0.181	29.8	5.5	1	1	1	1	1	1	1	1	1	1	1	1	1	1	1	1	1	1	1	1	1	1	1	1
C094A	140	D14	2.4	0.210	0.162	0.063	8.016E-03	0.389	30.0	2.6	0	0	0	0	0	1	1	1	1	1	1	1	1	1	1	1	0	0	1	1	1	1	1	1
C063A	30	C10	4.8	0.212	0.333	0.063	1.648E-02	0.189	29.7	5.3	0	0	0	0	1	1	1	1	1	1	1	1	1	1	1	1	1	1	1	1	1	1	1	1
C063A	30	D14	2.4	0.212	0.340	0.063	1.682E-02	0.185	29.7	5.4	1	1	1	0	1	1	1	1	1	1	1	1	1	1	1	1	1	1	1	1	1	1	1	1
C085B	45	E8	2.4	0.209	0.153	0.064	7.691E-03	0.418	30.6	2.4	0	0	0	0	1	0	0	1	1	1	1	1	1	0	0	1	1	1	1	1	1	1	1	1
B023	230	DE10	4.8	0.227	0.190	0.064	9.550E-03	0.337	28.2	3.0	0	0	0	0	0	0	0	1	1	1	1	0	1	1	1	1	1	1	1	1	1	1	1	1
B009	60	CD8	2.4	0.223	0.460	0.064	2.312E-02	0.139	28.7	7.2	1	1	1	1	0	0	1	1	1	1	1	1	1	1	1	1	1	1	1	1	1	1	1	1
C111A	100	BC14	2.4	0.208	0.171	0.067	8.998E-03	0.392	32.2	2.6	0	0	0	0	0	1	1	1	1	1	1	1	1	1	1	1	1	1	1	1	1	1	1	1
C117B	220	E13	3.6	0.208	0.183	0.068	9.773E-03	0.372	32.7	2.7	0	0	0	0	0	1	1	1	1	1	1	1	1	1	0	1	1	1	1	1	1	1	0	1
C077A	45	E8	2.4	0.206	0.182	0.071	1.015E-02	0.390	34.5	2.6	0	0	0	0	0	0	0	1	1	1	1	1	1	1	1	1	1	1	1	1	1	1	1	1
C110A	145	B14	2.4	0.209	0.185	0.074	1.075E-02	0.400	35.4	2.5	1	0	0	0	0	1	1	1	1	1	1	1	1	1	1	1	1	1	1	1	1	1	0	1	1
C063A	30	DE6	0.0	0.212	0.381	0.076	2.274E-02	0.199	35.8	5.0	1	1	0	1	0	1	1	1	1	1	1	1	1	1	1	1	1	1	1	1	1	1	1	1
C096A	180	B14	2.4	0.207	0.392	0.077	2.371E-02	0.196	37.2	5.1	1	1	1	1	1	1	1	1	1	1	1	0	1	1	1	1	1	1	1	1	1	1	1	1
B022	230	CD4	2.4	0.212	0.444	0.080	2.790E-02	0.180	37.7	5.6	1	1	1	1	0	0	0	1	1	1	1	1	1	1	1	1	1	1	1	1	1	1	1	1
B009	60	EF10	4.8	0.223	0.478	0.080	3.003E-02	0.167	35.9	6.0	1	1	1	1	1	1	1	1	1	1	1	1	1	1	1	1	1	1	1	1	1	1	1	1
B018	130	BC7	1.2	0.210	0.458	0.084	3.022E-02	0.183	40.0	5.5	1	1	1	1	0	0	0	1	1	1	1	1	1	1	1	1	1	1	1	1	1	1	1	1
C020A	230	EF7	1.2	0.226	0.478	0.086	3.229E-02	0.180	38.1	5.6	1	1	1	1	1	0	1	1	1	1	1	1	1	1	1	1	1	1	1	1	1	1	1	1
B018	130	CD16	0.0	0.210	0.498	0.088	3.442E-02	0.177	41.9	5.7	1	1	0	1	0	0	0	1	1	1	1	1	1	0	0	1	1	1	1	1	1	1	1	1
B018	130	FG9	3.6	0.210	0.458	0.090	3.237E-02	0.197	42.9	5.1	1	1	1	1	1	0	1	1	1	1	1	1	1	1	1	1	1	1	1	1	1	1	0	1
B024	230	BC13	3.6	0.211	0.512	0.090	3.619E-02	0.176	42.7	5.7	1	1	1	1	1	1	1	1	1	1	1	1	1	1	1	1	1	1	1	1	1	1	1	1
B005	32	DE13	3.6	0.213	0.506	0.092	3.656E-02	0.182	43.2	5.5	1	1	1	1	0	0	0	1	1	1	1	1	1	1	1	1	1	1	1	1	1	1	0	1
B006	32	EF5	1.2	0.211	0.508	0.092	3.671E-02	0.181	43.6	5.5	1	1	1	1	1	1	0	1	1	1	1	1	1	1	1	1	1	1	1	1	1	1	1	1

Specimen Characteristics											Radiographic Inspections							Penetrant Inspections							Ultrasonics Inspections					Eddy Current Inspections				
	Surface Finish		Incld Angle	Thick (t)	Length (2c)	Depth (a)	Area				A	B	C	D	E	F	G	H	I	J	K	L	M	N	O	P	Q	R	S	T	U	V	W	X
Specimen No.	(microinch)	Location	(degree)	(inch)	(inch)	(inch)	(inch^2)	a/2c	a/t	2c/a																								
B006	32	FG13	3.6	0.211	0.524	0.092	3.786E-02	0.176	43.6	5.7	1	1	1	1	0	0	1	1	1	1	1	1	1	1	1	1	1	1	1	1	1	0	1
B024	230	EF10	4.8	0.211	0.504	0.094	3.721E-02	0.187	44.5	5.4	1	1	1	1	1	0	0	1	1	1	1	1	1	1	1	1	1	1	1	1	1	1	1	1
B022	230	BC13	3.6	0.212	0.506	0.094	3.736E-02	0.186	44.3	5.4	1	1	1	1	0	1	1	1	1	1	1	1	1	1	1	1	1	1	1	1	1	1	1	1
B004	32	DE9	3.6	0.211	0.510	0.094	3.765E-02	0.184	44.5	5.4	1	1	1	1	1	1	0	1	1	1	1	1	1	1	1	1	1	1	1	1	1	1	1	1
B022	230	FG8	2.4	0.212	0.466	0.096	3.514E-02	0.206	45.3	4.9	1	1	1	1	1	1	1	1	1	1	1	1	1	1	1	1	1	1	1	1	1	1	1	1
C071A	35	D15	1.2	0.206	0.518	0.096	3.906E-02	0.185	46.6	5.4	1	1	1	0	1	1	1	1	1	1	1	1	1	1	1	1	1	1	1	1	1	1	1	1
C071A	35	B7	1.2	0.206	0.495	0.097	3.771E-02	0.196	47.1	5.1	1	1	1	1	1	1	1	1	1	1	1	1	1	1	1	1	1	1	1	1	1	1	1	1
B023	230	BC11	5.9	0.227	0.470	0.098	3.618E-02	0.209	43.2	4.8	1	1	1	1	1	0	0	1	1	1	1	0	1	1	1	1	1	1	1	1	1	1	1	1
C091B	145	BC11	5.9	0.205	0.500	0.103	4.045E-02	0.206	50.2	4.9	1	1	0	1	1	1	1	1	1	1	1	1	1	1	1	1	1	0	1	1	1	1	1	1
B011	60	EF13	3.6	0.224	0.512	0.104	4.182E-02	0.203	46.4	4.9	1	1	1	1	0	0	0	1	1	1	1	0	1	1	1	1	1	1	1	1	0	1	1	1
C072A	50	E6	0.0	0.207	0.326	0.105	2.688E-02	0.322	50.7	3.1	1	0	0	0	1	1	1	1	1	1	1	1	1	1	1	1	1	1	1	1	1	1	1	1
C078A	40	D15	1.2	0.207	0.494	0.106	4.113E-02	0.215	51.2	4.7	1	1	1	1	1	1	1	1	1	1	1	1	1	1	1	1	1	1	1	1	1	1	1	1
B016	130	DE12	4.8	0.225	0.520	0.106	4.329E-02	0.204	47.1	4.9	1	1	1	1	1	1	1	1	1	1	1	1	1	1	1	1	1	1	1	1	1	1	1	1
B003	32	BC11	5.9	0.223	0.526	0.106	4.379E-02	0.202	47.5	5.0	1	1	1	1	0	1	0	1	1	1	1	1	1	1	1	1	1	1	1	1	1	0	1
B012	60	DE9	3.6	0.221	0.530	0.106	4.412E-02	0.200	48.0	5.0	1	1	1	1	1	1	1	1	1	1	1	1	1	1	1	1	1	1	1	1	1	1	1	1
B016	130	CD4	2.4	0.225	0.534	0.106	4.446E-02	0.199	47.1	5.0	1	1	1	1	1	1	1	1	1	1	1	1	1	1	1	1	1	1	1	1	1	1	1	1
C066A	50	E7	1.2	0.206	0.459	0.107	3.857E-02	0.233	51.9	4.3	1	1	0	1	1	1	1	1	1	1	1	1	1	1	1	1	1	1	1	1	1	1	1	1
C066B	50	D11	5.9	0.206	0.489	0.107	4.109E-02	0.219	51.9	4.6	1	1	0	1	1	1	1	1	1	1	1	1	1	1	1	1	1	1	1	1	1	1	1	1
C093B	150	D11	5.9	0.208	0.492	0.107	4.135E-02	0.217	51.4	4.6	0	0	1	1	1	1	1	1	1	1	1	1	1	1	1	1	0	0	1	1	1	0	1	1
C060B	60	E10	4.8	0.209	0.475	0.108	4.029E-02	0.227	51.7	4.4	0	0	0	0	1	1	1	1	1	1	1	1	1	1	1	0	1	1	1	1	1	1	1	1
C105A	140	D15	1.2	0.209	0.495	0.108	4.199E-02	0.218	51.7	4.6	1	1	1	1	0	1	1	1	1	1	1	1	1	1	1	1	1	1	1	1	1	1	1	1
B014	130	DE7	1.2	0.221	0.522	0.108	4.428E-02	0.207	48.9	4.8	1	1	1	1	1	1	1	1	1	1	1	1	1	1	1	1	1	1	1	1	1	1	1	1
B011	60	CD5	1.2	0.224	0.530	0.108	4.496E-02	0.204	48.2	4.9	1	1	1	1	1	1	1	1	1	1	1	1	1	1	1	1	1	1	1	1	1	1	1	1
B012	60	CD3	3.6	0.221	0.534	0.108	4.530E-02	0.202	48.9	4.9	1	1	1	1	0	0	1	1	1	1	1	1	1	1	1	1	1	1	1	1	1	1	1	1
C079A	55	BC12	4.8	0.211	0.283	0.109	2.423E-02	0.385	51.7	2.6	0	0	0	0	1	0	0	1	1	1	1	1	1	1	1	1	1	1	1	1	1	0	1
C105B	140	D11	5.9	0.209	0.466	0.109	3.989E-02	0.234	52.2	4.3	1	1	1	1	1	1	1	1	1	1	1	1	1	1	1	1	1	1	1	1	1	1	1	1
C107A	140	D11	5.9	0.210	0.503	0.109	4.306E-02	0.217	51.9	4.6	1	1	1	1	1	1	1	1	1	1	1	1	1	1	1	1	1	1	1	1	1	1	1	1
C014B	280	BC11	5.9	0.210	0.513	0.109	4.392E-02	0.212	51.9	4.7	0	0	0	1	1	1	1	1	1	1	1	1	1	1	1	1	1	1	1	1	1	1	1	1
C112A	175	D10	4.8	0.207	0.520	0.109	4.452E-02	0.210	52.7	4.8	1	0	0	1	1	1	1	1	1	1	1	1	1	1	1	1	1	1	1	1	1	1	1	1
C066A	50	C15	1.2	0.206	0.508	0.110	4.389E-02	0.217	53.4	4.6	1	1	1	1	1	1	1	1	1	1	1	1	1	1	1	1	1	1	1	1	1	1	1	1
C060A	60	C14	2.4	0.209	0.519	0.110	4.484E-02	0.212	52.6	4.7	1	1	0	1	1	1	1	1	1	1	1	1	1	1	1	1	1	1	1	1	1	1	1	1
B023	230	DE5	1.2	0.227	0.534	0.110	4.613E-02	0.206	48.5	4.9	1	1	1	1	0	0	1	1	1	1	1	0	1	1	1	1	1	1	1	1	1	1	1	1
B010	60	CD8	2.4	0.224	0.550	0.110	4.752E-02	0.200	49.1	5.0	1	1	1	1	1	1	1	1	1	1	1	0	1	1	1	1	1	1	1	1	1	1	1	1
C076A	50	B11	5.9	0.211	0.484	0.111	4.219E-02	0.229	52.6	4.4	1	1	0	1	1	1	1	1	1	1	1	1	1	1	1	1	1	1	1	1	1	1	1	1
C113A	280	BC6	0.0	0.210	0.514	0.111	4.481E-02	0.216	52.9	4.6	1	1	1	1	1	1	1	1	1	1	1	1	1	1	1	1	1	1	1	1	1	0	1	1
C112A	175	F6	0.0	0.207	0.521	0.112	4.583E-02	0.215	54.1	4.7	1	1	1	1	1	1	1	1	1	1	1	1	1	1	1	1	1	1	1	1	1	1	1	1
B021	230	FG6	0.0	0.227	0.538	0.112	4.732E-02	0.208	49.3	4.8	1	1	1	1	1	1	1	1	1	1	1	1	1	1	1	1	1	1	1	1	1	1	1	1
B017	130	CD8	2.4	0.212	0.474	0.114	4.244E-02	0.241	53.8	4.2	1	1	1	1	1	1	1	1	1	1	1	0	1	1	1	1	1	1	1	1	1	1	1	1
C113A	280	BC10	4.8	0.210	0.499	0.114	4.468E-02	0.228	54.3	4.4	0	0	0	1	1	1	1	1	1	1	1	1	1	1	1	1	1	1	1	1	1	0	1	1
B008	60	DE7	1.2	0.226	0.520	0.114	4.656E-02	0.219	50.4	4.6	1	1	1	1	1	1	1	1	1	1	1	1	1	1	1	1	1	1	1	1	1	1	1	1
C072B	50	E14	2.4	0.207	0.523	0.114	4.683E-02	0.218	55.1	4.6	1	1	1	1	1	1	1	1	1	1	1	1	1	1	1	1	1	1	1	1	1	1	1	1
C060A	60	C6	0.0	0.209	0.535	0.114	4.790E-02	0.213	54.5	4.7	1	1	1	1	1	1	1	1	1	1	1	1	1	1	1	1	1	1	1	1	1	1	1	1
C062B	40	E11	5.9	0.210	0.539	0.115	4.868E-02	0.213	54.8	4.7	1	1	0	1	1	1	1	1	1	1	1	1	1	1	1	1	1	1	1	1	1	1	1	1
C087A	160	BC6	0.0	0.209	0.559	0.115	5.049E-02	0.206	55.0	4.9	1	1	1	1	1	1	1	1	1	1	1	1	1	1	1	1	1	1	1	1	1	1	1	1
B011	60	BC11	5.9	0.224	0.496	0.116	4.519E-02	0.234	51.8	4.3	1	1	1	1	0	0	0	1	1	1	1	1	1	1	1	1	1	1	1	1	1	1	1	1
C093A	150	D7	1.2	0.208	0.535	0.116	4.874E-02	0.217	55.8	4.6	1	1	1	1	1	1	1	1	1	1	1	1	1	1	1	1	1	0	0	1	1	1	0	1	1
C105A	140	C7	1.2	0.209	0.543	0.116	4.947E-02	0.214	55.5	4.7	1	1	1	1	1	1	1	1	1	1	1	1	1	1	1	1	1	1	1	1	1	1	1	1
C072A	50	E10	4.8	0.207	0.568	0.117	5.219E-02	0.206	56.5	4.9	1	1	0	0	1	1	1	1	1	1	1	1	1	1	1	1	1	1	1	1	1	1	1	1
C113A	280	E14	2.4	0.210	0.509	0.119	4.757E-02	0.234	56.7	4.3	1	1	1	1	1	1	1	1	1	1	1	1	1	1	1	1	1	1	1	1	1	0	1	1
B024	230	DE6	0.0	0.211	0.472	0.124	4.597E-02	0.263	58.8	3.8	1	1	1	1	1	1	1	1	1	1	1	0	1	1	1	1	1	1	1	1	1	1	1	1
B012	60	EF6	0.0	0.221	0.478	0.126	4.730E-02	0.264	57.0	3.8	1	1	1	1	1	1	1	1	1	1	1	1	1	1	1	1	1	1	1	1	1	1	1	1
C093A	150	E15	1.2	0.208	0.610	0.126	6.037E-02	0.207	60.6	4.8	1	1	1	1	1	1	1	1	1	1	1	1	1	1	1	1	1	0	0	1	1	1	1	1	1
C087A	160	BC14	2.4	0.209	0.710	0.126	7.026E-02	0.177	60.3	5.6	1	1	1	1	1	1	1	1	1	1	1	1	1	1	1	1	1	1	1	1	1	1	1	1	1
B006	32	EF9	3.6	0.211	0.474	0.128	4.765E-02	0.270	60.7	3.7	1	1	1	1	1	1	1	1	1	1	1	1	1	1	1	1	1	1	1	1	1	0	0	1
B004	32	DE5	1.2	0.211	0.478	0.128	4.805E-02	0.268	60.7	3.7	1	1	1	1	1	1	1	1	1	1	1	1	1	1	1	1	1	1	1	1	1	1	1	1
B006	32	CD7	1.2	0.211	0.492	0.130	5.023E-02	0.264	61.6	3.8	1	1	1	1	1	1	1	1	1	1	1	1	1	1	1	1	1	1	1	1	1	1	1	1
B005	32	EF7	1.2	0.213	0.482	0.136	5.148E-02	0.282	63.8	3.5	1	1	1	1	1	1	1	1	1	1	1	1	1	1	1	1	1	1	1	1	1	0	1	1
B015	125	EF7	1.2	0.225	0.490	0.144	5.542E-02	0.294	64.0	3.4	1	1	1	1	1	1	1	1	1	1	1	0	1	1	1	1	1	1	1	1	1	1	1	0
C104A	280	D15	1.2	0.210	0.979	0.149	1.146E-01	0.152	71.0	6.6	1	1	1	1	1	1	1	1	1	1	1	1	1	1	1	1	1	1	1	1	1	1	1	1
C074B	45	BC7	1.2	0.208	0.496	0.178	6.934E-02	0.359	85.6	2.8	1	1	1	1	1	1	0	1	1	0	1	1	1	1	1	1	1	1	1	1	1	1	1	1